SKELETAL MUSCLE MECHANICS AND SPASTICITY MANAGEMENT: HUMAN AND ANIMAL EXPERIMENTS

by

Cemre Su Kaya Keleş

B.S., in Bioengineering, Yıldız Technical University, 2014

B.S., in Chemical Engineering, Yıldız Technical University, 2014

Submitted to the Institute of Biomedical Engineering

in partial fulfillment of the requirements

for the degree of

Doctor

of

Philosophy

Boğaziçi University

2022

ACKNOWLEDGMENTS

I would first like to express my most sincere gratitude to my advisor Prof. Dr. Can A. Yücesoy for his inspiring attitude, continuous support on several issues, and for all the opportunities he has offered me throughout the time we worked together. He has always been the most genuine guide for me to learn the requirements of a successful academic career.

I am indebted to Assoc. Prof. Dr. Fuat Bilgili for enabling me to take data during surgeries, and for all the valuable advice he gave as a member of my thesis progress committee. This thesis would not be accomplished without the collaboration of him and his team at Istanbul University, Faculty of Medicine, Department of Orthopaedics and Traumatology.

I owe my deepest thanks to Prof. Dr. N. Ekin Akalan, a respectable physiotherapist who does his job with great sincerity, for always answering my clinical questions with extensive information.

It gives me a great honor in acknowledging Prof. Dr. Yener Temelli, who allowed us to start human experiments on patients. I am glad to have the opportunity to participate in surgical operations with a doctor as experienced as himself.

I warmly thank Assoc. Prof. Dr. Zeynep Deniz Akdeniz Doğan and Dr. M. Taygun Oluklu, who have great contributions to animal experiments, for their surgical expertise, help in scheduling, and good company.

I wish to thank Assoc. Prof. Dr. Duygu Ege for her participation in my thesis progress committee, her insightful comments and encouragement, and allowing me to use her laboratory facilities to conduct the chemical tests associated with animal experiments.

It was my great honor and pleasure to have the opportunity to share my thesis outputs with Prof. Dr. Jaap Harlaar and Prof. Dr. Richard T. Jaspers, the external members of my dissertation committee. I am beyond grateful for them taking the time and providing a valuable and enjoyable discussion session.

I greatly appreciate Dr. Filiz Ateş for teaching everything practical about human and animal experiments and for her precious company. I am happy to meet such an experienced labmate that I can consult on her guidance to be successful both in my academic and in my personal life.

All my friends I worked with and had a good time with at the Institute of Biomedical Engineering, primarily Dr. Uluç Pamuk who has been here in all my work in the Biomechanics Laboratory and made my Ph.D. student life easier, thank you all.

All the patients and their families who participated in the human studies presented in this thesis are gratefully and humbly acknowledged. I am also thankful for the animals used in the experiments for their contribution to science.

Most importantly, my dear father who has the greatest enthusiasm in my orientation to the academy; my dear mother who inspires me to always be patient; and lastly, my precious sister who is my closest and irreplaceable relative for life are warmly acknowledged.

Finally, I dedicate this dissertation to Ahmet Doğukan Keleş who waited for me at the door of the examination hall while I was taking the research assistant exam, rushed to the hospital when I had a laboratory accident, and took all my tiredness away for all this long period. I enjoy being with you during this entire process and finally celebrating my doctorate with you. You made it all possible, my loving husband.

The studies in this thesis were supported by The Scientific and Technological Research Council of Turkey (TÜBİTAK) under grants 113S293 and 116S393.

ACADEMIC ETHICS AND INTEGRITY STATEMENT

I, Cemre Su Kaya Keleş, hereby certify that I am aware of the Academic Ethics and Integrity Policy issued by the Council of Higher Education (YÖK) and I fully acknowledge all the consequences due to its violation by plagiarism or any other way.

Name :

Signature:

Date:

ABSTRACT

SKELETAL MUSCLE MECHANICS AND SPASTICITY MANAGEMENT: HUMAN AND ANIMAL EXPERIMENTS

Being the most common motor disability in childhood, cerebral palsy (CP) describes a movement disorder for which the exact underlying mechanism is unclear, and no cure is available. Yet, local injection of botulinum toxin type-A (BTX-A) is used for spasticity management. In this thesis, the relationship between the mechanics of spastic muscles and the impaired joint motion was investigated in patients, and the long-term effects of BTX-A on muscular mechanics were assessed in animals. Experiments on spastic knee flexors showed that passive muscle forces are much less than active forces (e.g., 26%), and epimuscular myofascial force transmission (EMFT) arising from intermuscular mechanical interactions significantly increases active forces (up to 132%). Combined with musculoskeletal models developed based on gait analysis data, EMFT effects were shown to be compatible with metrics characterizing patients' pathological gait, indicating that intermuscular mechanical interactions may be a source of high flexor forces in flexed joint positions. Experiments in the rat anterior crural compartment showed that long-term after injection, BTX-A yields in addition to decreased active forces, both unintended (a narrower range of force exertion by 23% and increased passive forces by 12%, for the injected muscle) and uncontrolled effects (similar effects on compartmental muscles due to the spread of the toxin). BTX-A also leads to collagen content increase (by several folds) for muscles exposed, which explains elevated passive forces and impacts also active forces. These effects are of high potential clinical importance as they conflict with therapeutic goals. Particularly, controlling the effects of BTX-A on connective tissue adaptation is critical for better spasticity management.

Keywords: Epimuscular myofascial force transmission, Cerebral palsy, Spastic muscle, Muscle force-joint angle/length characteristics, Gait analysis, OpenSim, Botulinum toxin type-A, Rat anterior crural compartment, Collagen.

ÖZET

İSKELET KASI MEKANİĞİ VE SPASTİSİTE YÖNETİMİ: İNSAN VE HAYVAN DENEYLERİ

Çocukluk çağındaki en yaygın motor engellilik olan serebral palsi (SP), altta yatan mekanizmanın belirsiz olduğu ve tedavisi bulunmayan bir hareket bozukluğunu tanımlar. Ancak botulinum toksin tip-A (BTX-A)'nın lokal enjeksiyonu spastisite yönetimi için kullanılmaktadır. Bu tezde, spastik kas mekaniği ve bozulmuş eklem hareketi arasındaki ilişki hastalarda; BTX-A'nın kas mekaniğine uzun süreli etkileri hayvanlarda araştırılmıştır. Spastik diz fleksörlerindeki deneyler, pasif kas kuvvetlerinin aktif kuvvetlerden çok az olduğunu (örneğin %26) ve kaslar arası mekanik etkileşimlerden kaynaklanan epimüsküler miyobağdokusal kuvvet iletiminin (EMKİ) aktif kuvvetleri önemli ölçüde arttırdığını (%132'ye kadar) göstermiştir. Yürüme analizi verilerine dayanarak geliştirilen kas-iskelet sistemi modelleriyle birleştirildiğinde, EMFT etkilerinin hastaların patolojik yürüyüşünü karakterize eden ölçütlerle uyumlu olduğu gösterilmiştir ki bu kaslar arası mekanik etkileşimlerin, bükülmüş eklem pozisyonlarındaki yüksek fleksör kuvvetlerin bir kaynağı olabileceğini işaret eder. Sıçan anterior krural kompartmanındaki deneyler, enjeksiyon sonrası uzun dönemde, BTX-A'nın azalmış aktif kuvvete ek olarak, kasıtsız (enjekte edilen kas için %23 daha dar bir kuvvet etkime aralığı ve %12 artan pasif kuvvetler) ve kontrolsüz etkiler (toksin sızması nedeniyle kompartman kaslarında benzer etkiler) yarattığını göstermiştir. BTX-A maruz kalan kaslarda kolajen içeriği artışına da (birkaç kat) yol açmaktadır ki bu artan pasif kuvvetleri açıklar ve ayrıca aktif kuvvetleri de etkiler. Bu etkiler, tedavi hedefleriyle çeliştikleri için yüksek potansiyel klinik öneme sahiptir. Özellikle, BTX-A'nın bağ dokusu adaptasyonu üzerindeki etkilerini kontrol etmek, daha iyi spastisite yönetimi için kritiktir.

Anahtar Sözcükler: Epimüsküler miyobağdokusal kuvvet iletimi, Serebral palsi, Spastik kas, Kas kuvveti-eklem açısı/uzunluk özellikleri, Yürüme analizi, OpenSim, Botulinum toksin tip-A, Sıçan anterior krural kompartmanı, Kolajen.

TABLE OF CONTENTS

LIST OF FIGURES

LIST OF TABLES

LIST OF SYMBOLS

$^{\circ}$	degree
Δl_{mt}	muscle-tendon length change
μg	microgram
μl	microliter
ρ	Spearman's rank correlation coefficient
C	Celcius
cm	centimeter
g	gram
h	hour
Hz	hertz
kg	kilogram
kHz	kilohertz
mA	milliampere
mg	milligram
ml	milliliter
min	minute
mm	millimeter
mm^2	square millimeter
ms	millisecond
N	Newton
N	Normality
nm	nanometer
P	probability value
s	second
U	unit

LIST OF ABBREVIATIONS

Ant	Anterior
Abs	Absorption
ACL	Anterior Cruciate Ligament
ANOVA	Analysis of Variance
ASIS	Anterior Superior Iliac Spine
BF	Biceps Femoris
BTX-A	Botulinum Toxin Type-A
C7	Seventh Cervical Vertebrae
$C_{\text{mid-thigh}}$	Mid-thigh Circumference
CP	Cerebral Palsy
DHP	Distal Half Paralyzed
ECM	Extracellular Matrix
EDL	Extensor Digitorum Longus
EHL	Extensor Hallucis Longus
EMFT	Epimuscular Myofascial Force Transmission
Ext	Extension
F_a	Active muscle force
F_{GRA}	Gracilis muscle active force
$F_{\text{GRA\_passive}}$	Gracilis muscle passive force
F_p	Passive muscle force
F_{ST}	Semitendinosus muscle active force
$F_{\text{ST\_passive}}$	Semitendinosus muscle passive force
Flx	Flexion
GC	Gait Cycle
Gen	Generation
GMFCS	Gross Motor Functional Classification System
GRA	Gracilis
HA	Hip Angle

KA	Knee Angle
l_{range}	Length Range of Active Force Exertion
LSE	Longer Sarcomere Effect
L_{thigh}	Thigh Length
MAS	Modified Ashworth Scale
MHP	Middle Half Paralyzed
MTS	Modified Tardieu Scale
MTU	Muscle-Tendon Unit
PA	Popliteal Angle
RF	Rectus Femoris
PHP	Proximal Half Paralyzed
Pos	Posterior
SD	Standard Deviation
SM	Semimembranosus
ST	Semitendinosus
TA	Tibialis Anterior
TD	Typically Developing

1. INTRODUCTION

1.1 Related Literature

1.1.1 Skeletal Muscle

Skeletal muscle, also called voluntary muscle due to its controllable function, is the motor that generates force and maintains body posture or produces motion. A better understanding of the biomechanical characteristics of muscular tissues and establishing their relationship with the joint movements are quite necessary to explain the restricted joint mobility observed in patients with movement disabilities, and thus to achieve the optimal treatment outcomes for them.

1.1.1.1 Anatomy and Physiology. The cell of muscle tissue is the muscle fiber, each of which contains hundreds to thousands of units of myofibrils roughly aligned parallel to the muscle fiber itself. Repeating subunits arranged end to end along the myofibril is referred to as a sarcomere, which is the basic functioning structure of a muscle, i.e., force-generating contractile elements within a muscle. Besides, like all tissue, the composition of muscle is not solely of cells, but an extracellular space between them is also present, namely extracellular matrix (ECM). Muscle fibers embedded in the ECM create a composite tissue in which cells are allowed to work and resist extension. The most abundant protein found in the ECM is collagen. Collagen fibers running in several directions create a complex network of muscular connective tissue in which muscle cells are functioning. Connective tissue sheets surround the various divisions of the muscle (i.e., the muscle fibers are surrounded by endomysium and form muscle bundles, namely fascicles; fascicles and their surrounding perimysium further form the muscle itself as they come together; the muscle is enveloped by the epimysium, which is continuous with the endomysial-perimysial stroma) and they are all linked together indicating continuity within intramuscular connective tissues (Figure 1.1).

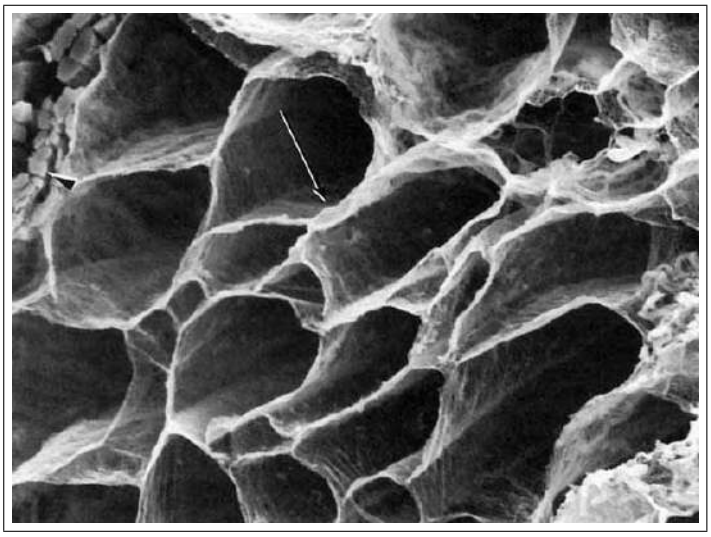

Figure 1.1 Scanning electron micrograph of the transversely cut surface of the collagenous stroma of the bovine skeletal muscle from which muscle fibers were removed [1]. The figure shows the continuous network of the endomysium (arrow) and the perimysium (arrowhead) surrounding tubular cavities within which muscle fibers operate.

The unique characteristic of muscular tissues is converting the chemical energy into mechanical energy (i.e., transforming the electrical signal into an endurance, balance, or movement incident) through a sequence of events, i.e., excitation-contraction coupling. Even though numerous phases and several specific proteins are needed for this process to occur, the initial step is the generation of an action potential in the motor neuron that innervates the muscle fibers to contract. The message from the motor neuron must then be passed to the muscle fiber through the neuromuscular junction. At the neuromuscular junction, the process termed exocytosis allows the release of acetylcholine by motor neurons into the synaptic cleft, that binds to receptors in the motor endplate, and this process ultimately causes muscle fibers to contract because of the change in the electrical potential of the sarcolemma (i.e., muscle membrane) it causes. Therefore, the discharge of acetylcholine-containing vesicles at the neuromuscular junction by exocytosis is essential for signal transmission, since without that muscle fibers cannot be physiologically activated.

Once the signal is taken, the muscle must contract to produce force. Contraction results from the formation of cross-bridges between the contractile proteins actin and myosin, through sliding of the actin chains on the myosin chains within the sarcomere.

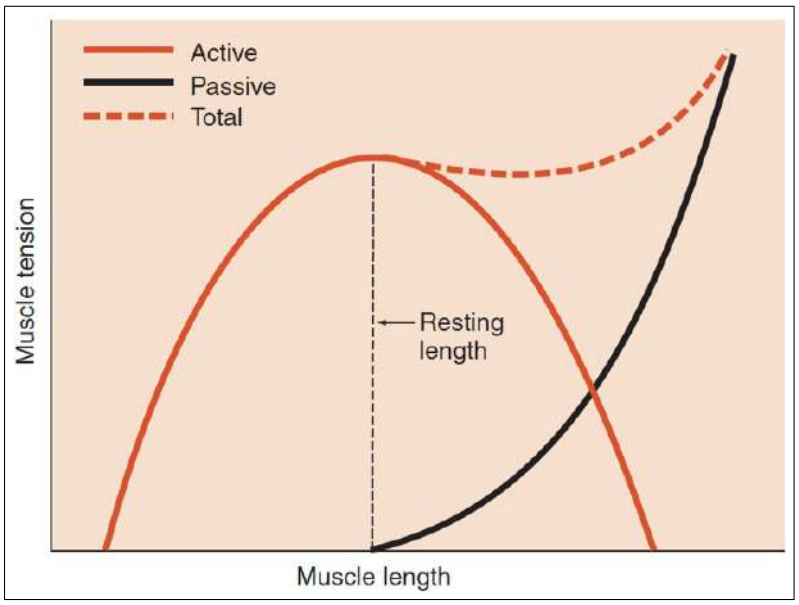

Figure 1.2 Muscle length-force relationship [2]. The passive and active forces are due to the non-contractile and contractile components, respectively. The total muscle force is the sum of the passive and active forces. Muscle passive force is usually negligible in the middle portion of the range of motion but increases as the muscle stretched such that at the end of the range it is dramatically elevated. The mechanical behavior of an activated muscle includes three regions: The ascending and descending limbs represent the muscle's decreasing active force output and are observed during movements that require a muscle to shorten considerably and to elongate beyond the resting length, respectively. The plateau region represents the optimum muscle force region, observed typically in the midrange of the anatomical range of motion.

Contraction of a whole muscle is the sum of singular contraction events occurring within the individual sarcomeres. Therefore, the arrangement of the skeletal muscles, with their attachments to bones by tendons allows the contraction of a sarcomere to move a bone eventually. In this process, numerous factors affect the ability of the muscle to create force (e.g., fiber length and distribution of its types, number of sarcomeres in series and in parallel, muscle physiological cross-sectional area, etc.), including the length of the muscle. The force a muscle can create has both active and passive sources. The active state forces are modulated by the behavior of the sarcomeres as mentioned, whereas the passive state forces come from the elastic properties of the noncontractile components of the muscle-tendon unit. When a muscle is passively lengthened, the muscle resists the lengthening. This resistance is thought to result from the stiffness in the noncontractile parts of the muscle (tendon, endomysium, perimysium, and epimysium) as well as the protein titin. Muscle passive force is a significant factor affecting movement at the extremities of joint range of motion. Figure

1.2 demonstrates the length-force characteristics of a whole healthy muscle. Additional to the architecture of the muscle itself, the ratio of contractile tissue to connective tissue in the muscle is an important factor determining the muscle's response to stretch as well [3].

1.1.1.2 Force Transmission Mechanisms. Force produced through a cascade of events needs to be transmitted from the interior of muscle fibers through the sarcolemma and ultimately onto the skeleton to maintain the body balance and to move the body parts. The older and most recognized approach of how forces are transmitted from the sarcomere to the bony skeleton is via the *myotendinous force transmission*. Force is assumed to be transmitted from a sarcomere to another connected in series, thereby transmitted from the muscle fiber to the tendon in the myotendinous junction. This in-series force transmission viewpoint roughly accepts muscles as independent actuators each of which is connected to the skeleton at their origin and insertion, and forces of all serially attached sarcomeres being as equal. Yet, today's literature points to additional pathways of force transmission arranged in parallel to the myotendinous path of force transmission to the bone, namely *myofascial force transmission*. These two different types of force transmissions describing the direct and inverse pathways, respectively, are simply distinguished whether the force is transmitted through the tendons or fasciae.

Myofascial force transmission [4] can be divided into two categories: *intra-* and *epimuscular myofascial force transmissions*. Transmission of force generated within the sarcomeres through trans-sarcolemmal molecules of the muscle fiber via the hierarchical intramuscular domain of the endomysial tubes, and the perimysial and epimysial tunnels [1, 5, 6], within which the muscle fibers and fascicles and also the whole muscle functioning is named intramuscular myofascial force transmission [4, 7, 8]. Besides, epimuscular myofascial force transmission (EMFT) is defined as the transmission of forces generated by a muscle to the skeleton via connective tissue linkages [7, 9, 10]. For such a force transmission to occur between a muscle and its surrounding tissues, the force must be passed beyond its outer limits (i.e., epimysium), which explains the

name given to the phenomenon. EMFT, therefore, refers to the force transmission from muscle to the bones by pathways other than the muscular origin and insertion, i.e., bypassing the myotendinous pathway [11]. Accordingly, the main characteristic effect of EMFT is the unequal forces exerted at the proximal and the distal ends (origin and insertion, respectively) of a muscle [11–17]. Another feature of a muscle involved in EMFT is that the relative position of a muscle varies its force due to the possible alterations in length, direction, and stiffness of connections with its surrounding muscular and non-muscular structures, even though the muscle itself is kept at constant length [13, 18–21]. EMFT is further distinguished as *inter-* and *extramuscular myofascial force transmissions*. Intermuscular myofascial force transmission [7, 14] defines the direct force transmission between two neighboring muscles via the continuous connective tissue along the full lengths of their interface, whereas extramuscular myofascial force transmission [7, 22] describing the force transmitted from the epimysium of a muscle to an adjacent non-muscular structure (i.e., neurovascular tracts and the compartmental connective tissues, which two are also connected to each other through muscular stroma).

1.1.2 Spastic Muscle Mechanics of Patients with Cerebral Palsy

Cerebral palsy (CP) describes a group of permanent motor disorders that are attributed to the damage to the central control system in the immature brain [23, 24]. Although the brain lesion, causing the neurological condition, is not progressive, it results in secondary muscle pathology due to abnormal motor control, which persists and does progress through the lifespan [25]. Therefore, the abnormality in motor control of CP leads to a disorder of posture and movement, causing functional limitations.

Patients with a spastic form of CP, by definition, have an increased velocity-dependent resistance to stretch [26]. Thus, hypertonia (i.e., increased muscle tone) is described as the central feature of spastic muscles [27]. Such persistently increased resistance to stretch [28] results in a sustained shortened state of the spastic muscle, causing contracture [27, 29]. Contracture adaptation of the muscles is associated with

an elevated joint and muscle stiffness [30–34] and a limited active and passive joint range of motion [35–37]. Patients with CP show gait disorders including additional to pathological hip and ankle conditions, crouch gait [38], and knee flexion deformity [39, 40]. However, the underlying mechanisms of the pathological joint condition observed in them are not clear. Moreover, although numerous structural changes for spastic muscles have been reported, the relationship of muscle level characteristics with the patients' gait patterns could not be explained yet.

Remarkably, joints being forcefully kept in a flexed position [41] mechanically indicate high force production of spastic flexor muscles in the active state. Using the intraoperative force measurement technique developed by Yucesoy et al. [42], previous studies [43–45] showed that the individual activations of main spastic knee flexor muscles (Figure 1.3A) are not representative of the mechanics of the pathology (i.e., the muscle produces only a small portion of its maximal force capacity in flexed knee positions, therefore no supreme force production at flexed joint positions in response to activation and no narrow operational joint range of force exertion were found). Moreover, the knee joint angle-muscle force characteristics of these individually activated spastic muscles have shown qualitative similarities with the previously reported forces of a healthy human muscle [42]. Still, testing of active force production capacities of thigh knee flexors for the whole operational joint range of motion yield a notable observation: Spastic gracilis (GRA) has the greatest capacity followed by the semitendinosus (ST) ascribable to non-zero GRA forces during the entire excursion and ascending portion of knee joint angle-muscle force curve which is wider than the one of semimembranosus (SM). Hence, focusing primarily on the activities of the spastic ST and GRA may be more useful to explain the pathology. However, obviously, the high flexor forces that limit knee extension in CP could not be ascribed to individual contributions of the knee flexors.

Notably, the study of Ates et al. [46] in which spastic GRA muscle forces were measured at specific knee joint angles, both when activated alone and also simultaneously with its antagonist muscle showed some remarkable mechanical features in co-activation condition, representing the pathology observed in the knee joint (i.e., high

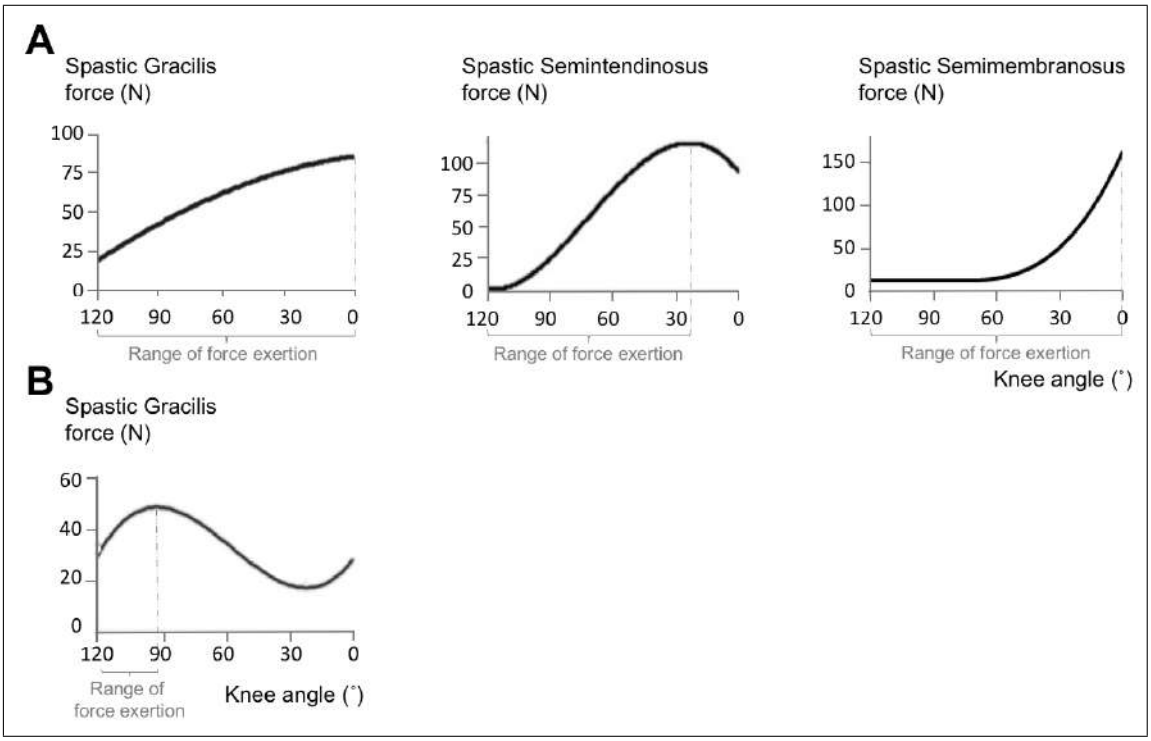

Figure 1.3 Selected typical knee joint angle-muscle force curves of spastic muscles in the lower extremity. Muscular force characteristics of (A) individually activated spastic gracilis, semitendinosus, and semimembranosus muscles and of (B) spastic gracilis co-activated with its antagonist, vastus medialis is shown. The figure is prepared based on [43–46].

active resistance capacity to stretch in flexed knee positions and narrow operational joint range of force exertion) (Figure 1.3B), although its selective stimulation did not lead those overall mechanics. In addition to these human studies, the previous model and animal studies also showed that EMFT can change force amplitude [13,14,18,47–49] and the length range of force exertion of a muscle [17, 50]. In spastic CP, this has been suggested as a factor affecting limited joint movement [7, 10]. Yet, how EMFT between synergist and/or antagonist muscles alter activated spastic muscle's mechanical behavior for the whole range of motion, and how such possible effects are clinically relevant to the patients' gait remain unknown. Moreover, spasticity clearly denotes the passive muscle stretch in the relaxed state, and therefore spastic muscle's passive forces are considered to be high. But, despite its major importance, the assessment of spastic muscle passive forces directly at the tendon has not been done. Thus, the current literature has missed knowledge and a better understanding of spastic muscle mechanics needs further examination.

1.1.3 Botulinum Toxin Type-A in the Management of Spasticity

As of yet, no cure is available for spastic CP, that is why the disability continues throughout the lifespan. The current approaches used in spasticity management aim to improve musculoskeletal functioning by preventing the development of fixed contractures and they are diverse, consisting of physiotherapy, followed by medical (oral or injectable agents) and orthopedic surgical management. These techniques are aimed to not only simply govern the spasticity (i.e., to reduce tone and to prevent contracture) but also improve the joint function [51–53].

A widely used technique for the management of spasticity arising from CP [54–56] is the injection of botulinum toxin type-A (BTX-A). The botulinum toxins are protein exotoxin products of the bacterium Clostridium botulinum [57]. Of the seven major serotypes of botulinum toxin (BTX-A to BTX-G) with varying properties (e.g., muscle-weakening efficacy, duration of action, and target protein), BTX-A has been introduced as optimum for long-term clinical use [58, 59]. Therefore, the focal intramuscular injection of BTX-A has currently a major role in the management of CP [60] and in delaying the need for surgical intervention. The toxin temporarily preventing the discharge of acetylcholine-containing vesicles at the neuromuscular junction by exocytosis results in presynaptic blocking in signal transmission, and thus causes muscle paralysis [61–66]. With inhibited acetylcholine release, muscle fibers cannot be physiologically fully activated [67], and this is what happens with focal BTX-A injections. A consequence is decreased muscle tone [68, 69] which mechanically implies a limited muscular force production capacity. Therefore, BTX-A treatment ultimately aims at increasing joint range of motion by reducing the muscle's elevated resistance in the joint.

There are studies that demonstrated the short-term effectiveness of BTX-A in reducing spasticity [70] and muscle tone [71], increasing joint range of motion [72], and improving gait pattern [73]. However, experiments in the rat anterior crural compartment have shown acutely that BTX-A has very complex effects (e.g., Yucesoy et al. [74] showed length-dependent reductions in muscle's active force). For the injected tibialis

anterior (TA) muscle in particular, although BTX-A aimed to widen the length range of the force exertion (l_{range}), it did not provide any improvement acutely, however, did elevate the injected TA muscle's passive forces [74]. Moreover, BTX-A leakage into the adjacent muscles [75], into synergistic muscles of a compartment [74, 76–78] and even across antagonistic compartments [79] have been reported in several animal studies. Such spread resulted in reduced forces [75, 80] and altered length-force characteristics (i.e., decreased l_{range}, increased passive forces, and elevated intramuscular collagen content) of also the non-injected muscles [74, 76, 78, 79]. Remarkably, some of these acute effects conflict with the expected BTX-A benefits. Even worse is that finite element modeling of the time course of BTX-A treatment predicted that such unintended adverse effects of BTX-A may get more pronounced in the long term because of the continuing elevated stiffness of the exposed muscles' ECM [81]. Since muscle exposed to BTX-A is still the motor for movement, understanding the mechanical and structural changes it creates, in the long run, deserves major attention.

1.2 Outline of the Thesis

1.2.1 Aims

The main themes of this thesis were the investigation of the relationship between the mechanical characteristics of spastic muscles and the impaired joint motion in order to shed light on the underlying mechanisms of pathology observed in patients with cerebral palsy (CP) and testing the effectiveness of the local application of Botulinum toxin type-A (BTX-A) in the management of spasticity. Additionally, the determinant role of epimuscular myofascial force transmission (EMFT) arising from intermuscular mechanical interactions was investigated for both human and animal limb muscles, and their clinical relevance was revealed. Specific aims were:

1. to show the effects of inter-synergistic EMFT on the overall mechanical characteristics of a primary knee flexor muscle, the activated spastic semitendinosus.

2. to directly measure the spastic muscles' passive forces for the first time, and further to identify the activated and passive muscle mechanical characteristics which are directly relevant to the pathological movement of the patients via clinical gait analysis.

3. to assess the muscle-tendon unit length change of the patients during gait in comparison with the typically developing children and to obtain the novel muscle-tendon unit length-force characteristics for spastic muscles.

4. to test if previously shown short-term adverse BTX-A effects (i.e., narrower length range of force exertion, increased passive forces, and increased extracellular matrix collagen) are persistent in the long term, in an animal model.

For these purposes, experiments were carried out on humans (muscle force measurements during surgery, 3D gait analyses, musculoskeletal models) and animals (muscle force measurements, histological testing).

1.2.2 Overview

The objectives of the thesis addressed in the following chapters are

Chapter 2 *"Effects of Inter-synergistic Mechanical Interactions on the Mechanics of Activated Spastic Semitendinosus Muscle"* addresses the first aim by performing intraoperative experiments. The effects of EMFT occurring due to co-stimulation of synergistic muscles of the upper leg are investigated, and the altered mechanics of activated spastic semitendinosus muscle (i.e., substantially increased active forces, whereas unchanged length range of force exertion and active stiffness of the muscle) are revealed.

Chapter 3 *"Passive and Active State Mechanics of Spastic Gracilis: Intraoperative Experiments and Gait Analyses"* provides spastic muscle's passive forces measured directly for the first time in patients with CP and combining intraoperative experiments with the patients' gait analysis indicates that active state muscular mechanics,

rather than passive, of spastic gracilis, present a capacity to limit joint movement in CP, the effects of which elevate due to intermuscular mechanical interactions.

Chapter 4 *"Passive and Active State Mechanics of Spastic Semitendinosus: Intraoperative Experiments and Patient-Specific Musculoskeletal Models"* describes intraoperatively measured passive and active state forces of the spastic semitendinosus muscle and presents muscular characteristics in relation to the terminal swing, loading response, and mid/terminal stance phases of the patients' gait. As well as using the OpenSim software, novel spastic muscle-tendon unit length - muscle force data are obtained which indicates no strong correlation between shorter operational muscle length and muscular mechanics for spastic semitendinosus, but EMFT does cause significant muscle force increases.

Chapter 5 *"The Force-Length Relations of Spastic Knee Flexor Muscles, Semitendinosus and Gracilis"* presents muscle force characteristics and effects of EMFT on them, particularly concerning gait-relevant lengths of spastic semitendinosus and gracilis muscles. The musculoskeletal models developed based on gait analyses of patients and typically developing controls reveal shorter muscle-tendon unit lengths for the tested knee flexors in patients compared to those in control. By combining intraoperatively obtained spastic muscle active and passive force data with the patient-specific musculoskeletal models, the force characteristics of spastic muscles in lengths encountered within a gait cycle and how co-working of different muscles, thus EMFT, contribute to the patients' pathological gait are shown. Therefore, in Chapter 3, Chapter 4, and Chapter 5, the second and the third aims are addressed.

Chapter 6 *"Long-term Effects of Botulinum Toxin Type-A on Mechanics of Muscles Exposed"* addresses the fourth aim by conducting an animal experiment and reveals the effects of local application of BTX-A on not only the injected but also the non-injected rat muscles. Muscle mechanical test and intramuscular collagen content quantification resulted in that previously reported unintended acute BTX-A effects persist and advance in the long term which is with potential clinical importance.

In Chapter 7 the main findings of the thesis are summarized, and the conclusions are stated. Clinical implications of the study are discussed and recommendations for future research are made.

1.3 List of Publications and Awards Resulting from the Thesis

1.3.1 Journal Articles

1. "Long-term effects with potential clinical importance of botulinum toxin type-A on mechanics of muscles exposed", C. S. Kaya, E. O. Yılmaz, Z. D. Akdeniz-Doğan, and C. A. Yucesoy, *Frontiers in Bioengineering and Biotechnology*, Vol. 8, Article. 738, 2020.

2. "Intraoperative testing of passive and active state mechanics of spastic semitendinosus in conditions involving intermuscular mechanical interactions and gait relevant joint positions", C. S. Kaya, F. Bilgili, N. E. Akalan, and C. A. Yucesoy, *Journal of Biomechanics*, Vol. 103, Article. 109755, 2020.

3. "Intraoperative experiments combined with gait analyses indicate that active state rather than passive dominates the spastic gracilis muscle's joint movement limiting effect in cerebral palsy", C. S. Kaya, F. Bilgili, N. E. Akalan, Y. Temelli, F. Ates, and C. A. Yucesoy, *Clinical Biomechanics*, Vol. 68, pp. 151-157, 2019.

4. "Effects of inter-synergistic mechanical interactions on the mechanical behaviour of activated spastic semitendinosus muscle of patients with cerebral palsy", C. S. Kaya, Y. Temelli, F. Ates, and C. A. Yucesoy, *Journal of the Mechanical Behavior of Biomedical Materials*, Vol. 77, pp. 78-84, 2018.

1.3.2 Conference Proceedings

1. "Muscle length and muscle force characteristics in patients with spastic cerebral palsy are weakly correlated", C. S. Kaya and C. A. Yucesoy, The 29th Annual

Meeting of the European Orthopaedic Research Society (EORS), Rome, Italy. *The Bone & Joint Journal - Orthopaedic Proceedings*, Vol. 103-B, SUPP_13, 2021.

2. "Using intraoperative spastic muscle force-joint angle data to model muscle-length relation during patients' gait", C. S. Kaya and C. A. Yucesoy, The 28th Annual Meeting of the European Orthopaedic Research Society (Virtual EORS). *The Bone & Joint Journal - Orthopaedic Proceedings*, Vol. 102-B, SUPP_11, 2020.

3. "Muscle-tendon unit length-spastic muscle force data by combined intraoperative-musculoskeletal modelling work", C. S. Kaya and C. A. Yucesoy, The 29th Annual Meeting of the European Society for Movement Analysis in Adults and Children (Virtual ESMAC), 2020.

4. "Force Production Characteristics of Spastic Knee Flexor Muscles: Intraoperative Tests and Patient-Specific Musculoskeletal Models", C. S. Kaya, U. Can, and C. A. Yucesoy, Medical Technologies Congress. Kuşadası, Turkey, 2019.

5. "Animal experiments reveal long-term effects with potential clinical importance of Botulinum toxin type-A on mechanics of muscles exposed", C. S. Kaya, Z. D. Akdeniz-Doğan, and C. A. Yucesoy, The 28th Annual Meeting of the European Society for Movement Analysis in Adults and Children (ESMAC). Amsterdam, The Netherlands. *Gait & Posture*, Vol. 73, Suppl 1, pp. 120-121, 2019.

6. "Botulinum toxin type-A effects on active and passive forces of the muscles exposed in the long-term", F. Ates, C. S. Kaya, Z. D. Akdeniz-Doğan, and C. A. Yucesoy, XXVII Congress of the International Society of Biomechanics, held in conjunction with the 43rd Annual Meeting of the American Society of Biomechanics (ISB-ASB). Calgary, Canada, 2019.

7. "Previously reported unintended acute Botulinum toxin type-A effects persist also in the long-term", C. S. Kaya, E. O. Yılmaz, Z. D. Akdeniz-Doğan, and C. A. Yucesoy, The 25th Congress of the European Society of Biomechanics (ESB). Vienna, Austria, 2019.

8. "Passive and active state mechanics of spastic semitendinosus: intraoperative tests and gait analyses", C. S. Kaya, F. Bilgili, N. E. Akalan, and C. A. Yucesoy, The 25th Congress of the European Society of Biomechanics (ESB). Vienna, Austria, 2019.

9. "O 043 - Mechanics of spastic semitendinosus altered by intermuscular interactions elevate its contribution to pathological resistance against knee extension during gait", C. S. Kaya, F. Bilgili, N. E. Akalan, F. Ates, and C. A. Yucesoy, The 27th Annual Meeting of the European Society for Movement Analysis in Adults and Children (ESMAC). Prague, Czech Republic. *Gait & Posture*, Vol. 65, Suppl 1, pp. 88-89, 2018.

10. "Intraoperative experiments combined with gait-analyses reveal the dominant determinant of limited knee extension in patients with spastic cerebral palsy", C. S. Kaya, F. Bilgili, N. E. Akalan, and C. A. Yucesoy, The 9th International Biomechanics Congress. Eskişehir, Turkey, 2018.

11. "Comparison of short-term and long-term effects of BTX-A on mechanics of the rat tibialis muscle", E. O. Yılmaz, C. S. Kaya, Z. D. Akdeniz-Doğan, and C. A. Yucesoy, The 9th International Biomechanics Congress. Eskişehir, Turkey, 2018.

12. "Pathological knee joint condition in children with cerebral palsy is associated with the active state muscular mechanics rather than passive", C. S. Kaya, F. Bilgili, N. E. Akalan, Y. Temelli, F. Ates, and C. A. Yucesoy, The 42nd Annual Meeting of the American Society of Biomechanics (ASB). Rochester, Minnesota, USA, 2018.

13. "Active (not passive) state mechanics and intermuscular interactions determine the pathological knee joint condition in cerebral palsy for gait relevant knee positions", C. S. Kaya, F. Bilgili, N. E. Akalan, Y. Temelli, F. Ates, and C. A. Yucesoy, The 8th World Congress of Biomechanics (WCB). Dublin, Ireland, 2018.

14. "Co-Activation of other muscles elevates spastic gracilis forces in agreement with the typical limited knee extension condition in CP", C. S. Kaya, F. Bilgili, Y.

Temelli, and C. A. Yucesoy, The 25th Annual Meeting of the European Orthopaedic Research Society (EORS). Munich, Germany, 2017.

15. "Effects of co-stimulating other muscles on mechanics of spastic gracilis at gait specific joint positions", C. S. Kaya, F. Ates, Y. Temelli, and C. A. Yucesoy, The 23rd Congress of the European Society of Biomechanics (ESB). Seville, Spain, 2017.

16. "The distal spastic semitendinosus tendon is not the right site to monitor high forces that limit knee extension in cerebral palsy", C. S. Kaya, Y. Temelli, F. Ates, and C. A. Yucesoy, The 8th National Biomechanics Congress. Ankara, Turkey, 2016.

17. "Spastic semitendinosus muscle of cerebral palsy patients tested intra-operatively does get affected by epimuscular myofascial force transmission but shows no abnormal mechanics", C. A. Yucesoy, C. S. Kaya, Y. Temelli, and F. Ates, The XXI Congress of the International Society of Electrophysiology and Kinesiology (ISEK). Chicago, Illinois, USA, 2016.

1.3.3 Awards

1. Best Oral Biomechanics Presentation Award, The 28th Annual Meeting of the European Orthopaedic Research Society (Virtual EORS), 2020.

2. Audience Best Paper, 3rd place award, The 28th Annual Meeting of the European Society for Movement Analysis in Adults and Children (ESMAC). Amsterdam, The Netherlands, 2019.

3. Travel Award, The 28th Annual Meeting of the European Society for Movement Analysis in Adults and Children (ESMAC). Amsterdam, The Netherlands, 2019.

4. Travel Award, The 25th Congress of the European Society of Biomechanics (ESB). Vienna, Austria, 2019.

5. Doctoral Student Presentation Competition, Finalist, The 42nd Annual Meeting of the American Society of Biomechanics (ASB). Rochester, Minnesota, USA, 2018.

2. EFFECTS OF INTER-SYNERGISTIC MECHANICAL INTERACTIONS ON THE MECHANICS OF ACTIVATED SPASTIC SEMITENDINOSUS MUSCLE

2.1 Introduction

Cerebral palsy (CP) is a movement disorder that occurs secondary to static lesions in the immature brain [23]. In patients with CP, patients increased resistance to stretch [28] results in a sustained shortened state of spastic muscle [27]. This causes soft tissue contracture [27,32,34], joint stiffness [33,82] and limits joint movement [37]. However, muscle is the motor for movement, and patients with CP show muscle hypertonicity [29, 83]. Upper extremity joints being forcefully kept in a flexed position [41] indicate high force production of spastic flexor muscles in active state. Patients with CP show gait disorders including additional to pathological hip and ankle conditions, crouch gait [38], and spastic knee flexion deformity [39, 40]. Besides, elevated stiffness of spastic muscles has been reported in passive state (e.g., [34]) and is considered highly plausible in active state. Therefore, the amplitude of activated spastic muscle's force, stiffness, and the range of its active force exertion are central to the joint movement limitation. However, studies quantifying such parameters in intraoperative experiments are sparse [44, 84–86]. Moreover, daily activities involve simultaneous activation of several muscles such as co-activation of the semitendinosus (ST) with the semimembranosus (SM) and gracilis (GRA) during walking and sit-to-stand [87–89]. Yet, the effects of added stimulation of synergistic muscles on spastic muscle's mechanical behavior are unknown.

Connective tissue linking muscle bellies via e.g., collagen-reinforces neurovascular tracts allow epimuscular myofascial force transmission (EMFT) between synergistic muscles [9, 90]. EMFT can change the force amplitude of a muscle held at constant length in response to imposed length changes or activation of its synergists [13,14,18,46–49]. EMFT effects rely on the connections between the muscle fibers

and the extracellular matrix (ECM) along their full peripheral lengths [91], which can transmit force [4,6]. Shear linkage was shown to exist between them [1,5,92,93]. Consequently, forces originating from the synergistic muscles transmitted onto the ECM can affect the force production of a sarcomere by manipulating its length [90]. Heterogeneity of sarcomere lengths across muscle fibers affects muscle optimum length [16,17,50]. Therefore, inter-synergistic EMFT can change a muscle's length range of force exertion. In spastic CP this can be a factor affecting the limited joint movement [7, 10]. The current understanding of tissue adaptations in CP indicates elevated ECM stiffness [34]. Kreulen et al. [94] showed that the epimuscular connections of tenotomised spastic flexor carpi ulnaris limit its shortening in response to stimulation. Therefore, also these connections must be highly stiff, and overall, stiff muscle-related connective tissues in CP suggest that EMFT effects can be more pronounced than in healthy individuals. This not only can limit the passive joint movement but also can alter activated spastic muscle's mechanical behavior unfavorably for mobility, which needs to be tested.

Intraoperative testing allows measuring forces of activated knee flexor muscles directly at the tendon [42]. Employing this methodology, the aim was to test the following study hypotheses: added activation of SM and GRA muscles of patients with CP changes (1) forces, (2) stiffness, and (3) joint range of force exertion of activated spastic ST due to inter-synergistic EMFT.

2.2 Materials and Methods

Surgical and experimental procedures, in strict agreement with the guidelines of the Helsinki declaration, were approved by a Committee on Ethics of Human Experimentation at Istanbul University, Istanbul. The patients and/or their parents gave informed consent to the work.

Table 2.1
Patient characteristics. L_{thigh} = thigh length; $C_{mid\text{-}thigh}$ = mid-thigh circumference. GMFCS = Gross Motor Functional Classification System. GMFCS level II: patients in need of physical assistance for walking in order to avoid a fall and rapid build-up of fatigue and support for sitting and standing. GMFCS level IV: patients in need of additional aids including a wheelchair or a body support walker for mobility. PA = popliteal angle (i.e., the angle between hip and knee at the hip in 90° flexion): mean (SD) = 76.7° (12.5°).

Patient	Limb	Age	L_{thigh} (cm)	$C_{mid\text{-}thigh}$ (cm)	GMFCS	PA (°)
1	1	5	23.0	26.5	IV	70
1	2	5	23.0	26.0	IV	65
2	3	5	23.0	29.0	IV	70
2	4	5	23.0	28.5	IV	50
3	5	6	27.0	30.5	II	75
3	6	6	27.0	29.0	II	70
4	7	8	27.0	28.0	IV	90
4	8	8	26.0	27.0	IV	90
5	9	17	39.0	39.0	II	90
6	10	15	41.0	39.5	II	80
7	11	5	22.5	24.0	IV	90
7	12	5	22.0	23.0	IV	80

2.2.1 Study Design

Seven patients (all male: at the time of surgery, mean age 8 years 9 months, range 5-17 years, standard deviation 5.1 years) diagnosed with spastic CP, however, with no prior remedial surgery, were included in the study. The Gross Motor Functional Classification System (GMFCS) was used to assess the mobility of the patients. Those who participated attained scores of at least level II, with four of them attaining level IV (Table 2.1). The popliteal angle (PA) is a key measurement made in the clinic to characterize the passive range of motion. Compared to conventions for abnormality (i.e., PA$>$ 50° [95]), the patients' PA values (between 50° and 90°) show their limited knee joint mobility. Overall, pre-operative clinical examinations indicated a severely limited range of knee joint motion and led to a decision that all patients required remedial surgery including the release of hamstrings. Six of the patients were operated on bilaterally. For five of them, separate experiments were performed on both legs. For the remainder patients, only one leg was experimented with due to time limitations imposed by subsequent multilevel surgery. Therefore, a total of twelve knee angle (KA)-ST muscle force F_{ST} data sets were collected. The spastic ST was stimulated exclusively (condition I), and simultaneously with its synergistic muscles GRA and SM (condition II) to assess the effects of inter-synergistic EMFT.

2.2.2 Surgical and Experimental Procedures

The patients received general anesthesia, and no muscle relaxants or tourniquets were used. All experimental preparations and data collection were performed within 30 minutes (the maximal study duration allowed by the ethics committee), after routine incisions to reach the distal ST tendon, and before any other routine surgical procedures. Using a scalpel blade (number 18), a longitudinal skin incision was made immediately above the popliteal fossa.

After cutting the adipose tissue, the distal ST tendon was exposed. Subsequently, a buckle force transducer (TEKNOFIL, Istanbul, Turkey) (Figure 2.1A) was

mounted and fixed over the tendon. The key transducer characteristics include S-shape; dimensions: width= 12 mm length= 20 mm and height= 9 mm; maximal force range= 400 N; for test range 0-200 N: accuracy< 3%, (<0.19% below 100 N); resolution= 0.62 N and high linearity (R^2= 0.99963, peak nonlinearity= 1.31%). Note that prior to each experiment, the force transducer was (i) calibrated using bovine tendon strips (with rectangular cross-section, dimensions 7x2 mm^2 representative of that of the ST distal tendon) and (ii) sterilized (using gas sterilization at maximally 50 °C).

The patient was positioned using an apparatus composed of three components (Figure 2.1B): (i) The *upper leg component*, (ii) the *knee angle adjuster*, and (iii) the *lower leg component*. The upper leg component was secured with two fixtures to the slot of the surgery table. The knee angle adjuster combining the upper and lower leg components allowed setting the KA and fixing it during the contractions. A circular slot machined in the knee angle adjuster and angles marked on it (in 0.5° increments) allowed adjusting the KA to experimental knee joint positions. The *leg holders'* position is adjustable on the upper leg component. This allows supporting the upper leg and aligning it based on the following: (a) the hip joint position was set to 0° both in sagittal and frontal planes. (b) the axis of the knee joint rotation corresponded to the center of the rotation of the knee angle adjuster. The *ankle holder*, the position of which is adjustable on the lower leg component allowed supporting the lower leg. The leg holder and ankle holder were sterilized components. The non-sterile remainder parts were covered with sterile fabric before an antiseptic agent was applied to the skin and the patient's leg was positioned and secured to the apparatus.

Isometric spastic F_{ST} was measured at various muscle lengths imposed by manipulating the KA. Earlier animal experiments indicated that previous active contraction of the muscle at long length affects its forces measured at short length [12]. Such length history effects were also shown in human [42]. Taking this into account, before acquiring data, muscle-tendon complexes and their epimuscular connections were preconditioned by isometric contractions, alternatingly at extended and flexed knee positions, until spastic ST forces at flexed knee position were reproducible. In addition, the measurements for data acquisition were started in a highly flexed knee (120°),

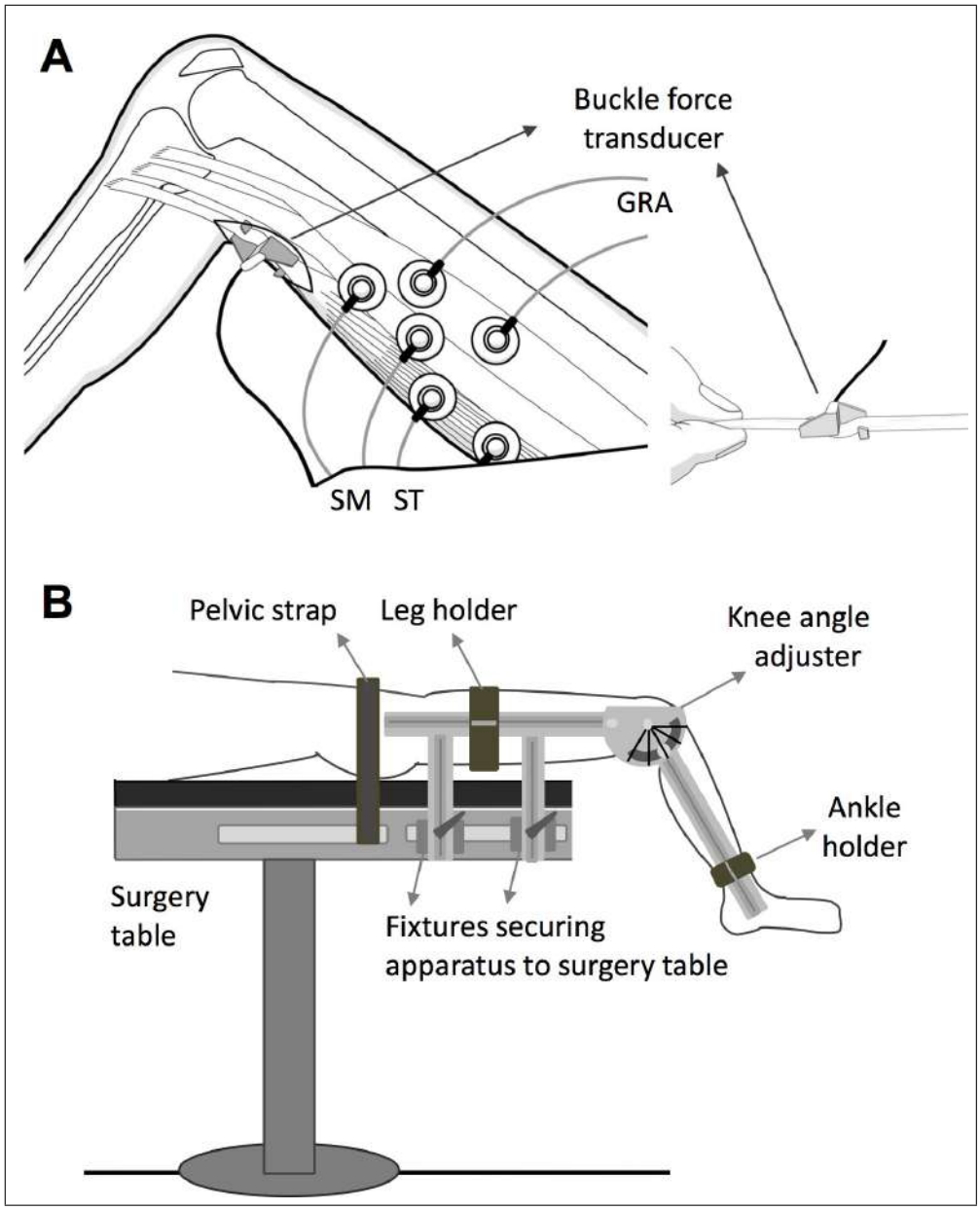

Figure 2.1 Intraoperative muscle mechanics experimental setup used for measurement of spastic ST forces at the neutral hip position. (A) Illustration of how the buckle force transducer is mounted over the target muscle's tendon. Inset shows the transducer mounted over a tendon strip. The three pairs of skin electrodes placed over the ST, GRA, and SM muscles are also illustrated. (B) An apparatus designed for intraoperative tests in lower extremities is composed of three components: (i) The *upper leg component* incorporating a leg holder, which has an adjustable position on it allows fixing the hip angle (to 0° both in the sagittal and frontal planes). This component is secured to the slot of the surgery table via fixtures. (ii) The *lower leg component* incorporating an ankle holder that has an adjustable position on it supports the lower leg. (iii) The *knee angle adjuster* links together the upper and lower leg components and allows setting the knee angle and fixing it during a contraction.

and the muscle length was manipulated by extending the knee by 30° increments at 120°, 90°, 60°, 30° and 0° (full knee extension). Testing was completed for both conditions before attaining a different knee angle. After each contraction, the muscle was allowed to recover for 2 minutes. A data acquisition system (MP150WS, BIOPAC Systems, CA, USA, 16-bit A/D converter, sampling frequency 40 kHz) was used with an amplifier for the transducer (DA100C, BIOPAC Systems, CA, USA).

Three pairs of gel-filled skin electrodes (EL501, BIOPAC Systems, CA, USA) were placed on the skin, over the spastic ST, GRA, and SM muscle bellies. Muscle bellies were located by palpation. The reference electrodes were placed as distal as possible to the incision with their positions having an offset. The location of the second electrode was determined according to the following procedure: The minimum center-to-center inter-electrode distance was ensured to be 30 mm for successful electrode function [96] and muscle excitation [97]. At KA= 120°, a tentative location for the second electrode was determined accordingly. The contraction responses were assessed in response to twitch stimuli evoked separately for each muscle. Successful stimulation of spastic ST was monitored from the measured force, and leakage of current into other muscles than the one stimulated was controlled by palpation. This was repeated at, KA= 60° and 0°. If necessary, the second electrode position was optimized by iteration.

A custom made, constant current high voltage source (cccVBioS, TEKNOFIL, Istanbul, Turkey) was used to impose supramaximal muscle stimulation (transcutaneous electrical stimulation with a bipolar rectangular signal, 160 mA, 50 Hz): two twitches were evoked which, after 300 ms, were followed by a pulse train for 1000 ms to induce a tetanic contraction and a subsequent twitch (see Figure 2.2 for superimposed examples of force-time traces for spastic ST muscle at five KAs).

In an additional test, in one patient outside the study group, but with similar characteristics (13 years old, L_{thigh}= 36.0 cm, $C_{mid\text{-}thigh}$= 40.5 cm, GMFCS: II, PA= 60°), stimulation of spastic ST selectively was confirmed. An additional buckle force transducer was mounted over the spastic GRA tendon and in response to stimulation of spastic ST using the protocol described above; forces of both muscles were measured

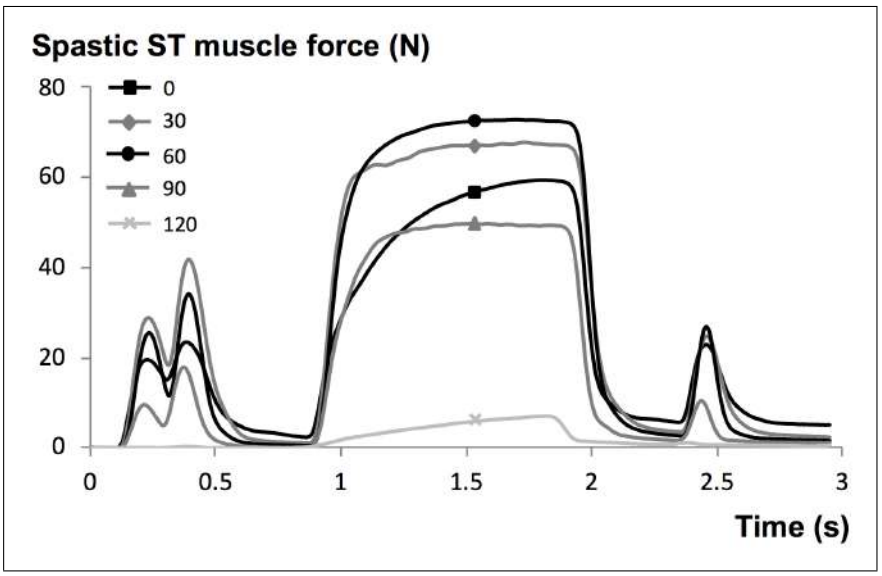

Figure 2.2 Typical examples of force-time traces for spastic ST muscle. Superimposed traces recorded for ST muscle at the five knee angles studied are shown.

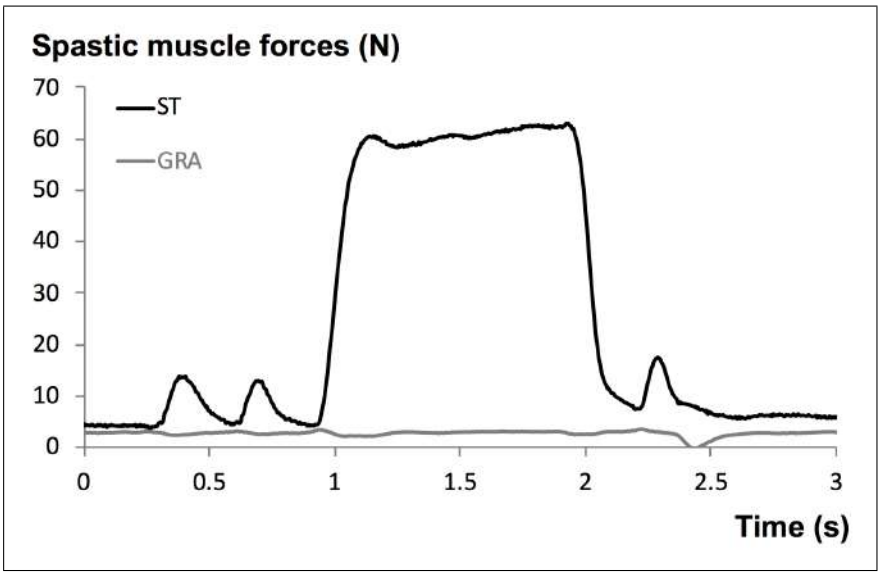

Figure 2.3 The force-time traces of spastic ST and GRA muscles obtained during the individual stimulation of ST.

simultaneously. Figure 2.3 exemplifies their force-time traces at KA= 60° showing no change in spastic GRA forces. This is valid also for other knee positions and indicates a lack of activation of this muscle. During the actual experiments, palpation was used to ensure the lack of possible contraction of spastic GRA and SM muscles.

2.2.3 Processing of Data

F_{ST} measured during a 500 ms period in the middle of the tetanus were averaged and recorded as muscle total force for each KA tested.

Using a least-squares criterion, KA-F_{ST} data were fitted with a polynomial function (Eq. 2.1).

$$F_{ST} = a_0 + a_1 \cdot KA + a_2 \cdot KA^2 + ... + a_n \cdot KA^n \tag{2.1}$$

a_0, a_1 ... a_n are coefficients determined in the fitting process.

The lowest order of the polynomials that still added a significant improvement to the description of changes of KA-F_{ST} data were selected using a one-way analysis of variance, ANOVA. The fitted KA-F_{ST} data for each condition were used to calculate the mean of ST forces and standard deviations per KA tested as well as in the calculation of the operational and hypothetical joint range of F_{ST} exertion.

2.2.4 Experimental Measures

The following key metrics were calculated to characterize the mechanical behavior of spastic ST: $ST_{Stiffness}$ i.e, stiffness of activated spastic ST muscle defined as the slope of the ascending limb of KA-F_{ST} curve represented by the KA range 90-30°; $KA_{FSTpeak}$ i.e., the KA at which the peak ST muscle force was exerted; Range-F_{ST} i.e., operational joint range of F_{ST} exertion defined as the KA range between $KA_{FSTpeak}$ and KA at which F_{ST} is the minimum within the experimental KA range. Range-

$F_{ST\_extrapolated}$ i.e., hypothetical joint range of F_{ST} exertion defined as the KA range between $KA_{FSTpeak}$ and active slack KA (the KA-F_{ST} curve was extrapolated linearly until F_{ST}= 0 N). Note that, Range-F_{ST} has clinical relevance, as it is determined from the actual knee positions tested during the experiment. However, Range-$F_{ST\_extrapolated}$ allows for a comprehensive characterization of the spastic muscle's mechanical behavior.

2.2.5 Statistical Comparisons Between Conditions

Two-way ANOVA for repeated measures (factors: KA and condition) was used to analyse the overall effects of inter-synergistic EMFT on KA-F_{ST} characteristics. Differences were considered significant at $P < 0.05$. If significant main effects and an interaction were found, Bonferroni post hoc tests were performed to further locate significant within-factor force differences.

The key metrics were used to assess specific aspects of the effects of inter-synergistic EMFT on spastic ST's mechanical behavior. Shapiro-Wilk test was used to check if the data are normally distributed. The key metrics calculated for each limb in both conditions were then compared using the paired-t test or Wilcoxon signed-rank test where appropriate. Differences were considered significant at $P < 0.05$.

Changes in KA-F_{ST} characteristics were used to test hypothesis 1. Changes in the key metrics $ST_{Stiffness}$ (hypothesis 2) and $KA_{FSTpeak}$, Range-F_{ST}, and Range-$F_{ST\_extrapolated}$ (hypothesis 3) were used to test the remainder hypotheses.

2.3 Results

Figure 2.4 shows KA-F_{ST} characteristics as the mean (SD) of ST forces of tested limbs as a function of KA. In condition I, the minimum F_{ST} is observed in the most flexed knee position. Subsequently, F_{ST} increases in response to added knee extension reaches a maximum, and decreases (e.g., F_{ST} = 3.1 N, 84.3 N, 78.0 N at KA= 120°, 15°,

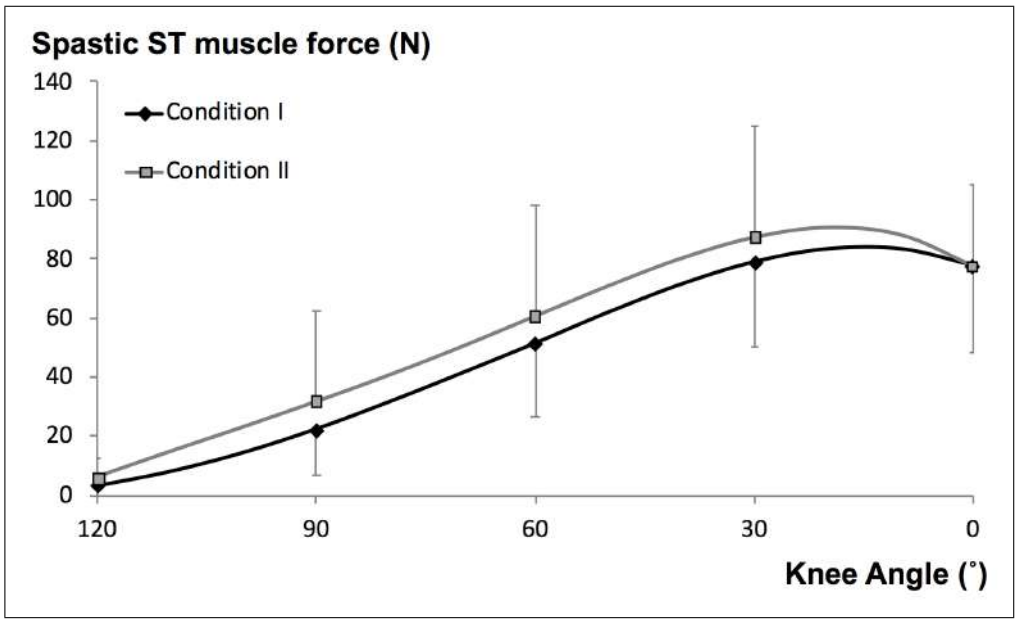

Figure 2.4 The mean (SD) of spastic ST forces of intraoperatively tested limbs per KA across the conditions tested. Spastic ST was activated alone (condition I) and simultaneously with its synergists GRA and SM (condition II).

and 0°, respectively). ANOVA (factors: KA and condition) showed significant main effects of both factors on spastic ST forces, but no significant interaction. In condition II, spastic F_{ST} increased on average by 33.3% compared to condition I. Therefore, hypothesis 1 is confirmed.

Table 2.2 shows the experimental metrics for each limb tested as well as the mean (SD) of these values for both conditions. For $ST_{Stiffness}$, $KA_{FSTpeak}$ and Range-F_{ST} the paired-t test and for Range-$F_{ST\_extrapolated}$ the Wilcoxon signed-rank test showed no significant differences between the two conditions. Therefore, study hypotheses 2 and 3 are rejected.

2.4 Discussion

Direct measurements of human muscle forces involve difficulties due to limited access to the tendons and technical challenges of measuring the tendon forces. This was done during remedial surgery of patients with CP, in the upper extremity (e.g.,

Table 2.2
The key metrics data for each limb tested. $ST_{Stiffness}$ = stiffness of activated spastic ST muscle; $KA_{FSTpeak}$ = the knee angle at which the peak ST muscle force was exerted; Range-F_{ST} = operational joint range of F_{ST} exertion i.e., the KA range between $KA_{FSTpeak}$ and KA at which F_{ST} is the minimum within the experimented KA range; Range-$F_{ST\_extrapolated}$ = hypothetical joint range of F_{ST} exertion i.e., the KA range between $KA_{FSTpeak}$ and KA at which F_{ST} is zero (the KA-F_{ST} curve was extrapolated linearly until F_{ST}= 0 N).

	Condition I				Condition II			
Limb	ST $_{Stiffness}$ (N/°)	KA $_{FSTpeak}$ (°)	Range - F_{ST} (°)	Range-$F_{ST\_}$ extrapolated (°)	ST $_{Stiffness}$ (N/°)	KA $_{FSTpeak}$ (°)	Range - F_{ST} (°)	Range-$F_{ST\_}$ extrapolated (°)
1	0.29	47	73	175	0.29	46	74	219
2	0.53	29	91	120	0.30	19	101	149
3	0.80	0	120	142	0.56	0	120	173
4	0.26	0	120	122	0.48	0	120	121
5	1.09	0	120	122	0.76	36	84	171
6	1.81	5	115	116	2.00	13	107	108
7	1.75	24	96	97	1.67	19	101	102
8	1.06	32	88	106	1.26	35	85	103
9	0.72	0	120	121	0.77	0	120	121
10	1.26	11	109	110	1.48	14	106	107
11	1.04	20	100	101	0.78	29	91	116
12	0.77	26	94	114	0.83	23	97	113
Mean	0.95	16.2	103.8	120.5	0.93	19.5	100.5	133.6
(SD)	(0.50)	(15.8)	(15.8)	(20.8)	(0.55)	(15.2)	(15.2)	(36.7)

[86,98]). Kreulen and Smeulders [99] measured forces of spastic flexor carpi ulnaris after releasing it from its insertion and obtained valuable data showing muscle force-length characteristics. Studies testing the effects of co-activation of several human muscles on muscular mechanics are even rarer. Previously, Ates et al. [44, 46] reported spastic muscle's potential to contribute to joint moment and range of motion in the lower extremities and tested effects of co-activation of an antagonistic muscle. A major novel contribution of the present study is that effects of added stimulation of its synergistic muscles on activated spastic ST muscle's mechanics were assessed and this yielded substantial force increases. This provides evidence for EMFT in patients with CP. However, the tested co-activation did not affect other characteristics of the spastic ST muscle's knee angle-force relationship.

The study hypotheses were based on possible inter-synergistic EMFT effects on spastic ST sarcomere lengths. Validation of that with data is difficult due to major technical challenges. However, elaboration on that is necessary to explain the present findings. Heterogeneity of lengths of sarcomeres arranged in series within muscle fibers was shown earlier by Huxley and Peachey [100]. Recent studies indicate that even within human muscles in vivo [101–103]. We anticipated that inter-synergistic EMFT can cause spastic ST sarcomeres to attain lengths favorable for force production, closer to their full myofilament overlap. Accordingly, for flexed joint positions prior to $KA_{FSTpeak}$, force increases of the activated spastic ST shown indicate less shortening of sarcomeres functioning in the ascending limb of their force-length curves. Beyond $KA_{FSTpeak}$, less lengthening of sarcomeres functioning in the descending limb can explain increased muscle force. On the other hand, we also anticipated shape changes of the KA-F_{ST} curves yielding elevated stiffness of activated spastic ST and decreased joint range of force exertion. Increased heterogeneity of sarcomere lengths across muscle fibers causes a shift of muscle's peak force to longer muscle lengths [50]. This increases the muscle's length range of force exertion and inter-synergistic EMFT can cause that [16, 17]. However, patients with CP show limited knee joint movement. Accordingly, if inter-synergistic EMFT is responsible for the narrow joint range of force exertion, we expected an opposite effect of shifting of $KA_{FSTpeak}$ to a flexed knee position in the present experiment. Yet, lack of change in joint range of force exertion

confirms no shape changes of the KA-F_{ST} curves due to inter-synergistic EMFT. Lack of stiffness change is in concert with that. In the light of this assessment, the present findings indicate two possible explanations. First, inter-synergistic EMFT caused spastic ST sarcomeres to operate at lengths favoring more force exertion, but without altering the heterogeneity of mean sarcomere lengths in different muscle fibers. Second, some of the forces of the co-activated GRA and SM muscles were transmitted via the connective tissue network on the spastic ST and were integrated into its force measured at the distal tendon, without affecting its sarcomeres.

The first explanation is tenable provided that myofascial loads act on the muscle belly and affect the contractile apparatus. Based on tendon forces in animal studies, inter-synergistic EMFT effects in physiologically relevant conditions were argued to be small [11, 104]. Conversely, human studies in vivo showed that global gastrocnemius strains imposed by knee movement caused much higher amplitudes of heterogeneous local strains to occur within the calf [105] and the remaining muscles of the limb [106]. This is explained by myofascial loads and indicates that muscle strains can be affected by inter-synergistic EMFT unproportionally with the loading on the tendon. do not cross the knee. This is explained by myofascial loads and indicates that muscle strains can be affected by inter-synergistic EMFT unproportionally with the loading on the tendon. The mechanism responsible for myofascial loads is muscle relative position changes (Figure 2.5). Due to differences in moment arms, knee angle changes may involve different length changes in each muscle co-activated. In healthy individuals, ST has a bigger knee flexion moment arm than the SM (as well as biceps femoris) [107] and GRA [108] in most knee positions. The ST attaining relatively longer lengths distally will stretch epimuscular connections in the distal direction. Hence, proximally directed myofascial loads plausibly act on distal parts of spastic ST. Additionally, the GRA is a hip flexor in contrast to the hamstrings [109]. The experimental test condition keeps it at a longer length than the other muscles, stretching epimuscular connections in the distal direction. Therefore, proximally directed myofascial loads plausibly act also on proximal parts of spastic ST. These loads can limit sarcomere lengthening with joint extension maintaining myofilament overlap favorable for force production. Note that, this mechanism should be effective already in condition I. The shape of KA-

F_{ST} curve does indicate that the muscle exerts low forces in flexed knee positions and its peak forces in response to knee extension. Therefore, myofascial loads originating from the compartmental connective tissues appear to eliminate sarcomere overstretch although this is considered as a property of spastic muscle due to adaptations in CP [110, 111]. Added activation of the SM and GRA in condition II must have elevated those myofascial loads. This can explain the increased spastic ST forces measured. Earlier, peak force of spastic GRA co-activated with its antagonist vastus medialis was measured in flexed knee positions [46], whereas if stimulated alone, this was encountered only in response to joint extension [44]. Therefore, unlike the present findings, EMFT effects vary among different spastic muscles and/or inter-antagonistic EMFT causes more pronounced effects also on the shape of the KA-F_{ST} curve are plausible suggesting that they can vary among different spastic muscles and/or inter-antagonistic EMFT causes more pronounced effects on spastic muscles' mechanical behavior. New studies are indicated to further understand EMFT effects in patients with CP.

Yet, supporting the second explanation, certain previous studies indicate that myofascial forces can also be transmitted via the connective tissue network without affecting fiber [103, 112] or sarcomere lengths, or their heterogeneity [13, 21]. A unique recent finding is also relevant. Flexor carpi ulnaris muscle biopsies from patients with CP compared to healthy controls showed a particular thickening of the tertiary perimysium [32] suggesting elevated stiffness of these structures. Notably, tertiary perimysial structures constitute the connective tissue reinforcement of neurovascular tissues penetrating the muscle. However, they traverse the muscle without enveloping fascicles from their origin to insertion unlike the other levels of the perimysium. Therefore, they can be considered to comprise an EMFT pathway inside, but through only a part of the muscle. The remainder, however, follows the stiffer pathway inside the muscle and leaves it via the neurovascular tracts at other parts of the muscle belly and reaches the joint. As no particular effects on sarcomere lengths and related changes to the shape of the KA-F_{ST} curve are considered, the second explanation is in concert with the lack of altered spastic ST stiffness and joint range of force exertion shown. However, the present study is incapable of isolating elevated stiffness of particular ECM elements of the spastic ST. We also don't have the data to test if inter-synergistic myofascial loads

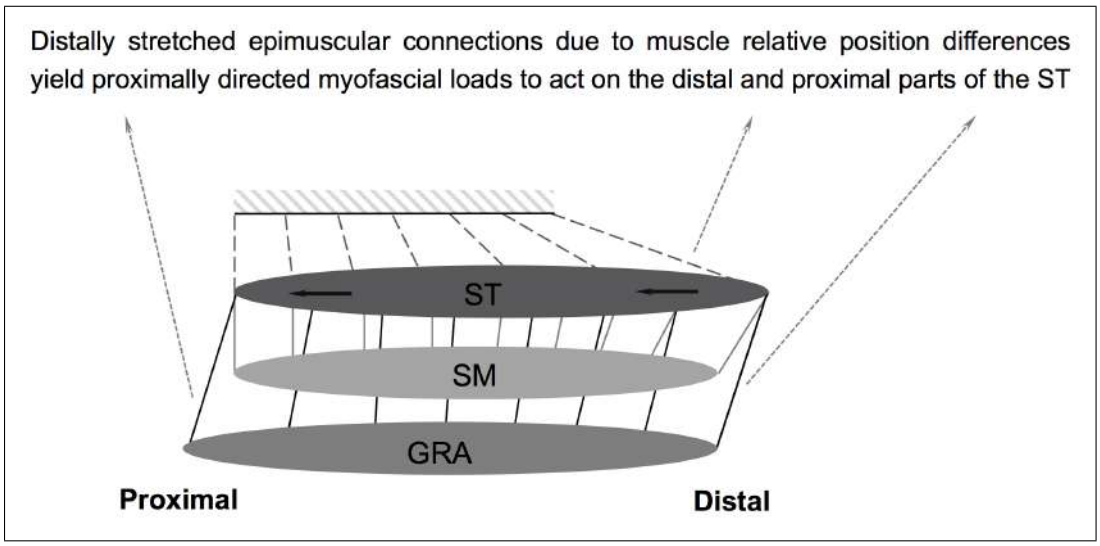

Figure 2.5 Schematic illustrating myofascial loads on the ST due to muscle relative position differences between the GRA and SM muscles and the ST. Relative position changes in an extended knee position are illustrated and exaggerated for clarity. Distally, relative position differences can occur due to differences in moment arms among the studied muscles and stretch their mutual epimuscular connections distally (solid lines interconnecting the ST to the SM and GRA). In addition, the target muscle's relative position changes with respect to the remainder of the hamstrings, and the bone are represented (dashed lines connecting the ST to the mechanical ground). Proximally, relative position differences occur due to the experimental condition. This keeps the GRA at a longer length than the other co-activated muscles and stretches the epimuscular connections (solid lines interconnecting the ST to the GRA) distally. Epimuscular connections stretched distally will lead to proximally directed myofascial loads to act on the distal and proximal parts of the ST (illustrated by solid black arrows on the ST belly). These loads include passive forces originating from muscles and connective tissues in condition I and also some of the active forces of co-activated GRA and SM muscles in condition II. Myofascial loads can affect the mechanics of the spastic ST by manipulating its sarcomere lengths (first explanation in text), or by being integrated into its force (second explanation in text), or a combination of these.

not encountered in the tendon may affect knee flexor moment as a source of limited knee joint mobility in CP. These issues were beyond our research questions posed but can be relevant for an improved understanding of the pathological joint condition and require specific testing in new studies.

If one of the two explanations was the dominant determinant of inter-synergistic EMFT effects shown cannot be decided. Additionally, the data is not capable of indicating whether the EMFT effects are different in patients with CP compared to typically developing children. EMFT was argued to play a role in the impaired joint function in CP and consequently, mechanical interactions between muscles were considered to impose greater effects on spastic muscles' mechanics than in healthy people [7, 10]. In contrast, in a rat model of spasticity, Olesen et al. [113] showed no differences in

mechanical interactions between synergistic lower hindlimb muscles compared to the control group. Although the pathology mechanisms between CP patients and a rat model can be quite different, new studies are indicated to compare EMFT effects in CP and typically developing children. On the other hand, plausibly, the limited knee joint mobility in CP stems from multiple factors. Haberfehlner et al. [114] showed a shift of passive knee moment-angle curve towards more flexed knee angles indicating a higher stiffness but could not explain this entirely with altered ST morphology. They suggested that elevated stiffness of intra- and epimuscular connective tissues as well other structures around the knee may play a role. Note that, the majority of the present participants were not independently ambulant, but all positions of knee extension in the testing protocol could be reached in the passive state. In contrast, in a similar group of patients, this was not possible [46]. Therefore, active state mechanics of spastic muscles appear not to agree with parameters characterizing the passive state. For self-ambulant children with CP, gait, and sit-to-stand involve a knee joint range approximating 30° to 100° [115,116]. We cover a wider range of knee positions, but the data indicate that EMFT may affect the pathological condition in the joint via force increases. The patients' high GMFCS values implying limited weight-bearing suggest that muscle weakness may be an issue at the time of testing. However, assuming that their muscle-related connective tissues have adapted to become stiffer during their development, a greater role of EMFT is plausible for them to become non-ambulant in the course of their pathological condition. These issues are in need of new and specific research.

2.5 Conclusion

Inter-synergistic EMFT occurring due to co-stimulation of other knee flexors of the upper leg does increase forces of activated spastic ST substantially. However, this did not cause changes in active stiffness and joint range of force exertion of the muscle. Therefore, we conclude that inter-synergistic EMFT affects forces exerted at the spastic ST tendon, but not other characteristics of its angle-force relationship.

3. PASSIVE AND ACTIVE STATE MECHANICS OF SPASTIC GRACILIS: INTRAOPERATIVE EXPERIMENTS AND GAIT ANALYSES

3.1 Introduction

In individuals with spastic cerebral palsy (CP), the mechanism of pathological resistance against joint extension is unknown. This is ascribed to the passive and active properties of spastic muscles. Regarding the former, the range of joint motion can be limited even in the absence of any active force exertion [37, 117]. Therefore, passive forces of spastic muscles are expected to be high [118]. In contrast, in the upper extremity, intraoperative measurements revealed low passive forces for spastic flexor carpi ulnaris muscle [86, 99]. However, in the lower extremity, this has not been measured directly, whereas assessments using muscle biopsies (e.g., [34]), and dynamometry and ultrasound shear wave elastography (e.g., [119]) demonstrated greater passive muscle stiffness in children with CP compared to typically developing (TD).

Regarding active properties, the role of spasticity in disrupting voluntary active motion has been supported [40, 120] or rejected [121, 122] by various studies. However, the pathological restricted joint motion of CP patients is clear. In the upper extremity, if the limb is pulled on, the joint is forcefully kept in a flexed position [41], indicating the presence of high flexor forces, which can stem from active force production of spastic muscles. Intraoperative tests allow for the quantification of human muscles' forces directly as a function of joint angle [42] and measure their capacity to affect joint moments. A series of studies in patients with CP showed that activated spastic knee flexors, the gracilis (GRA), semitendinosus (ST) and semimembranosus (SM) muscles, produce only low forces in flexed knee positions [43–45]. Note however that, if another muscle is co-activated, spastic GRA muscle's overall mechanical characteristics were shown to change, with the peak force shifting to flexed knee positions for some patients [46]. This was ascribed to intermuscular mechanical interactions. This through

epimuscular myofascial force transmission (EMFT) [90] have been shown to change the force of a muscle explained by its altered force production due to manipulated sarcomere lengths [13]. Daily activities involve the simultaneous activation of several muscles [87]. Therefore, intermuscular mechanical interactions can affect the active state mechanics of spastic muscle in CP.

Despite the contribution of previous studies, there are major gaps in our understanding of the passive and active state mechanics of spastic muscles. Although spastic muscle's passive forces are considered to be high, they have not been assessed directly. Additionally, activated spastic muscle's force - joint angle relations were studied independently of gait-relevant joint positions. The aim was to fill in these gaps by combining intraoperative experiments with gait analyses in order to test the following hypotheses: (i) spastic GRA passive forces are high even in flexed knee positions, (ii) its active state forces attain high amplitudes within the gait-relevant knee angle (KA) range and (iii) increase with added activations of other muscles.

3.2 Methods

Surgical and experimental procedures, in strict agreement with the guidelines of the Helsinki declaration, were approved by a Committee on Ethics of Human Experimentation at Istanbul University, Istanbul. The patients and/or their parents gave informed consent to the work.

3.2.1 Participants

Seven patients (all male: mean age 9 years 2 months, range 6-13 years, standard deviation 2 years 10 months) with CP, however no prior remedial surgery, were included. Gross Motor Functional Classification System (GMFCS) levels of all participants were II. Clinical spasticity scores: popliteal angles measured according to Modified Tardieu Scale and Modified Ashworth Scale scores (Table 3.1). Prior to surgery, computerized

Table 3.1
Patient characteristics and spasticity scores. L_{thigh} = thigh length; $C_{mid\text{-}thigh}$ = mid-thigh circumference; PA, Popliteal angle (i.e., the angle between hip and knee at the hip in 90° flexion); MTS, Modified Tardieu Scale; R1 and R2, PA measurements according to MTS per fast and slow-sustained stretch, respectively; MAS, Modified Ashworth Scale. PA> 50° indicates a severely limited range of knee joint motion. MAS scores (0, 1, 1+, 2, 3, and 4) other than 0 indicate spasticity. 1: slight increase in muscle tone, manifested by a catch and release or by minimal resistance at the end of the range of motion when the affected part(s) is moved in flexion or extension, 1+: slight increase in muscle tone, manifested by a catch, followed by minimal resistance throughout the remainder (less than half) of the range of movement, 2: more marked increase in muscle tone through most of the range of motion, but affected part(s) easily moved. 3-4 (not present in the current study): for affected part(s), movement is difficult or rigid.

Patient	Limb	Age (years)	L_{thigh} (cm)	$C_{mid\text{-}thigh}$ (cm)	PA (°) R1 of MTS	PA (°) R2 of MTS	MAS score adductor	MAS score hamstring
1	1	13	36.0	40.5	65	60	1	2
1	2	13	36.5	39.0	70	65	2	2
2	3	8	30.0	32.5	70	50	1+	2
3	4	8	31.0	36.0	75	40	2	2
3	5	8	31.0	35.8	60	50	1+	1+
4	6	6	27.0	29.2	65	65	1+	2
5	7	11	35.0	43.0	80	80	2	2
6	8	12	37.0	37.0	80	80	2	2
6	9	12	38.0	39.5	70	70	1+	2
7	10	6	26.0	28.0	80	65	1+	1+

gait analysis was performed for an objective diagnostic assessment. Note that, we used this data to build a relationship between the specific spastic muscle level joint angle-muscle force measurements and global patient motion characteristics i.e., to judge the spastic muscle's mechanics against the patients' pathological movement. Overall, pre-operative clinical examinations indicated a severely limited knee range of joint motion and led to a decision that all patients required remedial surgery including the release of hamstrings and hip adductors.

3.2.2 Gait Analysis

A motion analysis system (ELITE 2002, BTS Bioengineering, Milan, Italy) with six infrared cameras and two force plates (Kistler Instrumente AG, Winterthur, Switzerland) was used implementing Helen Hayes Marker Placement Protocol [123]. Bilateral marker locations: the metatarsal head V, the heel, the lateral malleolus, the tibial wand, the femoral lateral epicondyle, the femoral wand, and the anterior superior iliac spine (ASIS). A single marker was placed onto the sacrum. Additionally, a marker on the seventh cervical vertebrae (C7) was used to detect initiation of walking, and to quantify shoulder tilt relative to horizontal in combination with two shoulder markers (on the flat portions of the acromion). Hip and knee joint angles and moments in the sagittal plane were used to relate the global gait metrics to intraoperative spastic muscle level mechanics.

3.2.3 Intraoperative Measurements

Six of the patients were operated on bilaterally. For three of them, separate experiments were performed on both legs. For the remainder patients, only one leg was experimented with due to time limitations imposed by subsequent multilevel surgery. Therefore, a total of ten knee angle GRA muscle force (KA-F_{GRA}) data sets were collected. The intraoperative measurements were done first in the passive state (condition I), then the spastic GRA was stimulated alone (condition II), simultaneously with its synergists ST and biceps femoris (BF) (condition III), and also with its antagonist rectus femoris (RF) (condition IV).

The patients received general anesthesia without the use of muscle relaxants or tourniquets. All experimental preparations and data collection were performed after routine incisions to reach the distal GRA tendon and before any other routine surgical procedures. Using a scalpel blade (number 18), a longitudinal skin incision was made immediately above the popliteal fossa. After cutting the adipose tissue, the distal GRA tendon was exposed. Subsequently, a buckle force transducer (TEKNOFIL,

Istanbul, Turkey) (Figure 3.1A) was mounted and fixed over the tendon. The key transducer characteristics include S-shape; dimensions: width= 12 mm length= 20 mm and height= 9 mm; maximal force range= 400 N; for test range 0-200 N: accuracy <3%, (<0.19% below 100 N); resolution= 0.62 N and high linearity (R^2= 0.99963, peak nonlinearity= 1.31%,). Note that prior to each experiment, the force transducer was (i) calibrated using bovine tendon strips (with rectangular cross-section, dimensions 7x2 mm^2 representative of that of the GRA distal tendon) and (ii) sterilized (using gas sterilization at maximally 50° C).

The patient was positioned, and target joint angles were adjusted using an apparatus (see Figure 3.1B for details). Isometric spastic $F_{GRA\_passive}$ and F_{GRA} were measured at various muscle lengths imposed by manipulating the joint angles. Data collection was done in the following sagittal hip and knee angles. The hip position was fixed at two different hip angles (HA) equalling 45° and 20° determined from gait analyses (see Results). For each HA, the KA was manipulated. Note that the hip was positioned in a neutral position for ab/adduction and internal/external rotation during testing. Length history effects of previous active contraction of the muscle at long length on forces measured at short length [12,42] were eliminated before acquiring data by preconditioning muscle-tendon complexes and their epimuscular connections. Isometric contractions were alternated at extended and flexed knee positions until spastic GRA forces at flexed knee positions were reproducible. Additionally, the data acquisition was started in a highly flexed knee (120°), and the muscle length was manipulated by extending the knee in 30° increments until 0° (full knee extension). Testing was completed for all conditions before attaining a different knee angle. After each contraction, the muscle was allowed to recover for a minute, and completion of the protocol approximated 30 minutes. A data acquisition system (MP150WS, BIOPAC Systems, CA, USA, 16-bit A/D converter, sampling frequency 40 kHz) was used with an amplifier for the force transducer (DA100C, BIOPAC Systems, CA, USA).

Four pairs of gel-filled skin electrodes (Kendall H92SG, Covidien, MA, USA) were placed on the skin, over the spastic GRA, ST, BF, and RF muscle bellies. Muscle bellies were located by palpation. The reference electrodes were placed as distal as

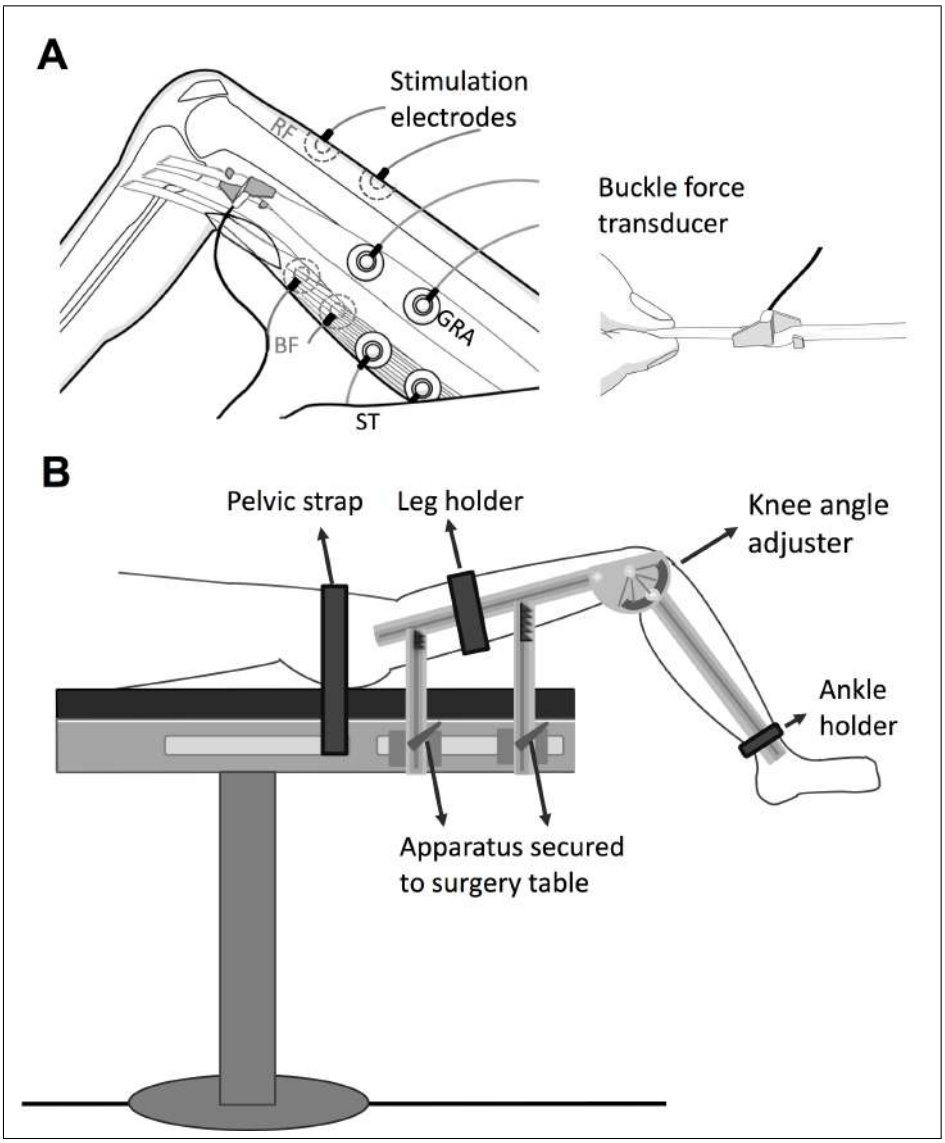

Figure 3.1 Intraoperative muscle mechanics experimental setup used for measurement of spastic GRA forces at flexed hip positions. (A) Illustration of how the buckle force transducer is mounted over the target muscle's tendon. Inset shows the transducer mounted over a tendon strip. Pairs of skin electrodes placed over the muscles are illustrated using solid (for the GRA and ST) or dashed (for the long head of BF and RF) circles. (B) An apparatus designed for intraoperative tests in lower extremities is composed of four components: (i) The *upper leg component* incorporating a leg holder, which has an adjustable position on it allows fixing the hip angle (to 45° or 20° both in the sagittal and frontal planes). This component is secured to the slot of the surgery table via fixtures. (ii) The *lower leg component* incorporating an ankle holder that has an adjustable position on it supports the lower leg. (iii) The *knee angle* and (iv) *hip angle adjusters* link together the upper and lower leg components and allow setting the knee and hip angle and fixing them during a contraction. Circular slots were machined in the knee and hip angle adjusters and angles were marked on them (in 0.5° increments) for the required joint position adjustments. The leg holders' position is adjustable on the upper leg component. This allows supporting the upper leg and aligning it such that the axis of the knee and hip joint rotations corresponded to the center of the rotation of the knee and hip angle adjusters, respectively. The ankle holder, the position of which is adjustable on the lower leg component allowed supporting the lower leg. The leg holder and ankle holder were sterilized components. The non-sterile remainder parts were covered with sterile fabric before an antiseptic agent was applied to the skin and the patient's leg was positioned and secured to the apparatus.

possible to the incision with their positions having an offset. The location of the second electrode was determined according to the following procedure: The minimum center-to-center inter-electrode distance was reported to be 30 mm for a successful electrode function [96] and muscle excitation [97]. At KA= 120°, a tentative location for the second electrode was determined accordingly. The contraction responses were assessed in response to twitch stimuli evoked separately for each muscle. Successful stimulation of spastic GRA was monitored from the measured force, and leakage of current into other muscles than the one stimulated was controlled by palpation. This was repeated at, KA= 60° and 0°. If necessary, the second electrode position was optimized by iteration.

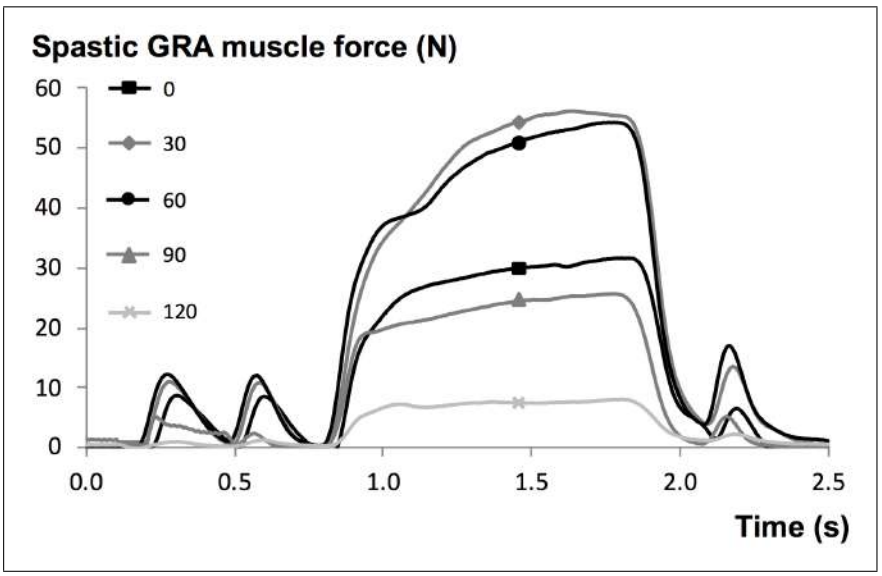

Figure 3.2 Typical examples of force-time traces for spastic GRA muscle. Superimposed traces recorded for GRA muscle at the five knee angles studied are shown.

A custom made, constant current high voltage source (cccVBioS, TEKNOFIL, Istanbul, Turkey) was used to impose supramaximal muscle stimulation (transcutaneous electrical stimulation with a bipolar rectangular signal, 160 mA, 50 Hz): two twitches were evoked which, after 300 ms, were followed by a pulse train for 1000 ms to induce a tetanic contraction and a subsequent twitch (see Figure 3.2 for superimposed examples of force-time traces for spastic GRA muscle at five KAs).

3.2.4 Processing of Data

For each KA tested, $F_{GRA\_passive}$ measured in passive state and F_{GRA} measured in active state, during a 500 ms period (in the middle of the tetanus for F_{GRA}) were averaged and recorded as muscle passive and total force, respectively.

Using a least-squares criterion, KA-F_{GRA} data were fitted with a polynomial function (Eq. 3.1).

$$F_{GRA} = a_0 + a_1 \cdot KA + a_2 \cdot KA^2 + ... + a_n \cdot KA^n \tag{3.1}$$

a_0, a_1 ... a_n are coefficients determined in the fitting process.

The lowest order of the polynomials and the exponential functions that still added a significant improvement to the description of changes of KA-F_{GRA} were selected using a one-way analysis of variance, ANOVA. KA-$F_{GRA\_passive}$ data were also fitted in the same way. The fitted data for each condition were used to calculate the mean of GRA forces and standard deviations per KA. Range-F_{GRA} (operational KA range of F_{GRA} exertion i.e., range between the KA's at which, the peak and minimum F_{GRA} is measured) was used as an active state metric.

3.2.5 Statistics

Two-way ANOVA for repeated measures (factors: KA and condition) was used to compare the overall mechanical characteristics of spastic GRA muscle in all conditions. If significant main effects and an interaction were found, Bonferroni post hoc tests were performed to further locate significant within-factor force differences. Shapiro-Wilk test was used to check if the key active state metrics data are normally distributed. Range-F_{GRA} calculated for each limb in condition III and condition IV were compared to those of condition II using paired-t test or Wilcoxon signed-rank test where appropriate. Differences were considered significant at $P < 0.05$.

3.3 Results

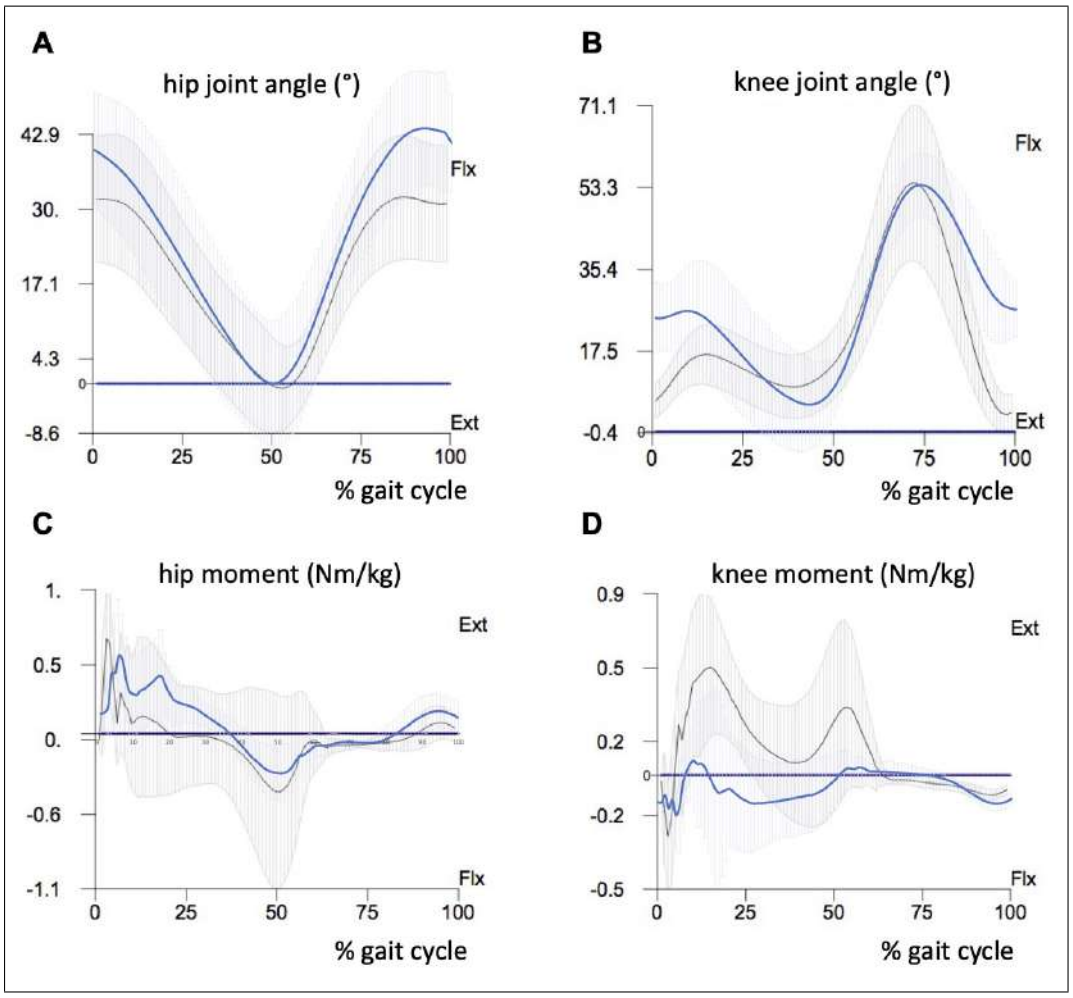

Figure 3.3 The patients' ensemble-averaged gait data (A) and (C) for the hip, and (B) and (D) for the knee, showing joint angles and moments, respectively. Blue curves indicate the patients' data, whereas the black curves indicate the reference data for the typically developing children (from the database of the BTS Bioengineering system). Flexion (Flx) and extension (Ext) are indicated.

Figure 3.3 shows the ensemble-averaged joint angles and moments in the sagittal plane. With less than one SD (for HA 11.1° and KA 8.8°) variation, the following parts of the gait cycle (GC) characterize the pathological joint condition of the patients and indicate gait-relevant KA range per HA tested intraoperatively: (i) Exaggerated knee flexion occurs for 0-30% GC and 75-100%. For the patients, this indicates that at the start and end of GC, their knee is highly flexed instead of being typically extended, which compromises heel strike leading even to toe landing. In the gait data, HA= 45° is observed for 0-12% and 77-100% GC, and this matches with KA= 17-61°. (ii) The knee moment is flexor for 16-51% GC instead of being typically extensor, which

also agrees with the patients' limited knee extension condition. In the gait data, HA= 20° is observed for 16-37% GC, and this matches with KA= 0-33°. Consequently, intraoperative data for KA= 17-61° at HA= 45° and KA= 0-33° at HA= 20° were determined to represent the pathological movement during loading response/terminal swing, and mid/terminal stance phases of the patients' gait, respectively.

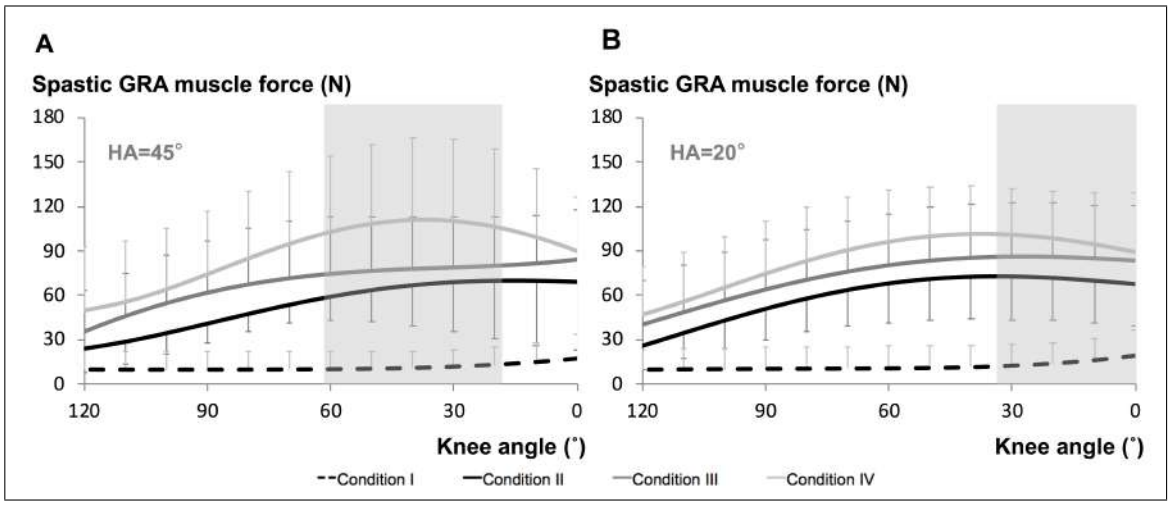

Figure 3.4 The mean (SD) of spastic GRA forces of intraoperatively tested limbs per KA across the conditions tested for both HAs studied. (A) for HA= 45° and (B) for HA= 20°. The spastic GRA forces in the passive states (condition I) are shown as dashed curves. The spastic GRA was activated alone (condition II), simultaneously with its synergists, semitendinosus (ST) and biceps femoris (BF) (condition III), and also with its antagonist rectus femoris (RF) (condition IV). The grey shaded areas show the gait-relevant KA-positions.

Figure 3.4 shows KA-F_{GRA} and KA-$F_{GRA\_passive}$ characteristics. For both HA, in conditions I and II: (1) passive forces start from non-zero, but low amplitudes in flexed knee positions and increase to maximally 26.1% (HA= 20°) of the peak total force measured in condition II. (2) Total forces attain their minimum in the most flexed knee position, show an increase in response to added knee extension, reach a maximum and decrease (for HA= 45°, F_{GRA}= 24.0 N, 70.1 N, 69.2 N at KA= 120°, 16° and 0°, and for HA= 20°, F_{GRA}= 25.8 N, 72.9 N, 67.6 N at KA= 120°, 34° and 0°, respectively).

ANOVA (factors: KA and condition) showed significant main effects of both factors on spastic GRA forces, but no significant interaction. Condition I: the passive forces measured at HA= 20° are significantly (on average by 6.5%) higher than those measured at HA= 45°. Condition II vs. III and IV: co-activation of the synergistic

Table 3.2
Effects of conditions on Range-F_{GRA} for each limb tested.

Limb	Range-F_{GRA} (°) for KA= 45°			Range-F_{GRA} (°) for KA= 20°		
	Condition II	Condition III	Condition IV	Condition II	Condition III	Condition IV
1	120	120	90	92	103	94
2	118	120	86	81	95	83
3	77	74	67	60	67	67
4	68	120	63	95	56	82
5	83	120	78	76	88	69
6	120	120	100	92	95	95
7	72	120	120	120	120	120
8	120	98	81	108	92	58
9	120	50	74	73	38	78
10	120	120	97	113	113	88
Mean (SD)	102 (23)	106 (25)	86 (17)	91 (19)	87 (26)	83 (18)

and antagonistic muscles caused spastic GRA total forces to increase significantly (on average, for HA= 45°, by 32.8% and 71.9%, and for HA= 20°, by 24.5% and 45.1% in conditions III and IV, respectively). Compared to HA= 45°, for HA= 20°, the total forces are higher in conditions II and III (on average by 12.9% and 6.1%, respectively) and lower in condition IV (on average by 4.6%). Condition I vs. IV: peak passive force is maximally 18.7% (HA= 20°) of peak GRA total force.

Condition II vs. III and IV: Wilcoxon signed-rank test (conditions III and IV at HA= 45°) and the paired-t test (conditions III and IV at HA= 20°) showed no significant differences in Range-F_{GRA} (Table 3.2). Across different HAs, no significant differences were shown in Range-F_{GRA} for condition II (Wilcoxon signed-rank test) and condition IV (paired-t test) but, in condition III, compared to HA= 45°, Range-F_{GRA} was significantly narrower (Wilcoxon signed-rank test) at HA= 20° (on average by 18.1%).

3.4 Discussion

Passive forces of spastic GRA muscle measured directly at the tendon for the first time maximally approximated a quarter of the active state forces in extended knee positions. Therefore, the hypothesis that spastic GRA passive forces are high even in flexed knee positions was rejected. However, the hypotheses that active state forces of spastic GRA attain high amplitudes within the gait-relevant KA range and increase with added activations of other muscles were confirmed.

The overall mechanical characteristics of spastic GRA in conditions I and II provide valuable novel information as the muscle's passive and active state mechanics can be compared. The fact that the passive state forces are only a certain fraction of the active state forces for most knee positions indicates that the passive state is not the dominant component of the spastic muscle's mechanics affecting the knee joint. This is valid also within the KA range relevant to gait. On the other hand, conditions involving co-activation of other muscles promote testing of the active state effects. Therefore, the intermuscular mechanical interaction effects in conditions III and IV characterize the change in the effects of the active state on the mechanics of spastic GRA. Accordingly, in condition III, elevated forces measured in response to the co-activation of synergistic muscles indicate an increased contribution of spastic GRA to knee flexion moment for gait-relevant joint positions due to EMFT. Moreover, further elevated forces of spastic GRA in response to added activation of an antagonist muscle in condition IV strengthen the judgment that the active state dominates the spastic muscle's effect at the joint to cause motion restriction. This is plausible also for other types of daily motions. For self-ambulant children with CP, sit-to-stand, and stair ascending/descending involve a KA range approximating 20° to 100° [116, 124] which is within the range of knee positions covered in the current study. Also, such key movements involve simultaneous activation of several lower-limb muscles including the GRA, ST, BF, and RF [88]. Therefore, conceivably EMFT may have similar effects on spastic muscle's mechanics contributing to the restricted joint movement for various types of movements. Note that, sit-to-stand involves further flexed hip positions, which is more pronounced in children with CP compared to TD [116]. This can cause the GRA to attain shorter

lengths proximally and based on the present findings may elevate the effect of EMFT. Hence, plausibly the active state may play a dominant role in limited joint mobility also for sit-to-stand motion. However, these issues require further specific testing.

Notably, (1) in condition IV, GRA forces measured at a HA of 45° were higher compared to those at a HA of 20°. (2) In condition III, Range-F_{GRA} determined for a HA of 20° was significantly narrower than that for a HA of 45°. These findings indicate the effects of epimuscular myofascial loads on the mechanics of spastic GRA. Altered HAs change a muscle's relative position with respect to other muscles, which stretches its epimuscular connections and causes myofascial loads to develop [13, 90]. This is the central mechanism for EMFT effects in which such loads can (i) integrate with the muscle's force, or (ii) alter its sarcomere lengths, hence changing the muscle's own force and movement production capacity. Regarding the latter, EMFT causes sarcomeres in the same muscle fibers to attain different lengths as well as the heterogeneity of mean sarcomere lengths across different fibers [102, 103, 125]. A consequence is an altered length range of force exertion [90, 126]. Additionally, myofascial loads can cause sarcomeres to attain lengths closer to their full myofilament overlap [50, 100]. Both mechanisms can be found in the present data suggesting that the present EMFT effects can be ascribed to both (i) and (ii). Such effects are plausible also for the other findings of the study, however, the amplitude and type of effects of epimuscular myofascial loads appear to vary across conditions. Nevertheless, the findings show that such loads did affect spastic GRA muscle's overall mechanics, particularly for the gait-specific joint positions studied. In order to assess if this reflects on the joint movement limitation, we sought a correlation between the severity of the patients' pathological gait and the increase in spastic GRA force via co-activation of other muscles (please see Appendices A and B for details). This assessment indicates that there is indeed a strong correlation between a characteristic metric representing per each limb, the limited knee extension of the patients, and the effect of EMFT causing elevated spastic GRA forces.

The present findings, which show that in cerebral palsy, active state, rather than passive dominates the spastic muscle's joint movement limiting effect, and the effects

of EMFT are a determinant of pathological gait, have clinical implications. One is for the clinical examination tests conducted prior to surgery. Ates et al. [44] studied muscle force-KA characteristics of individually activated spastic GRA intraoperatively and showed no correlation between the key determinants of the experimental measures (i.e., the KA and amplitude of peak spastic GRA force exertion and the percentage of it measured at the most flexed and extended knee positions tested) and the outcome of patients' pre-operative clinical examinations performed in the passive state (a metric combining the popliteal angle and hip abduction angle into a clinical score for a limited range of motion). The same general lack of active to passive state correlation was shown also for spastic ST [43] and semimembranosus [45] muscles. Therefore, we suggest that clinicians pay closer attention to a spastic muscle's impact on joint motion during active conditions as opposed to the typical passive range of motion assessments conducted. Intraoperative clinical testing is ideally a tool to be used for that purpose, but this technique is not widely available currently. However, gait analyses should be central and the use of e.g., supersonic shear imaging is capable of estimating muscle force as well as EMFT effects [127,128]. Additionally, new approaches to interventions are warranted that consider the effect of agonist/antagonist interactions on a spastic muscle's limiting joint motion. Muscle-related connective tissues also interconnecting those muscles are key to that. Tenotomy of spastic flexor carpi ulnaris was shown to be ineffective on wrist motion [94] and torque [129] unless accompanied with major dissection of the muscle's connective tissue envelope comprising epimuscular connections. Tendon transfer surgery involves partial dissection of connective tissues surrounding the muscle to be mobilized, which in return also interferes with the EMFT pathways [10]. Muscle lengthening surgery directly interferes with muscular connective tissues: (i) intramuscularly, muscle's extracellular matrix is torn after the aponeurosis is transacted, which is determines the acute effects [130]. (ii) However, also epimuscularly, the preparatory dissections done to perform the main intervention can be effective and for the non-targeted muscles as well [47]. Those studies show that intra- and epimuscular connective tissues affect the surgical outcome and the present study indicates they play a role in determining the spastic muscle's limiting joint motion. New studies should aim at determining if, in CP, those connective tissues are stiffer so as to provide pathological agonist/antagonist connections. Also, possible effects of their altered structure

and properties after the intervention should be accounted for to achieve the optimal outcome.

Limitations of the work should be acknowledged. Fee and Miller [131] showed in spastic CP that active muscle tone disappeared under neuromotor blockade anesthesia, which was not used in the current study. Therefore, our findings may not have isolated pure passive state properties. However, this suggests that the spastic GRA's passive forces may be smaller than those reported. The maximum contraction condition used in intraoperative testing is unlikely to occur during gait. Moreover, the isometric condition does not represent the dynamic gait-specific loadings. Therefore, the measured forces don't correspond directly to those acting on the joint during gait. However, the intraoperative data are important as the test conditions implemented to allow for the quantification of the maximal capacity of the spastic GRA in limiting knee extension and the effects of added activation of other muscles on that. Note that, a similar effect of such co-activation also on proximal GRA forces is plausible, which may elevate its motion limiting effect at the hip, but this needs to be tested. New studies are indicated to consider different joint positions that represent other functional activities including altering of hip position into the coronal or transverse planes. Also, testing of other medial hamstrings or plantar flexors is indicated for a broader understanding of the mechanics of spastic muscle and the effects of agonist/antagonist interaction on that.

3.5 Conclusion

Spastic muscle's passive forces measured directly for the first time in patients with CP maximally approximate a quarter of the active state forces, which attain peak values within the gait-relevant KA-range and elevate significantly after the added activation of other muscles. Therefore, active state muscular mechanics, rather than passive, of spastic GRA present a capacity to limit joint movement in CP, the effects of which elevate due to intermuscular mechanical interactions.

4. PASSIVE AND ACTIVE STATE MECHANICS OF SPASTIC SEMITENDINOSUS: INTRAOPERATIVE EXPERIMENTS AND PATIENT-SPECIFIC MUSCULOSKELETAL MODELS

4.1 Introduction

In cerebral palsy (CP) restricted knee joint range of motion can be seen even in conditions that do not involve any muscle activation [37,117]. Therefore, the pathological joint condition can be associated with non-contractile structures ascribed to stiff connective tissues such as the joint capsule or ligaments and/or high passive resistance of spastic muscles [118,132,133]. The former often is detected in pre-operative clinical examinations and may prohibit full knee extension in resting state (e.g., [46]). Passive knee moment-angle characteristics of spastic semitendinosus (ST) were shown to differ from those of typically developing (TD) children, indicating elevated epimuscular and intramuscular connective tissue stiffness in CP [114]. Using muscle biopsies, Smith et al. [34] reported greater passive state stiffness of spastic hamstring fascicles including the ST. However, despite its major importance, direct measurement of passive forces at the tendon of the spastic muscle has not been done.

In the active state, CP patients experience pathological restricted joint motion including knee flexion deformity during gait [39, 40]. If during clinical examination, the affected limb is pulled on, the joint is forcefully kept in a flexed position, which is ascribed to exaggerated stretch reflexes. However, this also indicates the presence of high flexor forces [41], conceivably originating from active state muscular force production. Yet, in flexed joint positions the muscle attains shorter lengths, which is not suitable for high force production. Therefore, spastic muscle could be characterized by altered contractile properties leading to a shift of the muscle's highest force production to flexed joint positions. In concert with that, spastic muscle is considered as a short-

ened muscle, which is derived from fewer series sarcomeres and not shortened sarcomeres [134]. This is supported by findings showing that sarcomeres attain longer lengths non-favorable for active force generation in extended positions [34]. However, accessing human tendons for direct force measurements to address those issues is difficult. Consequently, studies investigating patients' muscle mechanics are rare [85, 99, 129, 135]. Intraoperative experiments showed that selectively activated, spastic gracilis (GRA), ST, and semimembranosus (SM) muscles' forces are low in flexed, and high in extended knee positions [43–45], which could not reveal the source of aforementioned high flexor forces.

Daily activities involve co-activation of several muscles simultaneously [87, 136]. Resulting intermuscular mechanical interactions manipulate the muscle's force [90]. In patients with CP, co-activating other muscles with the target spastic knee flexor caused its force to increase [46, 137, 138]. However, although knee flexion deformity is often accompanied by increased hip flexion [139] the hip was kept at a neutral position. Therefore, assessments in conditions involving intermuscular mechanical interactions and in gait-relevant joint positions are lacking.

The present study aims at testing the following hypotheses by combining intraoperative experiments with the patients' gait data: (i) in both passive and active states, spastic ST per se shows its highest forces within gait-relevant knee angle (KA) range and (ii) due to intermuscular mechanical interactions, the active state forces are higher than those measured when the muscle is activated alone.

4.2 Methods

Surgical and experimental procedures, in strict agreement with the guidelines of the Helsinki declaration, were approved by a Committee on Ethics of Human Experimentation at Istanbul University, Istanbul. The patients and/or their parents gave informed consent to the work.

4.2.1 Participants

Seven patients (male: mean age 9 years 2 months, range 6-13 years, standard deviation 2 years 10 months) with CP, however no prior remedial surgery were included. The Gross Motor Functional Classification System (GMFCS) levels were II. The popliteal angle (PA) values show the patients' limited knee mobility (Table 3.1, please see Appendix C for a correlation assessment between clinical and intraoperative measures). Reference: seven age-matched TD children.

4.2.2 Gait Analysis

A motion analysis system (ELITE 2002, BTS Bioengineering, Milan, Italy) with six infrared cameras and two force plates (Kistler Instrumente AG, Winterthur, Switzerland) was used implementing Helen Hayes Marker Placement Protocol [123]. Bilateral marker locations were the metatarsal head V, the heel, the malleolus, the tibial wand, the femoral epicondyle, the femoral wand, and the anterior superior iliac spine (ASIS), and a single marker was placed onto the sacrum. In addition to the standard marker set, a marker on the seventh cervical vertebrae (C7) was used to detect the initiation of the walking. The gait data were used to associate the spastic muscle level mechanics with global patient motion characteristics.

4.2.3 Musculoskeletal Modeling

Musculoskeletal models were developed for each participant using OpenSim to establish the relationship between gait and muscle mechanics systematically in order to (i) assess the change in operational muscle-tendon unit (MTU) length of participants' ST muscle during gait and (ii) analyse MTU length-spastic muscle force data. The gait_2392 model which comprises 23 degrees-of-freedom, and 92 musculotendon actuators per leg [140] was used. Each model was scaled to the participants' anthropometry using the scale tool, based on body mass and surface marker locations obtained during

a static trial performed during the gait analysis. The inverse kinematic tool was used to calculate ST MTU lengths for each participant within the time frame of gait as well as ST MTU lengths corresponding to paired hip and knee joint angles used during intraoperative testing.

4.2.4 Intraoperative Measurements

Six patients were operated on bilaterally. For three of them, separate experiments were performed on both legs. For the remainder patients, only one leg was experimented with due to time limitations imposed by subsequent multilevel surgery. Therefore, a total of ten knee angle ST muscle force (KA-F_{ST}) data sets were collected. The intraoperative measurements were done first in the passive state (condition I). Then the spastic ST was stimulated alone (condition II), simultaneously with its synergists GRA and biceps femoris (BF) (condition III), and also with its antagonist rectus femoris (RF) (condition IV).

The patients received general anesthesia without the use of muscle relaxants or tourniquets. All experimental preparations and data collection were performed after routine incisions to reach the distal ST tendon and before any other routine surgical procedures. After the distal ST tendon was exposed, a buckle force transducer (TEKNOFIL, Istanbul, Turkey) (Figure 4.1A) was mounted and fixed over the tendon. The key transducer characteristics include S-shape; dimensions: width= 12 mm length= 20 mm and height= 9 mm; maximal force range= 400 N; for test range 0-200 N: accuracy$<$ 3%, ($<$0.19% below 100 N); resolution= 0.62 N and high linearity (R^2= 0.99963, peak nonlinearity= 1.31%). Note that prior to each experiment, the force transducer was (i) calibrated using bovine tendon strips (with rectangular cross-section, dimensions 7x2 mm^2 representative of that of the ST distal tendon) and (ii) sterilized (using gas sterilization at maximally 50° C).

The patient was positioned, and target joint angles were adjusted using an apparatus (Figure 4.1B). $F_{ST\_passive}$ and isometric F_{ST} were measured at two different hip

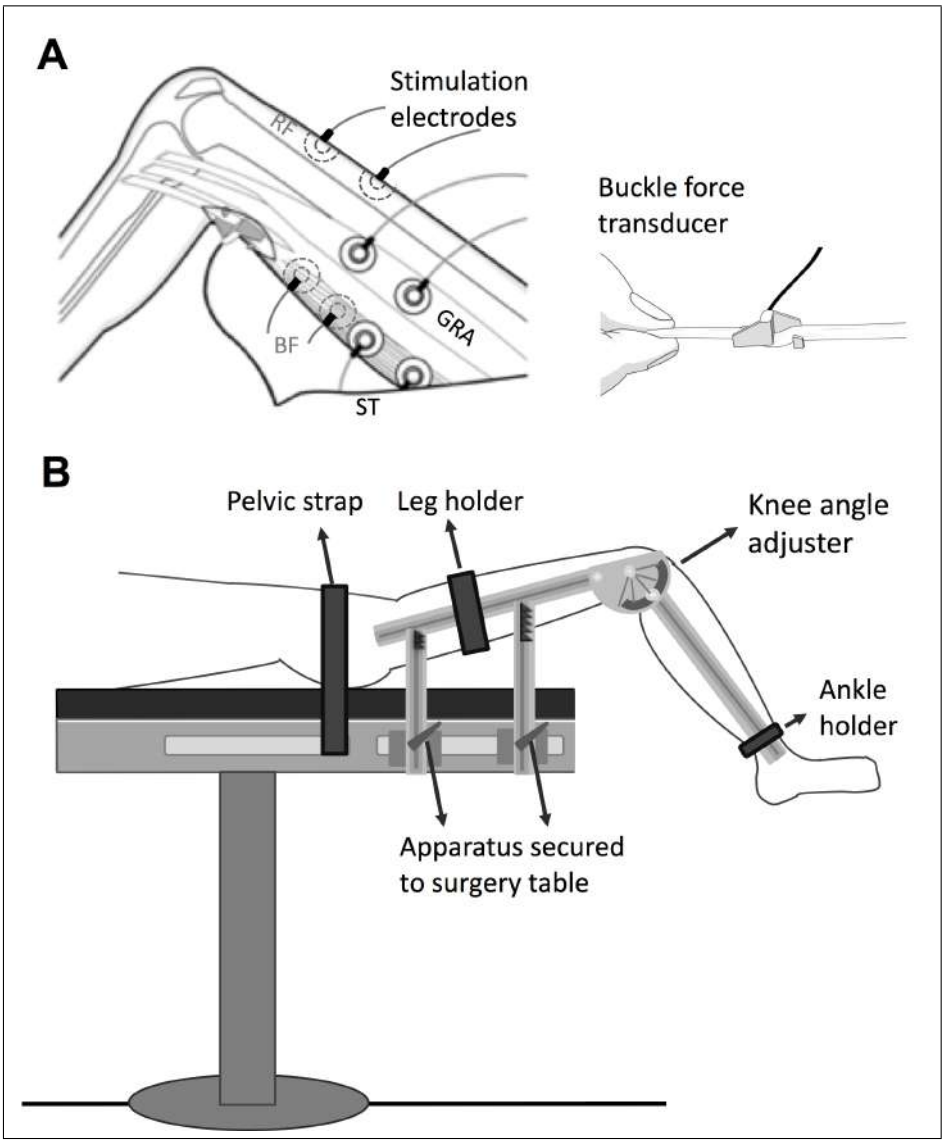

Figure 4.1 Intraoperative muscle mechanics experimental setup used for measurement of spastic ST forces at flexed hip positions. (A) Illustration of how the buckle force transducer is mounted over the target muscle's tendon. Inset shows the transducer mounted over a tendon strip. Pairs of skin electrodes placed over the muscles are illustrated using solid (for the ST and GRA) or dashed (for the long head of BF and RF) circles. (B) An apparatus designed for intraoperative tests in lower extremities is composed of four components: (i) The *upper leg component* incorporating a leg holder, which has an adjustable position on it allows fixing the hip angle (to 45° or 20° both in the sagittal and frontal planes). This component is secured to the slot of the surgery table via fixtures. (ii) The *lower leg component* incorporating an ankle holder that has an adjustable position on it supports the lower leg. (iii) The *knee angle* and (iv) *hip angle adjusters* link together the upper and lower leg components and allow setting the knee and hip angle and fixing them during a contraction. Circular slots were machined in the knee and hip angle adjusters and angles were marked on them (in 0.5° increments) for the required joint position adjustments. The leg holders' position is adjustable on the upper leg component. This allows supporting the upper leg and aligning it such that the axis of the knee and hip joint rotations corresponded to the center of the rotation of the knee and hip angle adjusters, respectively. The ankle holder, the position of which is adjustable on the lower leg component allowed supporting the lower leg. The leg holder and ankle holder were sterilized components. The non-sterile remainder parts were covered with sterile fabric before an antiseptic agent was applied to the skin and the patient's leg was positioned and secured to the apparatus.

angles (HA) equaling 45° and 20°, for each of which, the KA was manipulated. Length history effects of previous active contraction of the muscle at long length on forces measured at short length [12, 42] were eliminated by preconditioning. Additionally, the data acquisition (MP150WS, BIOPAC Systems, CA, USA) was started in a highly flexed knee (120°), and the muscle length was manipulated by extending the knee in 30° increments until 0° (full knee extension). Testing was completed for all conditions before attaining a different KA. After each contraction, the muscle was allowed to recover for a minute. A data acquisition system (MP150WS, BIOPAC Systems, CA, USA, 16-bit A/D converter, sampling frequency 40 kHz) was used with an amplifier for the force transducer (DA100C, BIOPAC Systems, CA, USA).

Four pairs of gel-filled skin electrodes (Kendall H92SG, Covidien, MA, USA) were placed over the spastic ST, GRA, BF, and RF muscle bellies. Muscle bellies were located by palpation. The reference electrodes were placed as distal as possible to the incision with their positions having an offset. The minimum center-to-center inter-electrode distance was 30 mm for a successful electrode function [96] and muscle excitation [97]. The tentative location for the second electrode determined accordingly was then optimized with twitch stimuli monitored at KA= 120°, 60°, and 0°.

A custom made, constant current high voltage source (cccVBioS, TEKNOFIL, Istanbul, Turkey) was used to impose supramaximal muscle stimulation (transcutaneous electrical stimulation with a bipolar rectangular signal, 160 mA, 50 Hz): two twitches were evoked which, after 300 ms, were followed by a pulse train for 1000 ms to induce a tetanic contraction and a subsequent twitch. Please see Appendix D for examples of muscle force-time traces showing tetanic contraction and selective stimulation of spastic ST.

4.2.5 Processing of Data

Gait analysis and musculoskeletal modeling: Modeled limb-specific data for hip and knee joint angle combinations were used to determine systematically the gait-

relevant joint angle ranges per each limb, borders of which characterize KA ranges for the participant group for each HA. Those ranges were narrowed using ensemble-averaged kinematic and kinetic data for KA ranges that characterize the clinical condition via exaggerated knee flexion positions and flexor moments. For each limb tested, the modeled MTU lengths were normalized per stride duration to match within 0-100% of the gait cycle (GC), and with respect to the participants' thigh lengths (Table 3.1).

Intraoperative measurements: For each KA tested, $F_{ST\_passive}$ measured in passive state and F_{ST} measured in active state, during a 500ms period (in the middle of the tetanus for F_{ST}) were averaged and recorded as muscle passive and total force, respectively.

Using a least-squares criterion, KA-F_{ST} data were fitted with a polynomial function (Eq. 4.1)

$$F_{ST} = a_0 + a_1 \cdot KA + a_2 \cdot KA^2 + ... + a_n \cdot KA^n \tag{4.1}$$

a_0, a_1 ... a_n are coefficients determined in the fitting process.

The lowest order of the polynomials that still added a significant improvement to the description of changes of KA-F_{ST} were selected using a one-way analysis of variance (ANOVA). KA-$F_{ST\_passive}$ data were also fitted in the same way.

The fitted data for each condition were used to calculate the mean (SD) of ST forces per KA. Range-F_{ST} (operational KA range of F_{ST} exertion i.e., range between the KA's at which, the minimum and peak F_{ST} is measured) was used as an active state metric.

Note that the same procedure was repeated to obtain MTU length-$F_{ST\_passive}$ and MTU length-F_{ST} data.

4.2.6 Statistics

Two-way ANOVA for repeated measures was used to compare (i) the overall mechanical characteristics of spastic ST muscle (factors: KA and condition), (ii) normalized MTU lengths (factors: %GC and participants). If significant main effects and an interaction were found, Bonferroni post hoc tests were performed to further locate significant within-factor force differences. Shapiro-Wilk test was used to check if the key active state metrics data are normally distributed. Range-F_{ST} calculated for each limb in Condition II, III and IV were compared with each other using paired-t test or Wilcoxon signed-rank test where appropriate. Differences were considered significant at $P < 0.05$.

4.3 Results

4.3.1 Gait-Relevant Joint Positions

Musculoskeletal modeling showed that for each limb tested, the KA ranges lie within 60.9-19.6° and 60.3-0° (for three limbs simulations yield hyperextension up to 2.3°) for HA= 45° and 20°, respectively.

Figure 4.2 shows the ensemble-averaged joint angles and moments in the sagittal plane. With less than one SD (for HA 11.1° and KA 8.8°) variation, the following parts of the GC characterize the pathological joint condition of the patients and indicate gait-relevant KA range per HA tested intraoperatively: (i) Exaggerated knee flexion occurs for 0-30% GC and 75-100%. For the patients, this indicates that at the start and end of GC, their knee is highly flexed instead of being typically extended, which compromises heel strike leading even to toe landing. In the gait data, HA= 45° is observed for 0-12% and 77-100% GC, and this matches with KA= 17-61°. (ii) The knee moment is flexor for 16-51% GC instead of being typically extensor and the knee power indicates absorption for 13-29% GC, which also agrees with the patients' limited

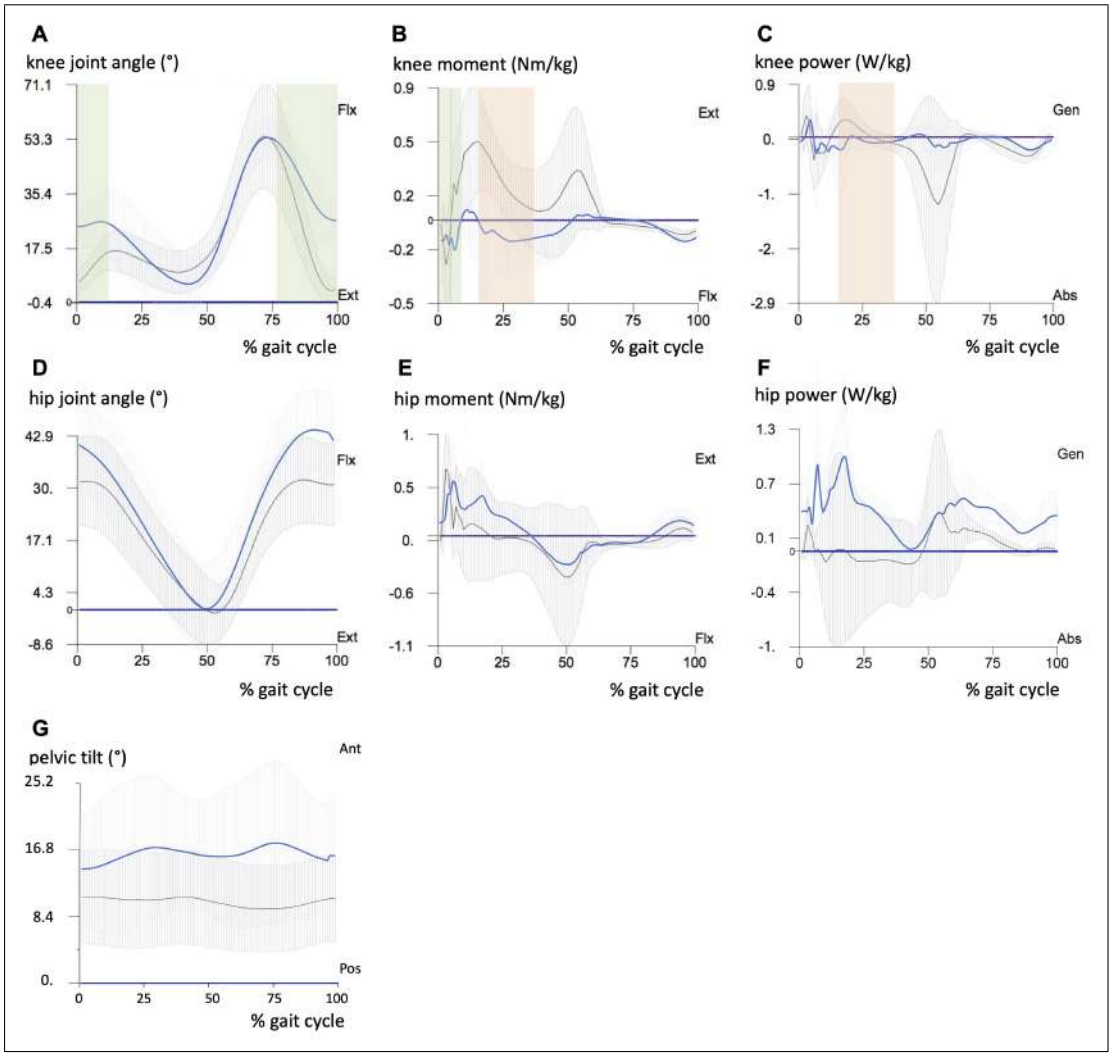

Figure 4.2 The patients' ensemble-averaged gait data (A), (B) and (C) for the knee, and (D), (E) and (F) for the hip (presented for completeness), showing joint angles, moments, and powers in the sagittal plane, respectively. Blue curves indicate the patients' data. The black curves show the normative data of BTS Bioengineering, Milan, Italy (TD children, n= 40, 5-12 years, 17-36 kg, 0.96-1.46 m evaluated using BTS Motion Analysis System and the Davis protocol in Motion Analysis Laboratory of San Raffaele Pisana Hospital, Rome, Italy). Flexion (Flx), extension (Ext), power generation (Gen), and absorption (Abs) are indicated. Shaded areas show gait data represented in intraoperative testing. Green: loading response (dotted line in (C) marks the beginning of flexor moment in CP) and terminal swing phases, orange: mid/terminal stance phases. Matching colored shaded areas indicate corresponding gait-relevant intraoperative data in Figure 4.3. Note that, unlike what (A) suggests, knee hyperextension was observed in only one of the limbs tested (Limb 10). This patient (7) showed exaggerated plantar flexion-knee extension couple. The reader is referred to Appendix A for individual knee joint angle data for each limb tested. (G) Shows anterior (Ant) and posterior (Pos) pelvic tilt, which indicates that high knee flexor moments are ascribable also to e.g., anterior pelvic tilt during gait.

knee extension condition. In the gait data, HA= 20° is observed for 16-37% GC, and this matches with KA= 0-33°. Consequently, intraoperative data for KA= 17-61° at HA= 45° and KA= 0-33° at HA= 20° were determined to represent the pathological movement during loading response/terminal swing, and mid/terminal stance phases of the patients' gait, respectively.

4.3.2 Intraoperative Data

Figure 4.3 shows KA-F_{ST} and KA-$F_{ST\_passive}$ characteristics for the entire KA range studied with the gait-relevant KA's indicated. ANOVA (factors: KA and condition) showed significant main effects of both factors on spastic ST forces, and a significant interaction ($P < 0.01$).

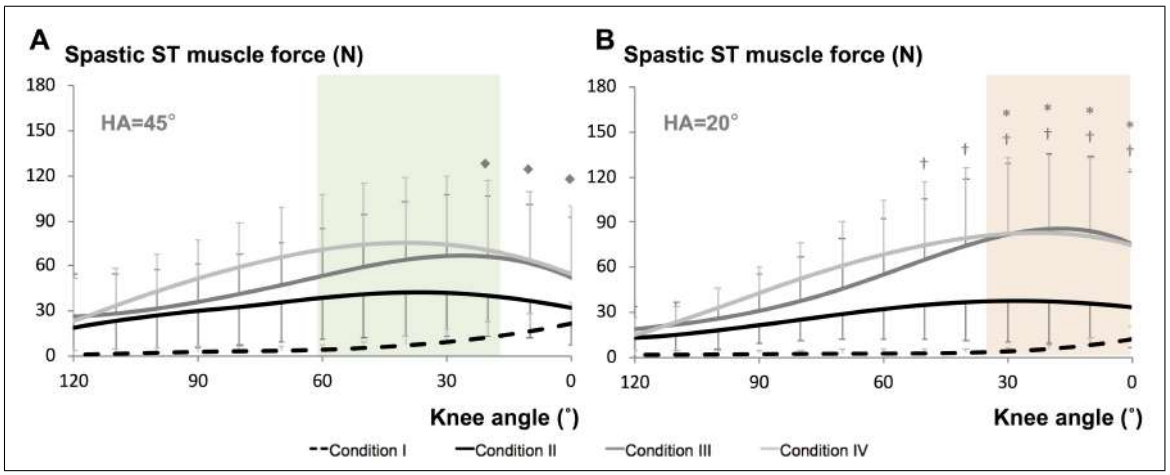

Figure 4.3 The mean (SD) of spastic ST forces of intraoperatively tested limbs per KA across the conditions tested for both HAs studied. (A) for HA= 45° and (B) for HA= 20°. The spastic ST forces in the passive state (condition I) are shown as dashed curves. The spastic ST was activated alone (condition II), simultaneously with its synergists, gracilis (GRA) and biceps femoris (BF) (condition III), and also with its antagonist rectus femoris (RF) (condition IV). Shaded areas show gait-relevant intraoperative data. Green: knee positions corresponding to loading response and terminal swing phases, orange: knee positions corresponding to mid/terminal stance phases. Significant differences among spastic ST forces at specific knee angles (Bonferroni post hoc test) are indicated: $\diamond$ shows for Condition I, the significant differences across the two HA tested indicating that spastic ST's passive forces for HA= 45° are higher in extended knee positions. $*$ shows for Condition II vs. III, and † shows for Condition II vs. IV, the significant differences for HA= 20°, indicating that co-activation of the synergistic and antagonistic muscles elevate spastic ST's active state forces in extended knee positions.

Passive and active state mechanics of spastic ST per se (conditions I & II) For both HA: (1) passive forces are low in flexed but increase towards extended knee positions with their peak equaling 52.2% and 31.4% of the peak active F_{ST} for HA= 45° and HA= 20°, respectively. Compared to HA= 20°, for HA= 45°, $F_{ST\_passive}$ are significantly higher (e.g., by 124.7% at KA= 20° within the gait-relevant KA-range, Figure 4.3 indicates specific KA's showing significant differences). (2) Total forces attain their minimum in the most flexed knee position, increase with knee extension till a maximum and decrease towards full knee extension (for HA= 45°, F_{ST}= 18.6 N, 42.2 N, 31.9 N at KA= 120°, 37° and 0°, and for HA= 20°, F_{ST}= 13.3 N, 37.9 N, 33.6 N at KA= 120°, 28°, and 0°, respectively). Compared to HA= 20°, for HA= 45°, F_{ST} are significantly higher in condition II (on average by 22.9%).

Effects of co-activation of other muscles (conditions III & IV) Compared to condition II, co-activation of the synergistic and antagonistic muscles caused spastic ST total forces to increase significantly ($P < 0.01$) in conditions III and IV: (i) For HA= 45°, on average by 42.0% and 72.5%, (ii) for HA= 20°, maximally by 131.8% and 123.7% (Figure 4.3 indicates specific KA's showing significant differences), respectively. Differences between active vs. passive state forces elevate: peak $F_{ST\_passive}$ equals maximally 33.0% (condition III, HA= 45°) and minimally 14.3% (condition IV, HA= 20°) of peak F_{ST}.

Table 4.1 shows Range-F_{ST} per each limb and their mean (SD). HA= 45°: no significant differences in Range-F_{ST} were found across any condition. HA= 20°: compared to condition III, Range-F_{ST} was significantly narrower in condition IV (by 18.1%, Wilcoxon signed-rank test, P= 0.018), whereas other comparisons showed no significant differences. Across different HAs, no significant differences were shown in Range-F_{ST} for conditions II and IV but, in condition III, compared to HA= 20°, Range-F_{ST} was significantly narrower for HA= 45° (by 33.2%, Wilcoxon signed-rank test, P= 0.022).

Table 4.1
Effects of conditions on Range-F_{ST} for each limb tested.

Limb	Range-F_{ST} (°) for KA= 45°			Range-F_{ST} (°) for KA= 20°		
	Condition II	Condition III	Condition IV	Condition II	Condition III	Condition IV
1	120	35	79	120	120	120
2	80	96	95	95	95	91
3	98	98	97	58	112	112
4	120	120	76	120	107	94
5	120	96	44	120	102	81
6	66	87	74	86	108	107
7	66	86	80	90	90	89
8	79	0	73	120	120	120
9	44	81	64	120	120	69
10	20	0	110	0	97	0
Mean (SD)	81 (34)	70 (43)	79 (18)	93 (39)	107 (11)	88 (35)

4.3.3 Modeled MTU Length Changes and MTU Length-F_{ST} Characteristics

ANOVA (factors: %GC and participants) showed significant main effects of both factors on normalized MTU lengths (Figure 4.4), but no significant interaction (on average 14.1% shorter in the patients). MTU length changes of spastic ST within the GC are below 14% (mean (SD) 13.4 (2.8)) with the longest lengths attained during the terminal swing phase.

Figure 4.5 shows per limb, MTU length-$F_{ST\_passive}$ and MTU length-F_{ST} characteristics with the gait-relevant MTU lengths indicated. Condition I: Passive forces are low in short MTU lengths but increase towards longer ones. Condition II: (i) at the shortest MTU length modeled, F_{ST} is maximally 45.0% (limb 8) and minimally 9.1% (limb 5) of peak F_{ST} for limbs 1-9, whereas for limb 10, 94.2% of that is encountered. (ii) At the shortest MTU length encountered during gait, F_{ST} is maximally 99.2% (limb

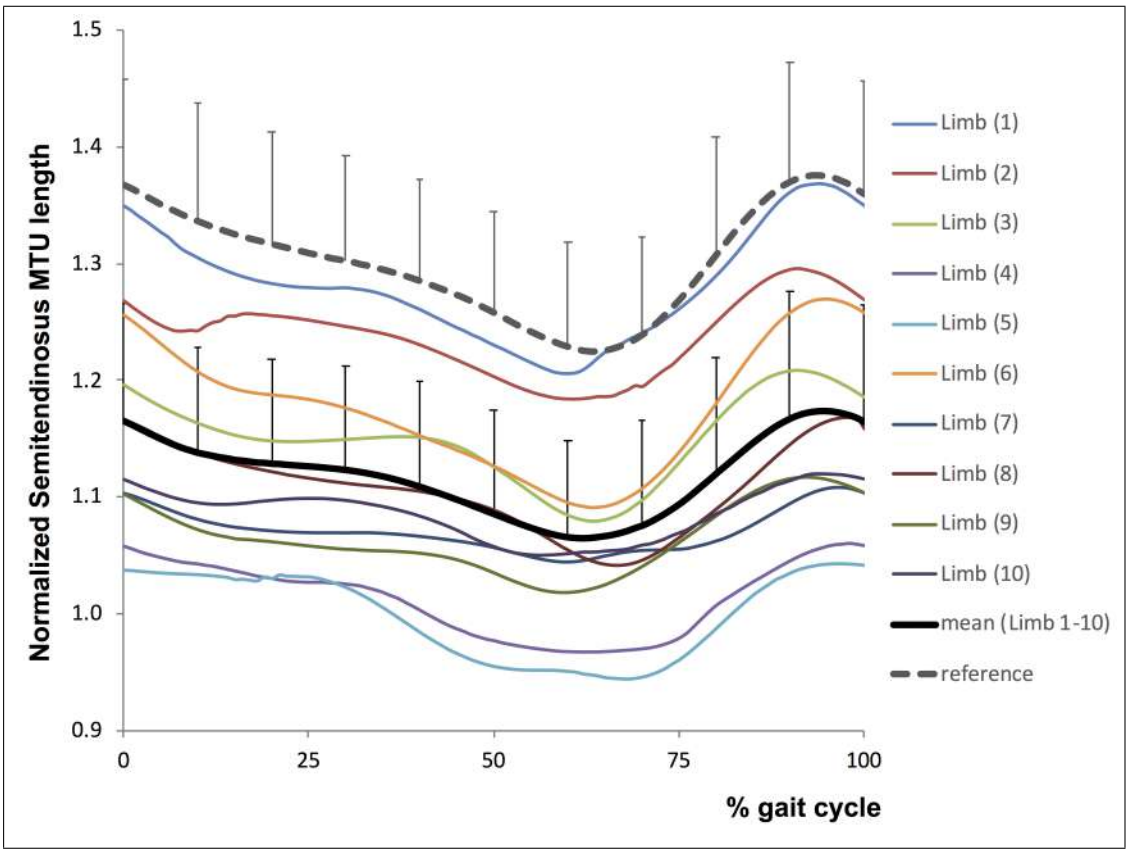

Figure 4.4 Normalized muscle-tendon unit lengths of ST within the GC. Patients' data for each limb tested intraoperatively were presented individually and as mean (SD) (black solid line). Reference participants' (n = 7, 7-9 years) data were shown as mean (SD) (grey dashed line). MTU lengths were normalized with respect to the participants' thigh lengths.

7) and minimally 16.5% (limb 5) of peak F_{ST} for limbs 1-9, whereas, for limb 10, 96.7% of that is encountered. (iii) At the longest MTU length, on the other hand, F_{ST} is high (minimally 81.2% of the peak F_{ST} for limb 3 and maximally 95.2% for limb 10), except for limb 5 (20.5% of the peak F_{ST}). Conditions III & IV: For limbs 3-8, co-activation of the synergistic and antagonistic muscles caused spastic ST total forces to increase (up to several folds for limb 3). However, for limbs 1-2 and 9-10 force changes are not consistent both in amplitude and direction (also force decreases are observed e.g., for limb 2 and in condition III).

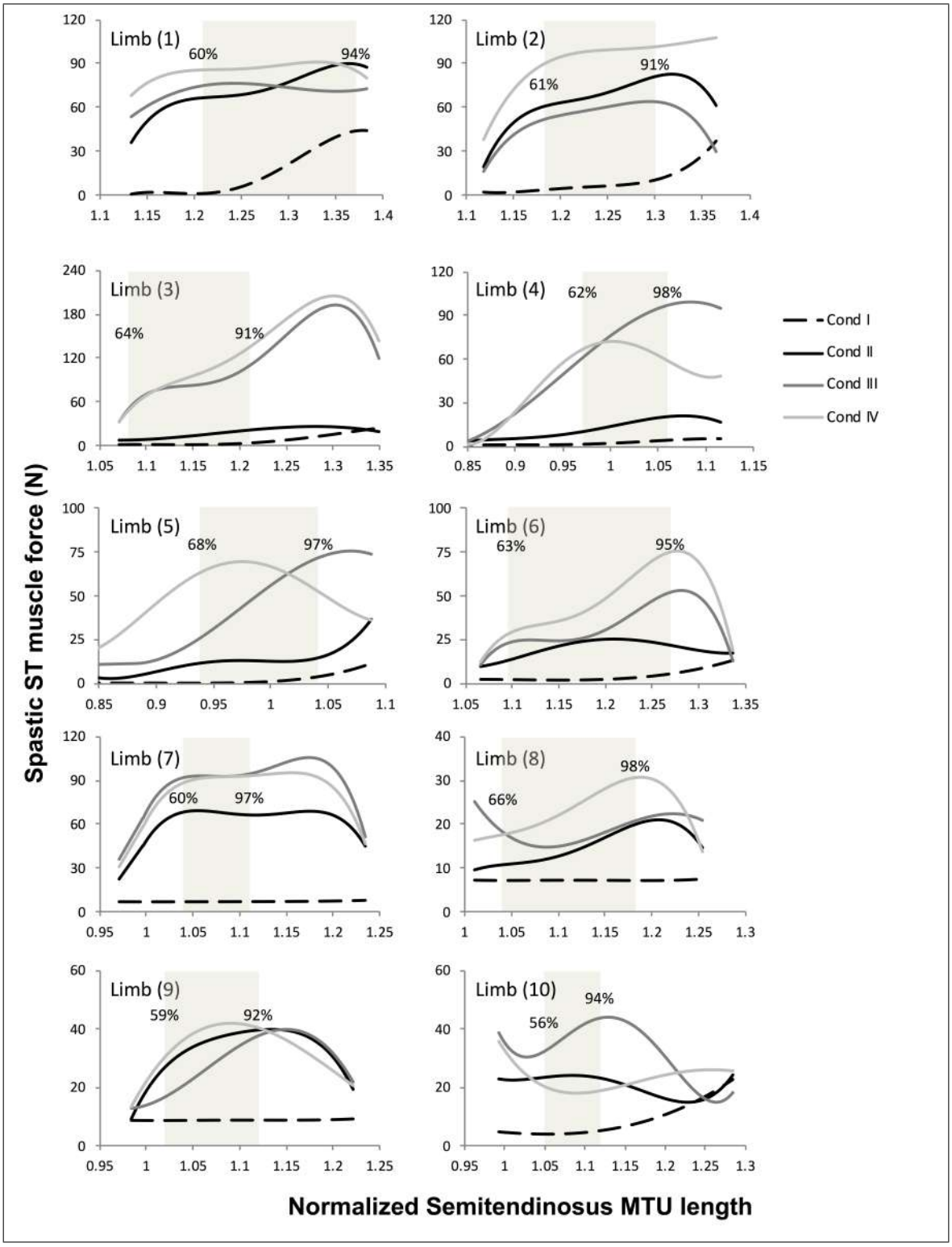

Figure 4.5 Modeled spastic ST forces of each limb as a function of normalized muscle-tendon unit lengths. The spastic ST forces in the passive state (condition I) are shown as dashed lines, whereas those in active states (conditions II-IV) are shown as solid lines. For each limb, the first and the last data points indicate the shortest and longest MTU lengths determined using the intraoperatively tested KA and HA combinations, whereas the shaded areas indicate gait-relevant data bound by the longest and shortest operational MTU lengths encountered within a gait cycle. The percentages indicated in each panel show the corresponding percent gait cycle as approximated by the musculoskeletal modeling. MTU lengths were normalized with respect to the patients' thigh lengths.

4.4 Discussion

The present study indicates the following: (1) $F_{ST\_passive}$ comprise only a certain part of F_{ST}. Therefore, active state forces dominate the tendon force for the entire KA range including the gait-specific KA range. Note that, the passive forces being higher in HA= 45° than in HA= 20° is ascribable to ST being longer in the more flexed hip position. (2) F_{ST} typically approximates its peak value in the gait-specific KA range and additionally (3) increases substantially in conditions III and IV, further establishing the role of active state via co-activation of other muscles. Therefore, intermuscular mechanical interactions affect spastic ST muscle's potential contribution to joint moment. Moreover, a narrower Range-F_{ST} shown indicates that this may affect spastic ST muscle's contribution to joint movement. Although adverse consequences are conceivable, implications of these effects on the patients' gait require specific testing.

In TD children, during the terminal swing, the knee attains an extended position to prepare the limb for the subsequent stance phase and at initial contact, the knee attains almost full extension. In the loading response, the knee starts to become flexed for absorbing the shock of weight transfer and to maintain stability. The hamstrings act to decelerate the swinging leg and later stabilize the knee in co-contraction with the RF. Both phases involve the activity of many lower limb muscles including the present target muscle ST and the other muscles co-activated in this study [89,141–143]. Terminal-swing knee extension was limited in the present participants (Figure 4.2A). Although the gait data show no change in the extensor knee moment for part of the loading response, for the remaining part (approximating 6-12% GC, Figure 4.2B), the knee moment is flexor. However, our intraoperative data cannot be directly related to that: (1) Collection of TD data intraoperatively was currently not possible, and normative TD children data of BTS Bioengineering (Figure 4.2) were utilized. (2) Externally applied moments to bring the leg in the passive state into the tested joint positions could not be measured. (3) In the active state, unlike the activation levels occurring during gait, the muscles were activated maximally. (4) Only distal ST forces were measured. Consequently, the findings are incapable of indicating the passive resistance at the joint. Besides, it is not known whether the tested co-activation

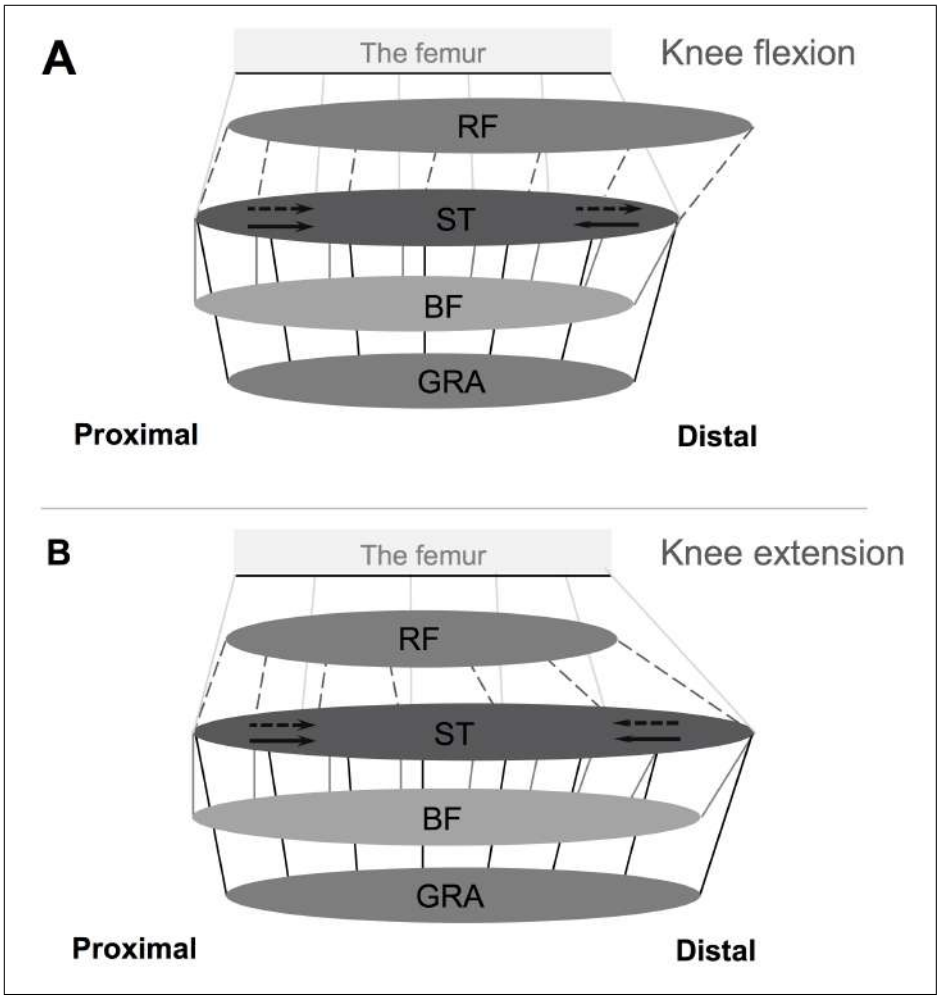

Figure 4.6 Schematic illustrating myofascial loads on the ST due to muscle relative position differences between the GRA, BF, and RF muscles and the ST. Relative position changes in (A) flexed and (B) extended knee positions are exaggerated for clarity. Actions of the studied muscles: in the knee, the ST, GRA, and BF are flexors and RF is an extensor; in the hip, the ST and BF are extensors and GRA and RF are flexors. Relative position differences can occur due to differences in moment arms and based on the actions of these muscles. This will stretch their mutual epimuscular connections (solid lines represent epimuscular connections interconnecting the ST to the GRA and BF and dashed lines represent those interconnecting the ST to the RF). Consequently, myofascial loads acting on the ST will develop due to its mechanical interaction with its synergists (solid arrows) and its antagonist (dashed arrows). Note that, if they are directly to be integrated into the force measured at its tendon, myofascial loads in the proximal direction can elevate the distal force of ST. However, not all of them are proximally directed suggesting that their mechanism of effects includes manipulation of sarcomere lengths such that they attain length favoring higher force production.

conditions increased also other hamstrings' forces and if a relatively higher force than the sum of the forces produced by each muscle when activated alone can be exerted at the knee joint. However, the present intraoperative data do show the target muscle's capacity to affect joint mechanics and indicate that compared to condition II, conditions III and IV elevated that substantially. The effect of condition IV remarkably shows that co-activation of an extensor muscle increases the force of a knee flexor and suggests the relevance of agonist-antagonistic mechanical interaction in CP. For such epimuscular myofascial force transmission (EMFT) [9, 90, 144] muscle relative position changes [13, 21] are central. ST's bigger moment arm than the GRA and BF [108] can cause different length changes among co-activated synergists. Besides, the GRA is a hip flexor unlike the ST and BF. Therefore, the ST was conceivably at a longer length both proximally and distally leading to relative position differences in tested joint positions. The position difference between the RF and the hamstrings is obvious as knee extension and its hip flexor function shorten the RF distally and proximally Figure 4.6. Consequently, epimuscular connections (e.g., neurovascular tracts and compartmental fasciae) get stretched, become stiffer, and exert forces and/or transmit some of the forces of the co-activated muscles on spastic ST. Such myofascial loads acting on its epimysium can impose effects internally via the continuity of intramuscular connective tissues and multimolecular mechanical linkages between the endomysium and the muscle fibers along their full-peripheral length [91]. Finite element modeling [17, 145–147] and in vivo imaging analyses [102, 103, 128, 148] showed effects of this mechanism manipulating length changes along muscle fibers and force production. Consequently, conditions III and IV may elevate spastic ST forces via the following mechanisms. Simple: myofascial loads are integrated into the distal force. In condition IV, the antagonist operates at longer lengths in flexed knee positions hence myofascial loads are plausibly distally directed (Figure 4.6A). This should reduce the distal force, but against the simple mechanism, the opposite was shown. Complex: myofascial loads impose effects inside the muscle and alter sarcomere lengths, causing them to operate at lengths favoring higher force production (e.g., those in the descending limb of their length force curves become shorter and others in the ascending limb become longer towards maximal myofilament overlap). This is tenable.

For the mid/terminal stance phase, the present gait data shows knee flexor moment and consequent power absorption for the mid-stance owing to knee extension (Figure 4.2B). Unlike the intraoperative testing conditions, this phase involves partial activity of lower limb muscles including ST [142]. However, pronounced EMFT effects are plausible at lower activation levels [149]. The narrower Range-F_{ST} (Figure 4.3B, condition IV) indicates again the complex mechanism as such change is associated with the parallel distribution of sarcomere lengths (i.e., differences in mean sarcomere lengths of different muscle fibers) [17, 50, 81, 125]. For HA= 20°, the RF is lengthened proximally, hence can produce higher forces in extended knee positions. Decreased Range-F_{ST} suggests that RF activation elevated myofascial loads, which reduced the heterogeneity of parallel distribution by limiting sarcomere lengthening in concert with the elevated active state forces.

Note the findings OpenSim analyses show. First, modeling indicates that spastic ST operates at shorter MTU lengths during gait. The muscle's length change within the GC is limited to 14%, which agrees with van der Krogt et al. [150]. It attains the longest lengths towards the end of the swing phase (Figure 4.4, 95% GC). Although no model data is available to distinguish the muscle belly and tendon lengths, intraoperatively measured highest spastic ST forces in extended knee positions don't support a short belly length. Second, assessment of intraoperatively measured spastic ST forces as a function of MTU lengths allows for further elaboration and indicates the following: (i) for a majority of the limbs for conditions I and II, muscle forces are low in shorter MTU lengths and increase only at longer MTU lengths. This does not support the presence of high flexor force exertion in short lengths of spastic ST both in passive and active states. Additionally, also the MTU length vs. muscle force data do not support that sarcomeres attain longer lengths non-favorable for active force generation. (ii) Yet one limb shows the opposite for short and another for long MTU lengths, indicating patient-specific variable mechanics of spastic ST. Similarly, the effects of conditions III and IV show variability across limbs. Note that, unlike the intraoperative experiments, the model does not account for the muscles' intermuscular mechanical interactions. Intraoperatively shown altered forces and Range-F_{ST}, therefore, implies that the mechanism of these effects may be more complex than a shortened muscle

belly, but maybe ascribed to sarcomere length changes within the muscle. However, this requires specific testing in new studies.

4.5 Conclusion

Combining intraoperative experiments with gait analyses, the present findings show that intermuscular mechanical interactions cause elevated active state forces of the spastic ST, compared to which, the passive state forces remain limited even in extended knee positions. The increased active state forces of the muscle in hip and knee joint position combinations representative of the terminal swing, loading response and mid/terminal stance phases agree with kinematic and kinetic metrics encountered in the CP patients, particularly with knee flexor moments, which are extensor in TD children. It has been considered that co-contraction is excessive in CP for reasons of stability but causes hampered movement due to increased joint stiffness (e.g., [151]). Our findings show that there is a mechanical reason for the co-activation of muscles affecting the joint movement adversely. We suggest that intermuscular mechanical interactions are different in CP patients compared to TD children possibly due to adaptations of myofascial structures and this leads to an improper influence of particularly antagonistic muscles on knee flexor action. This needs to be studied further with measurements conducted also in TD children.

5. THE FORCE-LENGTH RELATIONS OF SPASTIC KNEE FLEXOR MUSCLES, SEMITENDINOSUS AND GRACILIS

5.1 Introduction

Muscle belly length is a key metric to monitor a muscle's ability to lengthen and shorten, hence estimating its changes in vivo is of interest particularly in patients with cerebral palsy (CP). Much of our knowledge on such kinematics of muscle-tendon unit (MTU) in CP has been derived using ultrasound techniques. Several studies have focused on the ankle joint and showed that the spastic gastrocnemius muscle has a shorter muscle belly compared with that of typically developing (TD) children (e.g., [152]). Some of the studies [111, 153] have attributed that to a reduction in fascicle length in patients [154–156], whereas others showed no fascicle length change between CP vs. TD groups [30,118,157]. A shorter muscle belly has also been attributed to a reduction in the cross-sectional area of fascicles [158]. Barber et al. [30] showed a reduction in muscle volume without a reduction in fascicle length, leading to a conclusion that the main determinant for decreased muscle volume is the cross-sectional area, rather than a change in fascicle length. On the other hand, examination of length changes in the tendon component of the MTU is relatively limited. Spastic gastrocnemius MTU has been shown to exhibit a longer-than-normal tendon [153, 159], and remarkably, Wren et al. [153] pointed out that the gastrocnemius recession surgery or Achilles tendon lengthening does not restore normal MTU architecture, as longer tendon lengths and shorter muscle fascicles were observed in surgically treated children. As such architectural metrics affect the muscle's force-generation capacity, and hence its function, identification of MTU length changes of commonly surgically treated flexor muscles is relevant for a better operational outcome in patients with CP.

Although studies do not agree on the alterations observed in the microstructure of spastic muscles, as in fascicle length and diameter, clinically, spastic muscles of patients with CP, are considered as shortened (e.g., [34]) which are consequently expected

to produce high forces in flexed joint positions, hence at shorter muscle lengths. Orthopedic surgeries, therefore, aim at reducing the resistance at the joint to extension by limiting spastic muscle's resistance to lengthening.

Intraoperative studies in which activated muscles' forces were measured directly at the distal tendon and as a function of knee angle showed that spastic semitendinosus [43] and gracilis [44] muscles produce their peak force in extended knee positions and only a limited portion of that is measured in flexed positions. However, a relationship characterizing force production of spastic muscles as a function of changes in their MTU lengths is lacking. Recent intraoperative studies [160, 161] have obtained such directly measured muscle force data not only in the muscular activation state, but also in the passive resting state, and also allowed us to interpret the muscular forces for functional joint angles related to walking. Still, in addition to showing the relationship between joint angle and muscle force, revealing the direct relation of a muscle's force to its MTU length is meaningful in terms of testing the basic clinical expectation mentioned above. Therefore, combining intraoperative findings (spastic muscle forces measured at various muscle lengths by manipulating the joint angles during surgery, as well as in different conditions) with participants' musculoskeletal models developed based on their gait analyses, we aimed to obtain MTU length - muscle force data for spastic semitendinosus (ST) and gracilis (GRA) to study their muscular mechanics and EMFT effects on them concerning muscular lengths.

The following hypotheses were tested separately for the spastic ST and GRA muscles: within the gait-relevant MTU length range; spastic muscle (i) operates at short MTU lengths compared to that of TD children, exerts higher (ii) passive and (iii) active forces at shorter lengths, and (iv) shows increased forces due to co-activation of other muscles.

5.2 Methods

5.2.1 Gait and Muscle Force Datasets

Gait data are required for (i) performing patient-specific musculoskeletal modeling so that changes in target muscle lengths can be revealed throughout the gait cycle (GC), and for (ii) matching muscle forces corresponding to gait-related MTU lengths. For those purposes, 3D-gait analysis data belonging to the common patient group in our previously published articles [160, 161] were acquired. In those studies, seven patients (male: mean age 9 years 2 months, range 6-13 years, standard deviation 2 years 10 months) with spastic CP, however no prior remedial surgery were included. The Gross Motor Functional Classification System (GMFCS) levels were II. Overall pre-operative clinical examinations have indicated a severely limited knee range of joint motion for the patients and all of them were undergoing remedial surgery including the release of hamstrings and hip adductors.

The patients' pre-surgery 3D-gait analysis data were obtained by using a motion analysis system (ELITE 2002, BTS Bioengineering, Milan, Italy) with six infrared cameras and two force plates (Kistler Instrumente AG, Winterthur, Switzerland) and implementing Helen Hayes Marker Placement Protocol [123]. Kinetic and kinematic data were collected with the patient standing in an anatomical position and during walking at a self-selected speed.

Isometric spastic muscle forces were measured intraoperatively by fixing buckle force transducers (TEKNOFIL, Istanbul, Turkey) over the distal tendons of the ST and the GRA for a total of ten limbs. The measurement conditions included in the study were: (i) passive state (no muscular activation representing resting state), (ii) individual activation (ST or GRA was activated alone), and (iii) simultaneous activation (the ST, GRA, biceps femoris, and rectus femoris muscles were stimulated endorsing EMFT). Pairs of gel-filled skin electrodes (Kendall H92SG, Covidien, MA, USA) were placed over the target muscle bellies, and a custom made, constant current high voltage source (cccVBioS, TEKNOFIL, Istanbul, Turkey) was used to impose supramaximal muscle

stimulation. Muscle forces were measured at two different hip angles equaling 45° and 20°, for each of which, the knee angle was changed from 120° to full extension in 30° increments. Therefore, ST and GRA muscle forces measured in 10 different hip and knee joint angle combinations and at three different testing conditions were included in the study.

5.2.2 Musculoskeletal Modeling

Musculoskeletal models were developed for each participant (patients and age-matched TD individuals) using OpenSim to calculate MTU lengths of the ST and the GRA muscles corresponding to each hip and knee joint angle combination tested intraoperatively and to define patient-specific gait-relevant MTU length ranges, thereby, ultimately to analyze patient-specific gait-relevant spastic MTU length - muscle force data for muscles ST and GRA. The gait_2392 model which comprises 23 degrees-of-freedom, and 92 musculotendon actuators per leg [140] was used. Each model was scaled to the participants' anthropometry using the scale tool, based on body mass and surface marker locations obtained during a static trial performed during the gait analysis. The inverse kinematic tool was used to calculate MTU lengths of the target ST and GRA muscles for each participant within the time frame of gait as well as the muscles' MTU lengths corresponding to paired hip and knee joint angles used during intraoperative testing.

5.2.3 Data Processing and Statistics

For each limb tested, the modeled MTU lengths were normalized per stride duration to match within 0-100% of GC, and with respect to the participants' thigh lengths.

For each certain joint angle combination tested intraoperatively, muscle forces measured in the passive state and also in response to muscle activations ($F_{muscle\_passive}$

and F_{muscle}, respectively) were matched to the corresponding MTU lengths. Using a least-squares criterion, MTU length - F_{muscle} data were fitted with a polynomial function (Eq. 5.1).

$$F_{\text{muscle}} = a_0 + a_1 \cdot MTUlength + a_2 \cdot MTUlength^2 + ... + a_n \cdot MTUlength^n \quad (5.1)$$

a_0, a_1 ... a_n are coefficients determined in the fitting process.

The lowest order of the polynomials that still added a significant improvement to the description of changes of MTU length - muscle force was selected using a one-way analysis of variance (ANOVA). MTU length - $F_{muscle\_passive}$ data were also fitted in the same way.

Statistical analyses were performed separately for the ST and the GRA muscles. Two-way ANOVA (factors: %GC and participant groups) was used to compare the patients' normalized MTU lengths to those of the seven age-matched TD children to test the first hypothesis. To test the second and the third hypotheses, Spearman's rank correlation coefficient (ρ) was calculated to seek a correlation between the muscle's operational length (represented by mean MTU length within gait cycle) and muscular force characteristics (the percent force at shortest MTU length of peak force, either in passive or in active conditions), within gait-relevant MTU length range. The latest hypothesis was tested by using the mean percent muscle force increase within gait-relevant MTU length range calculated between conditions (ii) and (iii) as a metric for, and ρ was calculated to seek a correlation between the muscle's operational length and EMFT effects. Differences were considered significant at $P < 0.05$.

5.3 Results

5.3.1 Modeled MTU Length Changes

ANOVA showed significant main effects of both factors on normalized MTU lengths, but no significant interaction. MTU lengths of spastic ST and GRA are shorter (on average by 14.1% and 15.4%, respectively) compared to those of TD (Figure 5.1), confirming the first hypothesis.

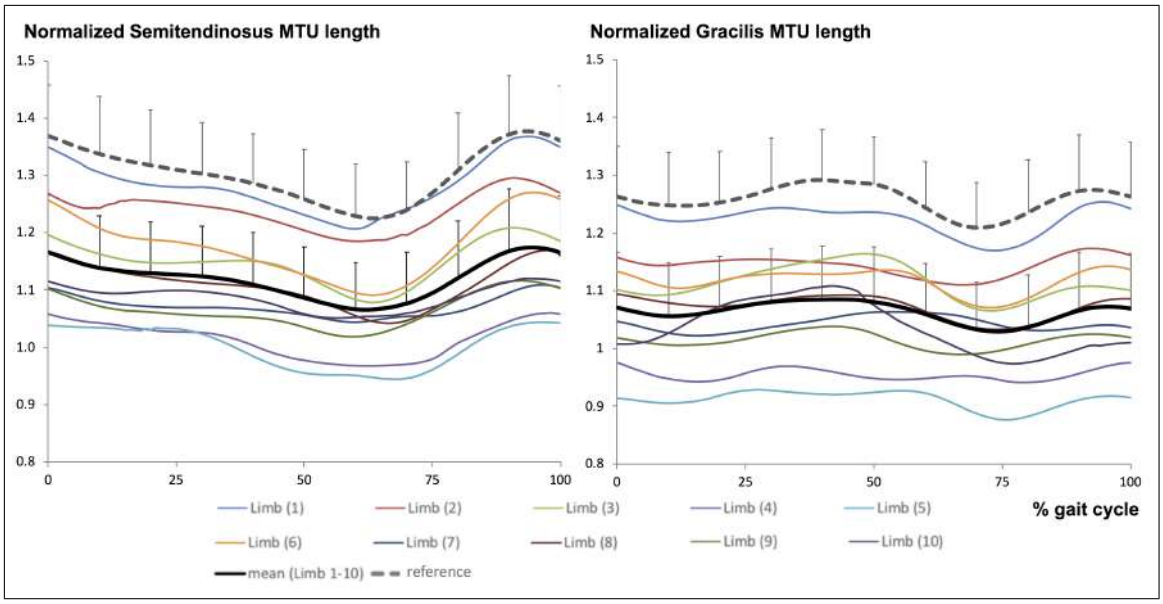

Figure 5.1 Normalized MTU lengths of the ST and the GRA muscles within the GC. Patients' data for each limb were presented individually and as mean (SD) (black solid line). Reference data were shown as mean (SD) (grey dashed line). MTU lengths were normalized with respect to the participants' thigh lengths.

5.3.2 MTU Length - Muscle Force Characteristics

Figure 5.2 and 5.3 show MTU length - muscle force characteristics for spastic ST and GRA muscles per limb, respectively, with the gait-relevant MTU length ranges indicated.

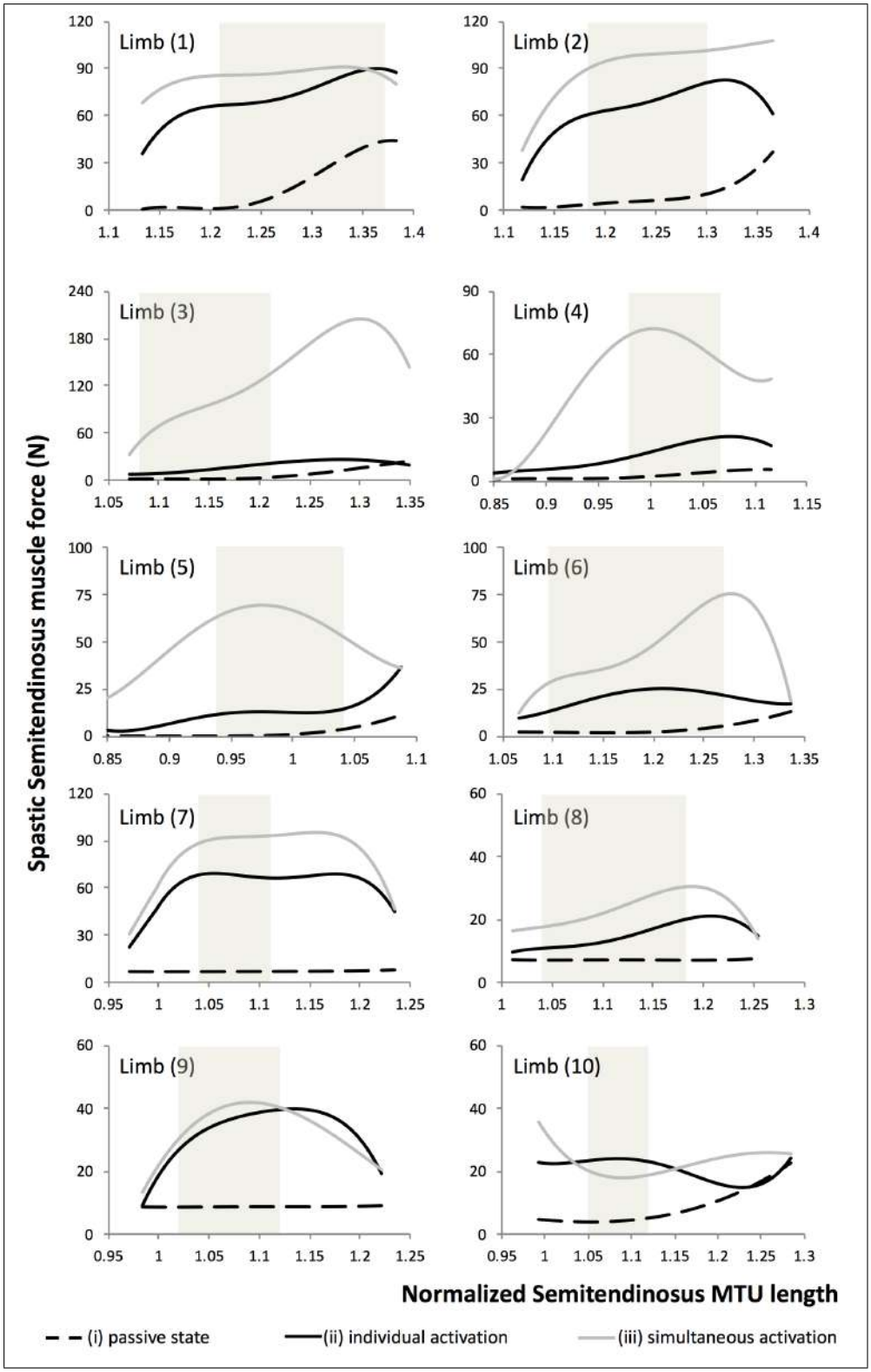

Figure 5.2 Spastic ST muscle forces of each limb tested as a function of its normalized muscle-tendon unit lengths. For each limb, the first and the last data points indicate the shortest and longest MTU lengths determined using the intraoperatively tested hip and knee joint angle combinations, whereas the shaded areas indicate gait-relevant data bound by the longest and shortest operational MTU lengths encountered within a gait cycle.

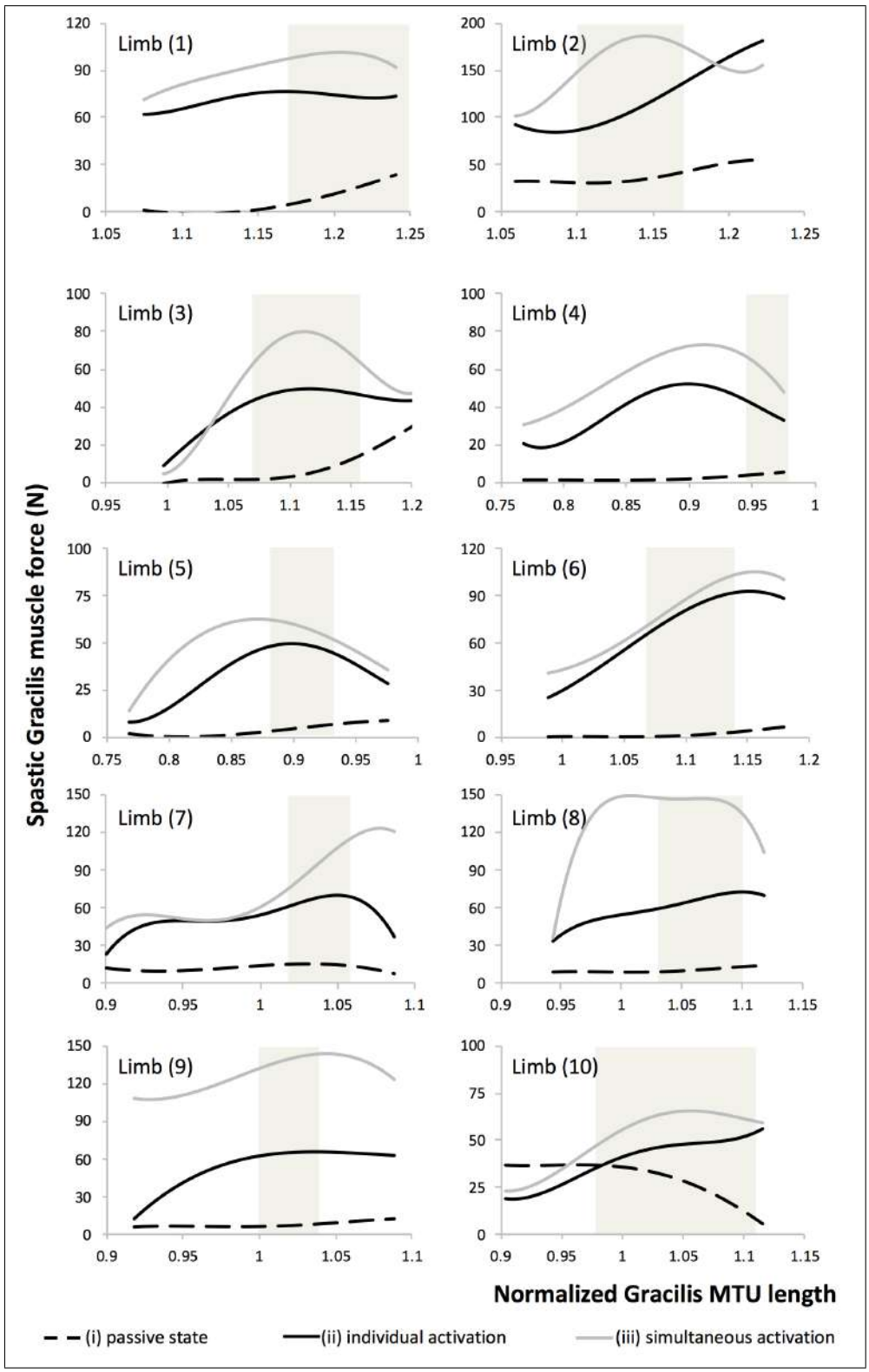

Figure 5.3 Spastic GRA muscle forces of each limb tested as a function of its normalized muscle-tendon unit lengths. For each limb, the first and the last data points indicate the shortest and longest MTU lengths determined using the intraoperatively tested hip and knee joint angle combinations, whereas the shaded areas indicate gait-relevant data bound by the longest and shortest operational MTU lengths encountered within a gait cycle.

Table 5.1
The key metrics on MTU length - ST muscle force characteristics for each limb tested. $\%F_{ST\_passive\ peak}$ | shortest MTU length = the percent of peak ST muscle passive force exerted at the shortest MTU length in measurement condition (i); $\%F_{ST\ peak}$ | shortest MTU length = the percent of peak ST muscle active force exerted at the shortest MTU length in measurement condition (ii); $\%F_{ST}$ change = the percent change of ST muscle active forces and direction of how the force changed between conditions (ii) and (iii) due to added simultaneous activation of other muscles. All data were calculated patient-specifically within their gait-relevant MTU length ranges.

Limb	Normalized MTU length (mean)	*Condition (i)* $\%F_{ST\_passive\ peak}$ | shortest MTU length	*Condition (ii)* $\%F_{ST\ peak}$ | shortest MTU length	*Condition (ii) vs (iii)* $\%F_{ST}$ change
1	1.282	2.16	73.96	16.38
2	1.238	35.08	75.81	41.50
3	1.148	21.47	39.88	592.70
4	1.013	32.04	47.30	362.61
5	0.999	3.36	81.14	410.23
6	1.175	44.55	48.79	114.27
7	1.070	99.19	99.23	35.85
8	1.107	99.57	56.78	69.25
9	1.064	98.66	65.97	11.05
10	1.086	77.52	97.47	-22.77
	Mean (SD)	51.4 (39.2)	68.6 (20.6)	163.1 (212.6)

At the shortest gait-relevant MTU length, the ST and the GRA passive forces were 51.4 (39.2)% and 55.8 (33.9)% of the peak passive force; and the active forces were 68.6 (20.6)% and 84.6 (13.7)% of the peak active force (Table 5.1 and 5.2, for ST and GRA muscles, respectively). Passive state forces show an increase at longer lengths, whereas active state force characteristics vary in a patient-specific way. Spearman's rank correlation indicated weak correlations between muscle's operational length and muscular force characteristics for the spastic ST (ρ= -0.16, P= 0.66, and ρ= -0.15, P= 0.68), and also for the GRA (ρ= -0.27 P= 0.45, and ρ= -0.30 P= 0.40, for passive and active states, respectively). Therefore, the second and the third hypotheses were rejected.

Table 5.2
The key metrics on MTU length - GRA muscle force characteristics for each limb tested. $\%F_{GRA\_passive\ peak}$ | shortest MTU length = the percent of peak GRA muscle passive force exerted at the shortest MTU length in measurement condition (i); $\%F_{GRA\ peak}$ | shortest MTU length = the percent of peak GRA muscle active force exerted at the shortest MTU length in measurement condition (ii); $\%F_{GRA}$ change = the percent change of GRA muscle active forces and direction of how the force changed between conditions (ii) and (iii) due to added simultaneous activation of other muscles. All data were calculated patient-specifically within their gait-relevant MTU length ranges.

Limb	Normalized MTU length (mean)	*Condition (i)* $\%F_{GRA\_passive\ peak}$ | shortest MTU length	*Condition (ii)* $\%F_{GRA\ peak}$ | shortest MTU length	*Condition (ii) vs (iii)* $\%F_{GRA}$ change
1	1.223	20.63	100.00	34.02
2	1.144	70.83	64.75	62.49
3	1.114	11.19	85.13	53.88
4	0.954	63.63	100.0	54.44
5	0.912	46.16	96.01	20.22
6	1.117	5.81	72.29	9.18
7	1.042	98.98	89.54	46.33
8	1.073	70.18	83.15	119.37
9	1.015	70.54	91.59	114.20
10	1.037	100.00	63.34	31.66
	Mean (SD)	55.8 (33.9)	84.6 (13.7)	54.6 (36.6)

5.3.3 Effects of EMFT on MTU Length - Muscle Force Characteristics

Simultaneous activation caused the target muscles' forces to increase significantly. The force increases between conditions (ii) and (iii) within the gait-relevant MTU length ranges were minimally by 11.1%, up to several folds for the spastic ST, whereas for the GRA the percent change was between 9.2-119.4. A very weak correlation between muscle operational length and EMFT effects was shown (ρ= -0.16 P= 0.65) only for the spastic ST. No correlation was found between GRA muscle's operational length and EMFT effects on its force characteristics. Therefore, the last hypothesis was rejected for both muscles.

5.4 Discussion

Combining previously published intraoperative muscle force data with newly performed musculoskeletal modeling, novel MTU length - muscle force relations for spastic knee flexors, ST, and GRA muscles were obtained.

The modeling showed in concert with the clinical considerations that both spastic ST and GRA may be shortened muscles that produce higher forces in shorter muscle lengths. However, this possibility implies dwelling on two points: (i) First, we consider that the availability of the peak muscle force at the lowest gait-relevant MTU length would provide an ideal match between the clinically diagnosed impaired movement and the experimentally determined MTU length - muscle force characteristics by means of representing pathology. In this regard, $\%F_{ST\_passive\ peak}$ | shortest MTU length and $\%F_{ST\ peak}$ | shortest MTU length data are very functional for interpreting whether the force-generating behavior of the spastic muscles is only in the descending portion of their MTU length - muscle force curve, exclusively. The ratio of the passive forces produced by both the spastic ST and GRA muscles of the shortest MTU length to their maximum passive force is around 50% percent within the gait-relevant GC. This may lead us to conclude that the passive forces of the spastic knee flexor muscles tested are high in shorter MTU lengths. However, notably, muscle force measurements

have not been done under neuromotor blockade anesthesia which disappears the active muscle tone [131], meaning that the presented passive forces may not have isolated pure passive state properties, and suggesting that the real passive state forces maybe even smaller than those reported. Moreover, the fact of this ratio is unknown in TD children prevents us from making a reasonable comparison between healthy and spastic muscles' passive force characteristics. Regarding muscle forces measured in response to selective muscular activation either of the ST or the GRA, a majority of the limbs exerted most of the maximum force they can produce at the shortest MTU length within the gait-relevant range. For spastic ST, this ratio is higher than 50% in seven out of ten limbs (Limbs 3, 4, 6), whereas for spastic GRA, all limbs showed fairly high percentages with a minimum of 63.34% for Limb 10. Therefore, it is plausible to conclude that comparing the forces produced by the muscle in the resting and activated states, the dominant component of the exaggerated force in shorter MTU lengths is the active force, rather than passive. Importantly, as the intraoperative force measurement technique applies the maximum muscular contraction to quantify the maximal capacity of the spastic muscles in limiting muscular extension, this would be wrong to think that these measured forces will be observed directly during walking. Yet, it can be clearly stated that force-generating capacity is high for spastic knee flexor muscles, ST, and GRA even in longer MTU lengths. (ii) Secondly, the present data contrasts intraoperative data [43,44] which show only low forces in flexed knee positions. However, those studies presented joint angle - muscle force characteristics of spastic muscles as mechanical structures, focusing on all possible knee joint angles, not functional joint ranges specific to certain movements like walking, and, therefore, made statistical analyses and inferences within the entire joint range to define spastic muscle functioning as a whole. The present study differs from the previous studies in this respect, as here all analyses were done within the patient-specific gait-relevant MTU length ranges. Still, because the model does not distinguish the muscle-belly and tendon lengths, it cannot isolate shorter muscle-belly lengths and how this compares to the data of TD children remains unknown.

Most importantly, the absence of a strong correlation between shorter operational muscle length and higher force production either in passive or in active conditions

highlights the influence of other factors (i.e., muscle structural proteins, and muscle mechanical characteristics including intermuscular interactions) on the pathology rather than ascribing it solely and/or directly to the length of a spastic muscle itself. Firstly, in relation to the muscular architecture, the adaptations observed at the muscle tissue level in patients with spastic CP need to be evaluated, since the muscle's structural organization is one of the major determinants of its force-generation capacity. Friden and Lieber [162], for instance, demonstrated stiffer fibers from contractured muscles than controls which have been hypothesized to arise from the variations in muscle structural proteins such as titin and collagen. Although titin is directly considered as the passive load-bearing protein within the muscle fiber, its role in muscular activation as a part of the contractile machinery is also presented in the literature (e.g., [163–165]) and what is the active state titin's role in spastic muscle function in CP remains to be determined. Remarkably, the present findings show that the active state muscle forces are elevated due to co-activating other muscles, compared to which, the passive state forces are rather limited. This makes it necessary to investigate the structure of active-condition muscle proteins in detail. Although muscle biopsy studies presenting altered passive muscle properties after spasticity is common in the literature (e.g., [34]), this is not the case for activated conditions and in vivo studies are further required. Besides, the effects of EMFT cause an increase of the spastic muscles' forces [98, 137, 138, 160, 161] are also observed in the present MTU length - muscle force data characterizing gait. EMFT is evident in healthy human muscles in vivo [106, 148, 166, 167] though, we suggest that the structures of the intermuscular mechanical pathways through which force transmission occurs may vary in patients. Since the effects of EMFT is based on the connective tissue linkages between the muscle fibers and the extracellular matrix (ECM) along their full peripheral lengths [91] and these linkages are shown to transmit force [4], altered mechanical characteristics of intermuscular interactions are the key for the pathology. Such transmission is plausibly more pronounced in patients with spastic CP, due to their muscle's relatively higher intramuscular connective tissue [168]. For the spastic ST and GRA muscles, in particular, higher stiffness of their ECM reported earlier [34] can partly explain the increased forces of the target muscles in co-activation conditions shown presently. Hereby, rather than the muscle shortness or altered muscle cross-sectional area in CP, both of which have not been definitively agreed upon in

the literature, the source of the clinically indicated exaggerated muscle stiffness could be related to other factors, such as above mentioned intramuscular connective tissue alterations and related altered myofascial loads of the epimuscular connections of the spastic muscle with its surrounding muscular and/or non-muscular structures [7]. Previously, de Bruin et al. [32] reported unchanged myofiber typing and cross-sectional area for biopsies of control and spastic flexor carpi ulnaris muscles, whereas the connective tissue composition of the spastic muscle altered exclusively by thickening of its tertiary perimysium (i.e., the intramuscular continuation of connective tissue branches of the main neurovascular tracts penetrating the muscle), instead of a thickening of all the muscular connective tissue stroma. As suggested by the authors and we agree, this creates a conducive environment (i.e., a stiffer path) for transmission of myofascial loads on the spastic muscle and contributes in a major way to the etiology of limitation of movement at the joint. This may also apply to spastic knee flexors and needs to be specifically studied.

5.5 Conclusion

Modeling work showed shorter MTU length for knee flexors, ST, and GRA muscles in patients with spastic CP. However, novel muscle force - MTU length data of those muscles do not match with the clinical consideration that spastic muscles produce higher forces in shorter lengths. The absence of a strong correlation between shorter operational muscle length and higher force production implies the necessity of taking the composition and organization of the muscle structural proteins and the intermuscular interactions into account for a better understanding of the muscles' force-generating behavior. Besides, our findings on EMFT shed light on how the simultaneous working of different muscles causes target muscle's force to increase within the MTU lengths characterizing gait. Therefore, if indeed spastic knee flexor muscles produce high forces in short muscle-belly lengths alone, elevated forces due to EMFT may be considered as a contributor to the patients' pathological gait. Otherwise, such EMFT effect may be the main determinant of the pathological condition.

6. LONG-TERM EFFECTS OF BOTULINUM TOXIN TYPE-A ON MECHANICS OF MUSCLES EXPOSED

6.1 Introduction

A widely used technique for management of spasticity arising from a wide range of conditions such as cerebral palsy (CP) [54–56], spinal cord injury [169, 170], multiple sclerosis [171, 172] and stroke [173, 174] is the injection of botulinum toxin type-A (BTX-A). The toxin temporarily paralyzes muscles by inhibiting the discharge of the acetylcholine-containing vesicles into the synaptic cleft, and hence transmission of nerve impulses to the muscle fibers at the neuromuscular junction [61,62,175]. A consequence is decreased muscle tone [68, 69] which mechanically implies a limited muscular force production capacity. BTX-A treatment aims at improving joint function [53] by reducing the passive resistance of the muscle in the joint [176] and increasing the joint range of motion [72].

Understanding BTX-A effects on muscular mechanics is of central importance because the muscle exposed continues to serve as the motor for movement, but this understanding remains limited. Length-dependent reductions in knee extension torque [67] and muscle force [74] shown in previous animal experiments indicate complex effects of BTX-A on joint mechanics. Additionally, experiments in the rat anterior crural compartment have shown acutely that BTX-A does not improve the muscle's length range of force exertion (l_{range}) and elevates passive forces of the injected tibialis anterior (TA) muscle [74]. In addition, the spread of BTX-A through muscle fascia was reported [177]. Such spread has been reported to reduce forces [37, 75] and cause changes in length-force characteristics of also the non-injected muscles [74, 76, 78, 79]. Remarkably, those changes in the short-term include effects contradicting treatment aims (i.e., decreased l_{range}, increased passive forces, and elevated intramuscular collagen content) [76]. Finite element analyses of that indicated that they do ascribe to a continuing elevated stiffness in the exposed muscles' extracellular matrix [81], testing

of which deserves major attention.

Whether the short-term effects persist in the long term is unknown, but very important. Therefore, in a rat model, we aimed at testing the following hypotheses. In the long term, BTX-A (1) maintains l_{range} and (2) increases the passive forces of the injected TA muscle, and (3) spreads into non-injected muscles also affecting their active and passive forces.

6.2 Methods

6.2.1 Assessment of Effects of BTX-A on Muscular Mechanics

Surgical and experimental procedures were approved by the Committee on the Ethics of Animal Experimentation at Boğaziçi University. Male Wistar rats were divided into two groups: control (n= 7; mean ± SD: body mass 386.3 ± 36.5 g and 406.9 ± 16.8 g for the times of injection and experiment, respectively) and BTX-A (n= 7; body mass 394.7 ± 29.0 g and 404.3 ± 34.3 g for the times of injection and experiment, respectively).

Using intraperitoneal ketamine (1 mg/kg), mild sedation was imposed. Subsequently, a region was shaved, bound within an approximately 15 mm radius from the center of the patella, where a marker was placed. Bringing the ankle to maximal plantar flexion and the knee to approximated 90° angle, the TA muscle was located by palpation. At a point 10 mm distal along the tibia, a second marker was placed. A line segment was drawn between the two markers and the injection location over the TA muscle was determined as a point 5 mm lateral to the second marker. At this location, the depth of the TA and the thickness of the skin approximated 5-5.5 and 0.7-1 mm, respectively. All injections were made exclusively into the TA, to a depth of 3 mm, therefore into the superficial half of the muscle. 100 U vial of vacuum-dried, botulinum type A neurotoxin complex (BTX-A) (BOTOX; Allergan Pharmaceuticals, Westport, Ireland) was reconstituted with 0.9% saline solution. For the BTX-A group,

the animals received a one-time intramuscular BTX-A injection. The total dose was 0.1 U and the injected volume was 20 μl. For the Control group, the animals received a one-time intramuscular injection of the same volume of 0.9% saline solution exclusively. All injections were performed 1-month prior to testing. The animals were kept in standard cages separately. The animal care room was thermally regulated and maintained a 12 h dark-light cycle. The animals were free to do their normal activity until the day of the experiment.

6.2.1.1 Surgical Procedures. The animals were anesthetized using an intraperitoneally injected urethane solution (1.2 ml of 12.5% urethane solution per 100 g of body mass). Additional doses were given if necessary (maximally 0.5 ml). Immediately following the experiments, the animals were euthanized by using an overdose of urethane solution.

To prevent hypothermia, the animals were kept on a heated pad (Homoeothermic Blanket Control Unit; Harvard Apparatus, MA, USA) during surgery and data collection. The control of the body temperature at 37 °C was obtained by adjusting the temperature of the heated pad utilizing a feedback system integrated with a rectal thermometer.

During surgery, the skin and the biceps femoris muscle of the left hindlimb were removed. After the anterior crural compartment was exposed, only a limited distal fasciotomy was performed to remove the retinaculae (i.e., the transverse crural ligament and the crural cruciate ligament). Consequently, the connective tissues of the muscle bellies within the compartment (i.e., the TA, extensor digitorum longus (EDL), and extensor hallucis longus (EHL) muscles) were left intact.

A reference position was selected as the combination of knee joint angle of 120° and ankle angle of 100°. This position matches with a combination of knee and ankle positions that the rat attains in vivo, during the stance phase of gait [178]. Maintaining the reference position, the following were done: using silk thread, the four distal tendons

of the EDL muscle were tied together. On the distal tendons of the EDL, TA, and EHL muscles, as well as on a fixed location on the lower leg matching markers were placed. Afterward, the distal EDL tendon complex as well as the TA and the EHL tendons were cut as distally as possible.

The femoral compartment was exposed for two purposes: (1) to reach the proximal tendon of the EDL and (2) to expose the sciatic nerve. Subsequently, keeping a small piece of the lateral femoral condyle still attached, the tendon was cut from the femur. The sciatic nerve was dissected free of other tissues. Once all nerve branches to the muscles of the femoral compartment were severed, the sciatic nerve was cut as proximally as possible.

The proximal tendon of the EDL, the tied distal tendons of the EDL, the distal tendon of the TA, and the distal tendon of the EHL muscles were sutured to four separate Kevlar threads in order to provide connection to force transducers.

6.2.1.2 Experimental Set-up. To mount the animal in the experimental set-up (Figure 6.1A) the following procedure was utilized: (1) in order to avoid obstruction of the Kevlar threads connecting the distal tendons to their force transducers, the ankle was brought to maximal plantar flexion (180°) in which position, the foot was fixed to the foot clamp. (2) The femur was fixed to the femur clamp such that the knee angle was set at 120°. (3) Taking care to ensure their alignments in the muscle's line of pull, each Kevlar thread was connected to a separate force transducer (BLH Electronics Inc.; Canton, MA, USA). (4) The distal end of the sciatic nerve was placed on a bipolar silver electrode (Figure 6.1B).

6.2.1.3 Experimental Conditions and Procedure. For the duration of the experiment room temperature was kept at 26 °C. To prevent dehydration, muscles and tendons were irrigated regularly by isotonic saline. The distal and proximal tendons of the EDL and the distal tendon of the EHL muscles were kept in their reference positions

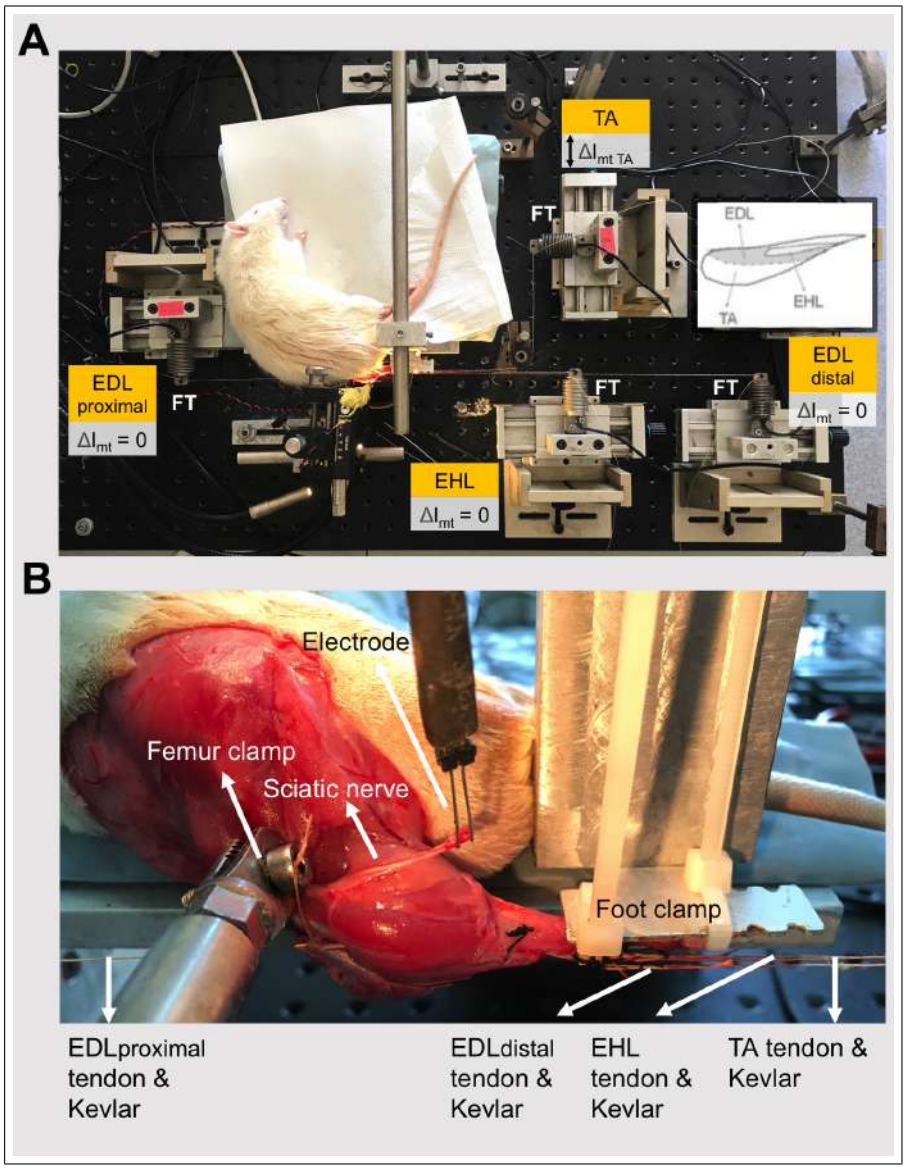

Figure 6.1 The animal experimental set-up. (A) The distal tendons of the TA and the EHL muscles as well as the proximal and the tied distal tendons of the EDL muscle (EDL proximal and EDL distal, respectively) were each connected to a separate force transducer by Kevlar threads. Throughout the experiment, the EDL and EHL muscles were kept at constant muscle-tendon complex lengths. Exclusively, the TA muscle was lengthened ($\Delta l_{mt\ TA}$) to progressively increasing lengths, at which isometric contractions were performed. Lengthening (indicated by double-headed arrow) started from muscle active slack length at 1-mm increments by changing the position of the TA force transducer. Inset shows relative sizes and positions of muscles of the anterior crural compartment. (B) The experimental reference condition for joint angles is 120° and 100° for knee and ankle angles, respectively. The femur and the foot were fixed by metal clamps. The distal end of the sciatic nerve was placed on a bipolar silver electrode.

at all times. Therefore, during the experiment, their lengths were not changed. However, the TA was brought to various muscle-tendon complex lengths, by repositioning its force transducer. The isometric forces of all muscles were measured simultaneously at each TA length. The measurement started at an active slack length of the TA and its length was increased in 1 mm increments until reaching 2 mm over its optimum length. TA muscle-tendon complex lengths are expressed as deviation from its active slack length ($\Delta l_{mt\ TA}$).

Subsequent to bringing the TA to a target muscle length, all muscles studied were activated maximally using a constant current of 2 mA (square pulse width 0.1 ms) delivered to the sciatic nerve (STMISOC; BIOPAC Systems, CA, USA) with the following stimulation protocol: (1) two twitches were evoked. (2) 300 ms after the second twitch, the muscles were tetanized (pulse train 400 ms, frequency 100 Hz). (3) 200 ms after the tetanic contraction, another twitch was evoked. Each completion of this protocol was followed by a recovery period of 2 min for all muscles. During the recovery period, the TA was kept near the active slack length. However, the EDL and EHL lengths were not altered.

6.2.2 Assessment of Changes in Intramuscular Connective Tissue Content Due to BTX-A

In a separate set of male Wistar rats, changes in intramuscular connective tissue content due to BTX-A were assessed. The animals were divided into two groups: control (n= 6; mean ± SD: body mass 404.3 ± 31.0 g) and BTX-A (n= 6; body mass 413.3 ± 46.2 g).

The collagen amount of each muscle was quantified using a colorimetric analysis of hydroxyproline content [179] 1-month after the injections. Subsequent to the above-described surgical procedures to expose the anterior crural muscles, biopsies were removed rapidly after euthanizing the animal. Purity of the muscle samples was provided by careful removing of all tendinous materials from the sample. Muscle biop-

sies were flash-frozen in liquid nitrogen and stored at -80 °C before running the assay within 4 weeks after removal. In short, each muscle was weighed prior to undergoing hydrolyzation at 130 °C for 12 h in 5 N HCl. Samples of the hydrolysate were oxidized at room temperature with a chloramine-T solution for 25 min incubation. Subsequently, the impurities were extracted and discarded by toluene treatment. To convert the oxidation product to pyrrole, the remaining aqueous layer containing the hydroxyproline products was heated for 30 min in boiling water. The final pyrrole reaction product is then removed in a second toluene extraction, and the final solution was mixed with Ehrlich's reagent for 30 min. Sample absorbances were read at 560 nm in triplicate using UV-Visible spectrophotometer (UV-1280; SHIMADZU, Kyoto, Japan).

6.2.3 Data Processing

Muscular tissues' capacity of mechanical resistance at a tested muscle-tendon length is characterized by muscle force in an unstimulated state. This is referred to as passive muscle force (F_p). Using the force-time traces obtained experimentally: (i) F_p was determined 100 ms after the second twitch (Figure 6.2). (ii) Muscle total force was determined as the mean force (for a 200 ms interval, 150 ms after evoking tetanic stimulation) during the tetanic plateau. Muscle active force (F_a) per muscle-tendon complex length was calculated by subtracting F_p from muscle total force.

A least squares criterion was used to fit the data for Fp and Fa, with a polynomial function (Eq. 6.1):

$$y = a_0 + a_1 \cdot x + a_2 \cdot x^2 + ... + a_n \cdot x^n \tag{6.1}$$

where y represents isometric muscle forces (i.e., F_p or F_a), and x represents the muscle-tendon complex length. a_0, a_1 ... a_n are coefficients determined in the fitting process.

Using one-way analysis of variance (ANOVA), the order of the polynomials was determined [180]. The lowest order was sought after with the criterion that a significant

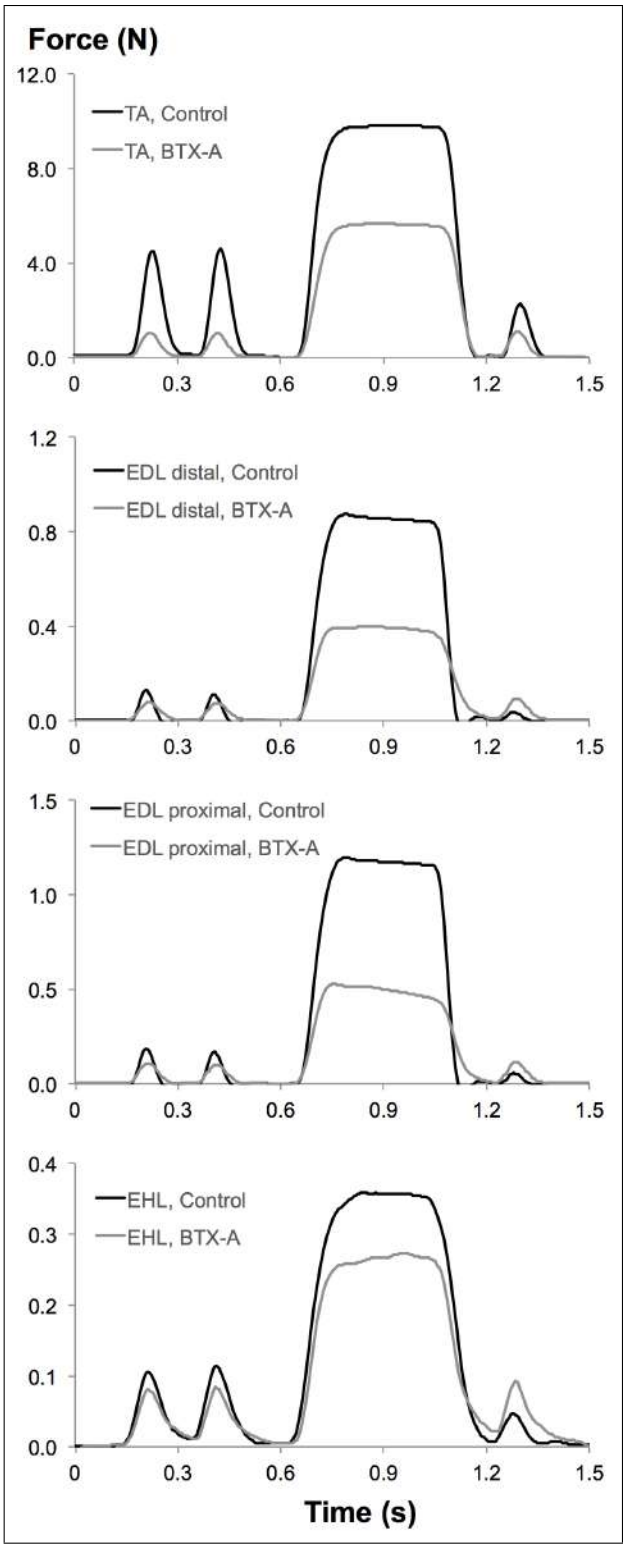

Figure 6.2 Typical examples of force-time traces measured at tendons of muscles from both control and BTX-A groups. Superimposed traces of (upper to lower) the TA force, the distal EDL force, the proximal EDL force, and the EHL force recorded at the optimum length of TA muscle.

improvement was still provided to the description of changes in muscle force data as a function of muscle-tendon complex length. These polynomials were used for calculating the mean and standard deviations (SD) of data: for each muscle studied, muscle forces at different TA muscle-tendon complex lengths were obtained. For each TA muscle-tendon complex length, muscle forces were averaged in order to determine the muscle force (mean ± SD) of the control and BTX-A groups.

Muscle length-force characteristics were studied using four key determinants defined as follows: (1) *muscle optimal force* is the maximum isometric force exerted by an active muscle. Muscle optimal force is often taken as an indication of a muscle's capacity for force production. (2) *muscle optimum length* is the muscle length at which muscle optimal force is encountered. (3) *muscle active slack length* is the shortest length at which an active muscle can still exert nonzero force. (4) *muscle length range of force exertion* is the length range from active slack length to optimum length. Within the potential joint range of motion, this is considered as a metric indicating movement capability, with active force exertion.

Also, to process these key determinants, the polynomials obtained were utilized in order to determine: the optimal TA force (i.e., the maximum active muscle force value of the fitted polynomial, for each individual TA muscle), the corresponding optimal muscle length, as well as TA active slack length. The TA length range of active force exertion (l_{range}) was determined as the muscle length range between muscle active slack length and muscle optimum length.

Hydroxyproline analysis was used to quantify changes in intramuscular collagen content for muscles exposed to BTX-A. Using the measured absorbance values of muscle samples, hydroxyproline contents of individual muscles were determined based on a reference (i.e., standard regression curve identifying the paired information of pre-known hydroxyproline amounts and their measured absorbance values) as μg hydroxyproline expressed per mg of muscle tissue wet weight. Hydroxyproline content was converted into intramuscular collagen content using a constant (7.46), which characterizes the number of hydroxyproline residues in one molecule of collagen [181].

6.2.4 Statistical Analyses

After using the Shapiro-Wilk test to seek for a normal distribution in l_{range} data of the TA, unpaired-t or Mann-Whitney U test was used to test for the effects of BTX-A injection on this metric.

Two-way ANOVA for repeated measures (factors: TA muscle-tendon complex length and animal group) was performed separately for the forces of each muscle. If significant main effects were found, Bonferroni post hoc tests were performed to further locate significant within-factor differences.

Forces of both groups were aligned for their optimum length. Decrease in muscle active force is calculated per TA muscle-tendon complex length, as the difference in mean force between the control and the BTX-A groups. This is expressed as a percentage of the mean force of the control group. The Spearman's rank correlation coefficient (ρ) was calculated to test if reductions in TA active forces due to BTX-A injection are correlated with TA muscle-tendon complex length. Correlations were considered significant at $P< 0.05$.

Shapiro-Wilk test was used to check if the collagen content data are normally distributed. The collagen amount calculated for each muscle in the BTX-A group was compared to those of the control group using unpaired-t or Mann-Whitney U test, where appropriate. Differences were considered significant at $P< 0.05$.

6.3 Results

6.3.1 Effects of BTX-A on Muscular Mechanics

TA Force-Length Characteristics: ANOVA (factors: TA length and animal group) showed both significant main effects on TA active forces, and a significant

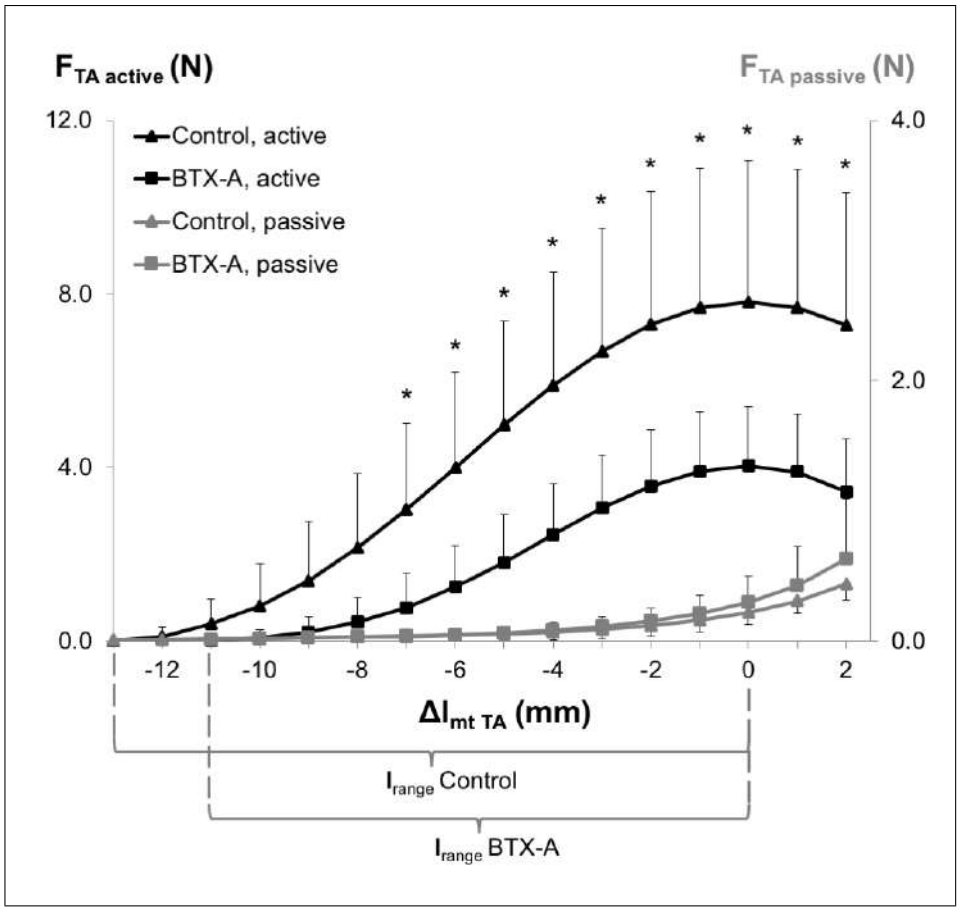

Figure 6.3 Forces of the TA as a function of increasing TA muscle-tendon length. Active and passive muscle forces are shown as mean and standard deviation values for the control and BTX-A groups. The TA muscle-tendon complex length is expressed as a deviation from its optimum length ($\Delta l_{mt\ TA}$). Significant differences between the TA active force of the control group and BTX-A group (Bonferroni post hoc test) are indicated by *.

interaction. Post hoc testing showed significant effects of BTX-A for most muscle lengths ($\Delta l_{mt\ TA} \geq$ -7 mm). TA active force reductions (e.g., 75.2%, 48.3%, and 52.8%, respectively, at $\Delta l_{mt\ TA}$= -7 mm, $\Delta l_{mt\ TA}$= 0 mm and $\Delta l_{mt\ TA}$= 2 mm) were inversely correlated with increasing TA muscle length (ρ=-0.94, P$<$ 0.001). The l_{range} of the BTX-A group (8.56 $\pm$ 2.05 mm) was significantly narrower compared to that of the control group (11.10 $\pm$ 1.58 mm) by 22.9%. ANOVA showed significant main effects also on TA passive forces, but no significant interaction. Compared to the control group, the passive forces are higher in the BTX-A group on average by 12.3% (Figure 6.3).

EDL Forces: ANOVA showed both distally and proximally, only a significant effect of animal group on EDL active and passive forces. However, neither significant effects of TA length nor a significant interaction were found. BTX-A caused significant active force decreases (on average by 66.8% distally and 55.4% proximally) and passive force increases (on average by 62.5% distally and more than twice proximally) compared to those of the control group (Figures 6.4A and 6.4B).

ANOVA also showed significant main effects of both factors on the EDL proximo-distal active force differences (Figure 6.4C), but no significant interaction. Whereas for the control group, both positive and negative proximo-distal active force differences were shown (distal EDL forces were higher than proximal ones for ($\Delta l_{mt\ TA} \leq$ -7 mm and vice versa at longer TA lengths), for the BTX-A group, the EDL proximal forces were higher than the distal forces for most of the TA lengths ($\Delta l_{mt\ TA} \geq$ -11 mm). Bringing the TA to longer lengths changed the proximo-distal active force difference measured at the shortest muscle length ($\Delta l_{mt\ TA}$= -13 mm) significantly for $\Delta l_{mt\ TA} \geq$ -8 mm and for $\Delta l_{mt\ TA} \geq$ -9 mm, for the control and BTX-A groups, respectively.

EHL Forces: ANOVA showed significant main effects of both factors on EHL active forces, but no significant interaction, and only a significant effect of BTX-A on passive forces, but no significant interaction. BTX-A caused a significant active force decrease (on average by 28.8%) and passive force increase (on average by more than twice) compared to those of the control group (Figure 6.5).

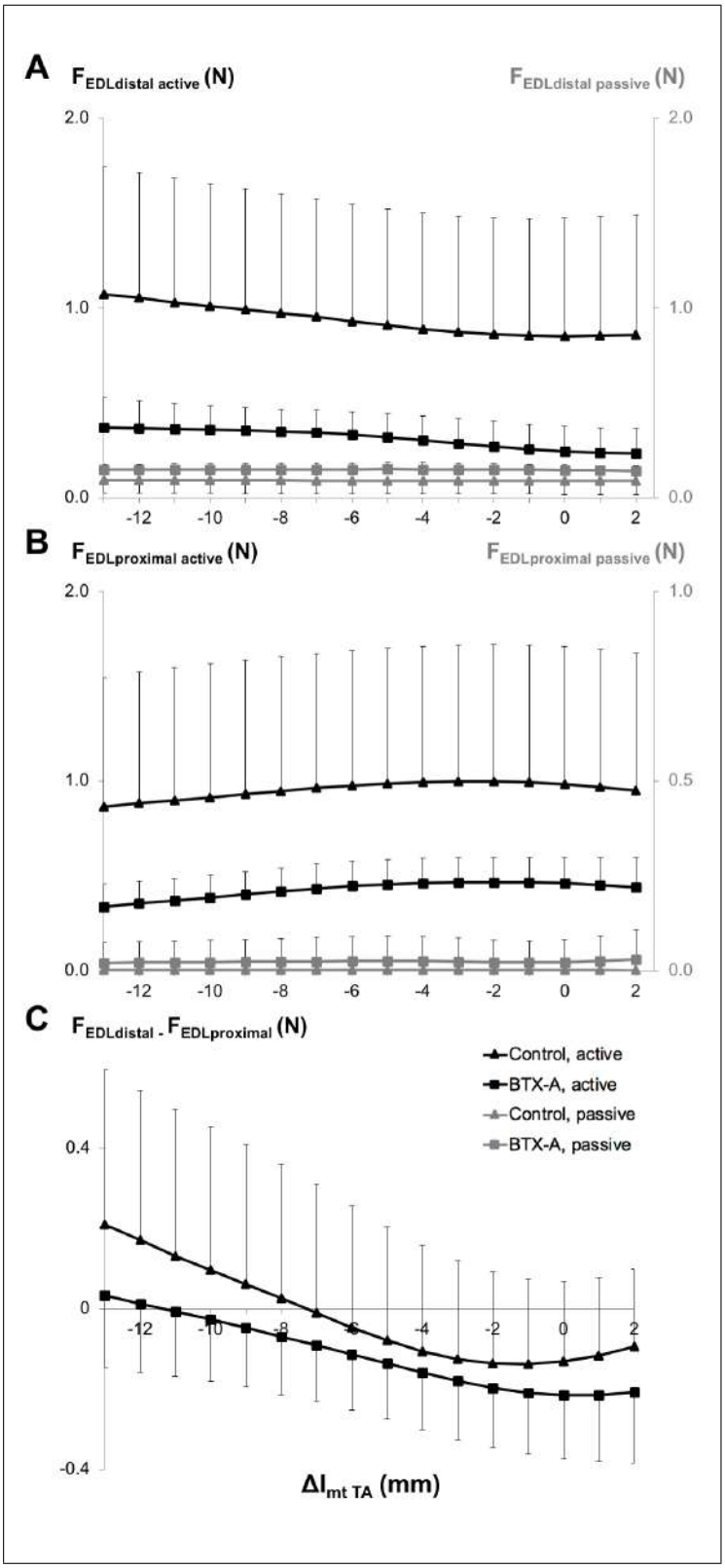

Figure 6.4 Forces of the EDL as a function of increasing TA muscle-tendon length. Active and passive forces of the EDL measured from (A) the distal tendon and (B) from the proximal tendon, and (C) proximo-distal active force differences of EDL ($F_{EDL\ distal}$ - $F_{EDL\ proximal}$). Isometric muscle forces are shown as mean and standard deviation values for the control and BTX-A groups. TA muscle-tendon complex length is expressed as a deviation ($\Delta l_{mt\ TA}$) from its optimum length.

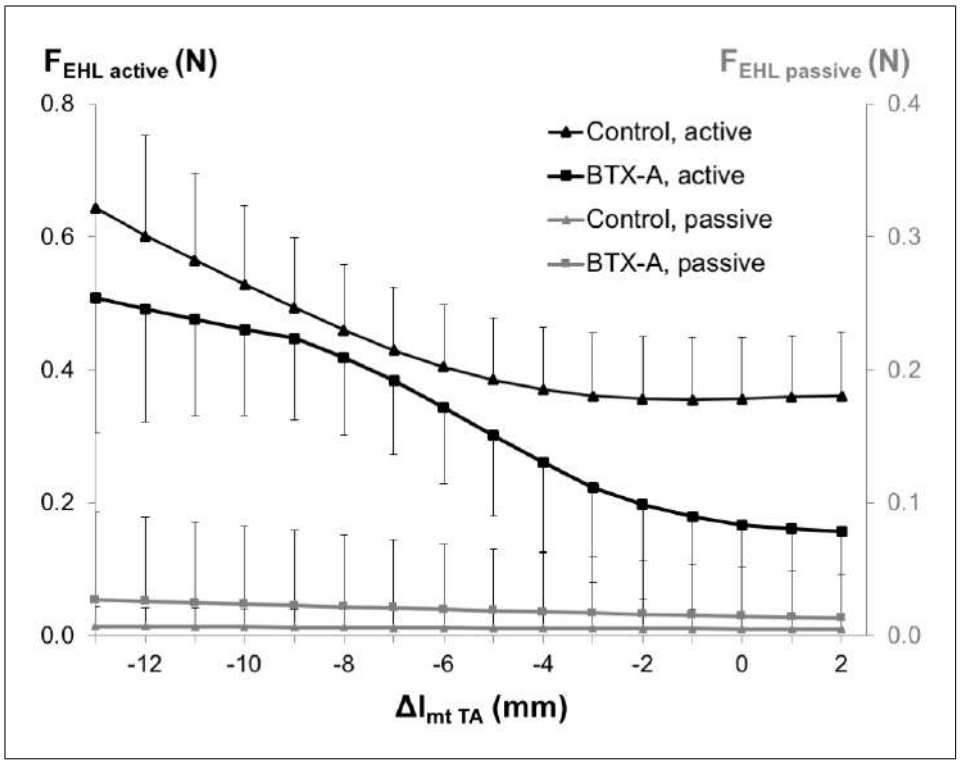

Figure 6.5 Forces of the EHL as a function of increasing TA muscle-tendon length. Active and passive muscle forces are shown as mean and standard deviation values for the control and BTX-A groups. TA muscle-tendon complex length is expressed as a deviation ($\Delta l_{mt\ TA}$) from its optimum length.

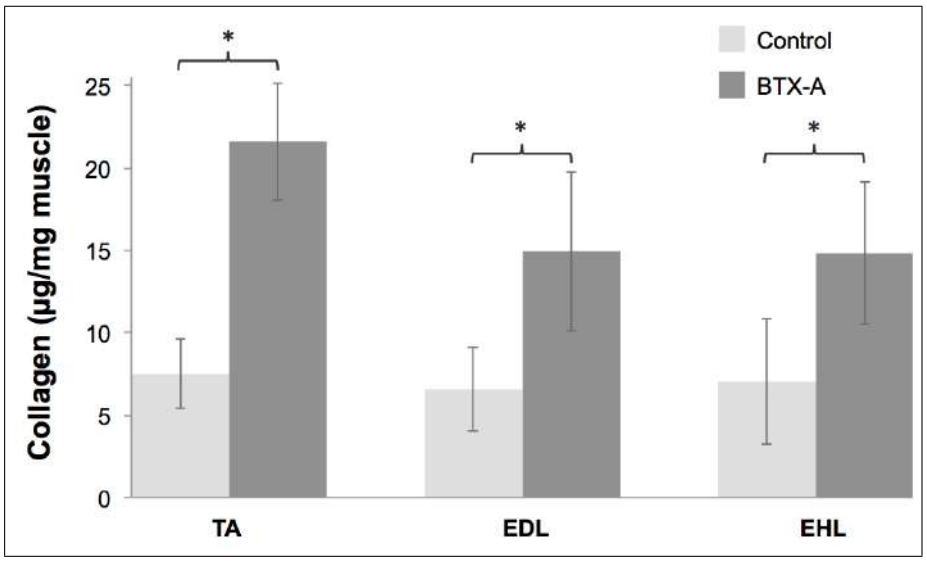

Figure 6.6 Collagen contents of the TA, EDL, and EHL muscles shown as mean and standard deviations for the control and BTX-A groups. Significant differences between the control and BTX-A groups are indicated by *.

6.3.2 Changes in Intramuscular Connective Tissue Content Due to BTX-A

For both injected TA muscle and non-injected EDL and EHL muscles, were the intramuscular connective tissue contents (Figure 6.6) significantly higher for the BTX-A group compared to those of the control group (BTX-A group: 21.61 ± 3.56, 14.94 ± 4.82, and 14.82 ± 4.32; Control group: 7.49 ± 2.08, 6.55 ± 2.55, and 7.05 ± 3.81 μg collagen/mg muscle; P= 0.005, 0.006, and 0.029 for the TA, EDL, and EHL, respectively). Note that, muscle masses in the BTX-A group were less than those of the control group (BTX-A group: 0.35 ± 0.04, 0.10 ± 0.01, and 0.01 ± 0.003 g; Control group: 0.65 ± 0.04, 0.16 ± 0.03, and 0.01 ± 0.01 g; P< 0.001, and P= 0.005, and 0.198 for the TA, EDL, and EHL, respectively).

6.4 Discussion

Rejecting the first hypothesis, the present data indicate a reduced l_{range} for the injected TA muscle. The hypothesis was based on our previous short-term experiment [74], which showed, unlike an expected increase, no significant changes in the l_{range}.

However, the present study showed that in the long-term, BTX-A leads to even a narrowing of the muscle's l_{range}. Elevated passive force of the injected TA muscle confirms the second hypothesis and is a consistent finding with the short-term effects of BTX-A shown earlier [74]. Active and passive forces of not only the injected muscle but all muscles within the anterior crural compartment were altered indicating the spread of BTX-A into also the non-injected muscles. This confirms the third hypothesis. Elevated intramuscular collagen combined with the muscle atrophy observed agrees with the increased muscle passive forces. Therefore, BTX-A-induced changes to the structure and mechanics of both targeted and untargeted muscles persist and advance in the long term.

6.4.1 Altered Mechanics of Muscles Exposed to BTX-A

The mechanism of effects of BTX-A on muscular mechanics and in particular how this reflects on muscle's l_{range} has been explored using finite element modeling [146]. The characteristic determinant for this mechanism was indicated as the "longer sarcomere effect" (LSE). In short, the inactivated muscle fibers modeled, which represent BTX-A-induced partial muscle paralysis do not shorten. This effect is reflected also in the activated ones via muscle fiber-extracellular matrix (ECM) mechanical interactions [90, 125] yielding overall a limited shortening of sarcomeres in muscle exposed to BTX-A compared to their counterparts in a BTX-A free muscle. Due to such LSE (please see Figure 6.7 for an illustration), the sarcomeres reach their maximal force production earlier causing the muscle's optimum length to shift to a shorter length. This explains the narrowing of l_{range}. Finite element modeling of the time course of BTX-A treatment further predicted that such an effect of BTX-A may get more pronounced in the long-term [81]. This was characterized by increased stiffness of the muscle's ECM, which, via a more pronounced LSE, was shown to cause sustained and/or increased shifting of muscle optimum length to shorter lengths. This mechanism is likely to explain the present experimental findings, which in contrast to no significant effects reported acutely [74] did show a narrowed l_{range} for the TA exposed long-term to BTX-A. Based on those earlier studies we consider that operation of the sarcomeres at

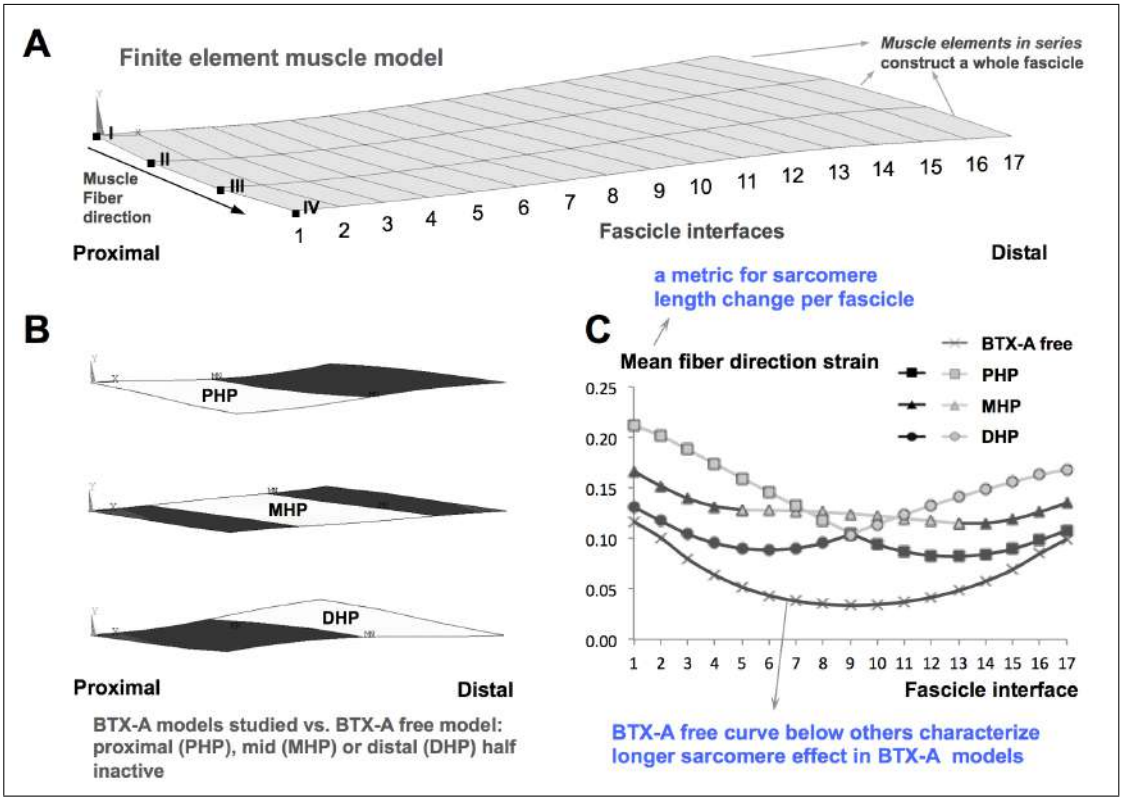

Figure 6.7 Illustration of the longer sarcomere effect (based on [146]. (A) The finite element muscle model consists of combinations of muscle elements arranged in series each of which constructs a whole fascicle. A combination of model nodes along one side of a fascicle is referred to as a fascicle interface. For example, the most proximal fascicle interface is a combination of the nodes indicated by Roman numerals from I to IV. Each fascicle interface is indicated by a number from 1 to 17. The local length changes along the muscle fiber direction i.e., fiber direction strain are analysed. (B) Schematic representation of BTX-A models studied. These are achieved by not activating muscle elements (representing BTX-A-induced partial paralysis) located in the proximal half (PHP), middle half (MHP), and distal half (DHP) of the muscle: white areas show paralyzed muscle parts whereas, the darker areas show the parts that are activated maximally. These models are studied vs. a BTX-A free model (i.e., the entire muscle is activated maximally). (C) The characteristic BTX-A effect i.e., the longer sarcomere effect shown earlier [146] exemplified. Mean fiber direction strain is the average of local length changes in nodes I to IV in each fascicle interface. Therefore, it is a metric characterizing sarcomere length change per fascicle. The mean fiber direction strain curve for the BTX-A free muscle is localized below those of the BTX-A models indicating that sarcomeres within muscle exposed to BTX-A attain longer lengths.

longer lengths within the BTX-A exposed muscle could plausibly be a mechanism explaining the present findings. However, specific new tests should be conducted in order to confirm that. Note that, the significantly higher total collagen content of muscles exposed to BTX-A is an important present finding. This is in concert with the elevated muscle passive forces shown and also with the increased ECM stiffness considered in previous finite element modeling. The hydroxyproline analysis conducted objectively addresses changes in intramuscular connective tissue content indicating increased collagen in muscle exposed to BTX-A. As collagen is the main load-bearing constituent of the ECM, this analysis was directly complementary for our aim of assessing the effects of BTX-A on muscular mechanics. Yet, an assessment of the expression and orientation of specific collagen isoforms and other elastic proteins such as titin [182] in future studies can make the analysis of BTX-A-induced structural and mechanical changes comprehensive.

6.4.2 BTX-A Effects at Large and on Mechanical Interactions Between Muscles

BTX-A can affect intermuscular mechanical interactions in two ways: (1) As a highly diffusive toxin, BTX-A can spread beyond the injected muscle through muscle fascia [177], bloodstream [183], and/or axonal pathways [184]. Mechanical effects of leakage of BTX-A into a neighbouring muscle [75], into synergistic muscles within a compartment [74, 76–78] and even across antagonistic compartments [79] have been reported in several animal studies. This resulted in at the least a dropped active muscle force, but also lead to elevated collagen content, stiffness, and passive force as well as a reduced l_{range} of non-injected muscles exposed acutely to BTX-A by diffusion. The effects of BTX-A investigated presently in the long term confirmed that BTX-A leads to a decrease in the active forces of all synergistic muscles within the compartment. On the other hand, BTX-A administration is clinically expected to improve agonist-antagonist force balance [185, 186]. However, assuming that inter-compartmental spread of BTX-A occurs in patients and is effective in the long term, BTX-A effects on such imbalance may not be as simple as weakening of the target muscle for a better match with the

force of the antagonist. Instead, mechanically this may involve also the weakening of the antagonist. However, BTX-A may decrease co-contraction of antagonistic muscles, which is exaggerated in children with CP [82]. Nevertheless, this may not be a controlled effect. More importantly, although positive effects of BTX-A against the neurological pathology are plausible, the present findings suggest that simultaneously occurring mechanical effects may not be favorable ones. (2) Muscles are connected to the joint through the tendons however, their bellies are interconnected via an integral system of myofascial connective tissue structures (e.g., collagenous connections providing integrity between the epimysia of adjacent muscles and collagen-reinforced neurovascular tracts interconnecting bellies of intra- and intercompartmental muscles). In BTX-A free conditions, epimuscular myofascial force transmission (EMFT) [9, 90] i.e., intermuscular mechanical interactions occurring through those connective tissue structures impose major effects on muscular mechanics including the following: magnetic resonance imaging analyses indicate heterogeneous local length changes (varying e.g., from 29% lengthening to 13% shortening) along muscle fibers of human medial gastrocnemius after imposing passive stretch [103] or submaximal activation [102]. Supersonic shear imaging analyses show similar local muscle stiffness changes (e.g., the shear modulus of the TA was higher in the extended knee compared to flexed knee position on average by 27%, despite the fact that ankle angle was restrained) [127]. Muscle mechanics experiments indicate changes in muscle's length-force characteristics in response to altered mechanical conditions within which the target muscle operates: (i) in animal experiments, those changes due to co-activation of synergistic muscles include elevated agonist muscle force amplitude (e.g., by 17%) and shift of muscle's maximal force production to a different length (e.g., by several mm's, yielding an increase in the muscles length range of force production by 24%) [10, 17]. (ii) In intraoperative experiments in CP patients, co-activation of synergistic and antagonistic muscles was shown to yield similar effects altering force production of the target spastic muscle compared to that measured after it is activated alone [137, 138, 160, 161]. However, previously, EMFT has been shown to be affected by BTX-A exposure in the short term [77]. One characteristic effect of EMFT is the proximo-distal force differences (i.e., unequal muscle forces exerted at both ends of a biarticular muscle, reaching up to 35%) [12, 16, 17]. This represents the net amount of epimuscular myofascial loads

(i.e., forces arising from stretching of the intermuscular connections due to muscle relative position changes) acting on the muscle [90]. The present results showed that exposure to BTX-A does affect proximo-distal force differences for the EDL muscle. At the shortest TA lengths, for both animal groups, distally exerted EDL active forces were higher than those exerted proximally. This indicates that proximally directed epimuscular myofascial loads act on the EDL belly. After imposing TA lengthening, the direction of those loads changed to become distally directed for both groups, but the amplitude of the net amount of epimuscular myofascial loads was higher for the BTX-A group. Previously, BTX-A injected into the TA was shown to acutely remove EDL proximo-distal force differences for all TA lengths studied [74]. Moreover, a specific test involving solely relative position changes of the EDL, which was kept at constant length showed minimized EDL proximo-distal force differences indicating diminished EMFT after exposure to BTX-A [77]. Although the latter test was not conducted presently, the findings (i) in contrast, do not show a diminished EMFT in the long term, but judging from the elevated distally directed myofascial loads, and (ii) indicate that intermuscular connective tissue linkages between the TA and the EDL should be stiffer. This issue is relevant because, for patients with CP, recent intraoperative experiments show that inter-synergistic EMFT [137, 138, 160, 161], and also the inter-antagonistic EMFT [46, 137, 160, 161] causes a significant increase in the force of spastic gracilis and semitendinosus muscles (above 30%, up to 70%). This suggests that the spastic hamstrings capacity to affect the pathological condition in the joint is changed by EMFT. Therefore, it is important to assess in new clinical studies if exposure to BTX-A in the long-term sustains or even elevates the stiffness of connective tissue structures, which provide intermuscular mechanical connections.

6.4.3 Limitations and Implications of the Study

The established time to assess the chosen long-term effects of BTX-A is based on concepts related to the process of exocytosis. This process allows the release of acetylcholine into the synaptic cleft at the neuromuscular junction, and any intervention targeting that including exposure to BTX-A yields presynaptic blocking in signal

transmission, hence muscle paralysis [61, 62, 65]. de Paiva et al. [187] showed that 4-weeks after BTX-A injection, no exocytosis occurs at the parent nerve terminals. However, (i) this changes beyond one-month duration (e.g., at day 63 the authors showed recovery in exocytosis in the parent terminals) and (ii) formation of a network of nerve-terminal sprouts takes place after BTX-A injection, showing an increase over time. Therefore, our choice of assessment of BTX-A effects one-month post-injection allows avoiding exocytosis in the parent terminals for consistent testing and is in concert with earlier animal studies [67, 75, 182, 188]. However, earlier research such as de Paiva et al. [187] suggests that due to a dynamic exocytosis process, involving varying influences of the parent terminals and nerve-terminal sprouts, also further longer-term BTX-A effects need to be studied for a comprehensive understanding. Nevertheless, our present study sheds light on such understanding and indicates the presence of novel mechanical effects that may affect the function of the treated muscle.

Note the differences between the injection protocol, BTX-A dosage, and volume used in the present animal study and in common clinical practice. The injected TA muscle was located by the manual placement method using anatomical landmarks and palpation. However, electrical stimulation, electromyography, or ultrasound-guided injection of BTX-A is suggested for clinical application in order to improve the accuracy and specificity of localization, especially for deep and/or very small muscles [60, 189–191]. Nevertheless, Picelli et al. [192] showed that such guidance does not provide a better outcome compared to the manual placement method for superficial muscles. Accordingly, we were confident in localizing the superficial TA muscle presently and also in standardizing the injection location and depth as bound by the protocol described in the Methods. On the other hand, the optimal clinical injection dosage per targeted muscle depends on the muscle volume, the degree of spasticity and the level of the muscle's involvement in the patient's pathological pattern of joint movement [193]. Heinen et al. [60] reported a safe total dose range for children with CP as 1 to 25 U/kg bodyweight. In lower extremity muscles, clinical BTX-A doses vary between 3 and 6 U/kg [70,80]. However, presently, the BTX-A quantity injected approximates only 0.32 U/kg. Therefore, a direct comparison suggests that the experimentally used quantity is much less than those typically used in clinical applications. Also, the presently injected

volume (approximately 64 μl/kg) is less than the clinically utilized volumes (2.5-8 ml/kg) in lower limb muscles [70, 72, 80]. However, the findings indicate substantial drops in the measured forces suggesting effectiveness and therefore, appropriateness of the present dose for the study purposes. Note also the considerable variability in the dose and volume injected across animal studies, conducted on different species. Reported per kg of the animal, those values include 8.3 U and 0.83 ml in the mouse [194], 1-10 U and 0.1 ml in the rabbit [195] and 3.5 U and 0.23 ml in the cat [75]. Therefore, in terms of the dose and injected volume of BTX-A, a general limitation for animal studies is the difficulty in building an explicit relationship with the clinical practice. This applies to the present study as well. Yet, animal studies do reveal major new phenomena and the present study indicates previously unknown remarkable long-term effects of BTX-A on mechanics of muscles exposed. However, those effects should be tested in the clinics.

Being also related to the dose-administered the issue of injection site also requires attention. Contrary to the common clinical practice, which typically involves multiple injection sites [55,62], presently only the mid-target muscle belly was injected. Taking into account high diffusivity of BTX-A [177], dividing the total dose per muscle between multiple injection sites, can be effective in preventing the spread of the toxin to other muscles [55, 193]. The present injection protocol involving a single site into which the entire dose was administered may plausibly have facilitated leakage of the toxin to the adjacent non-targeted muscles. Yet, also for protocols involving multiple injection sites, the spread of BTX-A was shown to occur beyond the injection site [177]. This makes controlling the effects of the treatment difficult and was considered as a side effect [55,171]. In contrast, Frasson et al. [80] suggested that the spread of BTX-A they showed from foot flexors to even antagonists could positively contribute to improving gait in patients with CP. Overall, such spread, which as indicated in previous animal studies can take place inter-compartmentally (e.g., [79]) implies at least uncontrolled effects occurring in non-targeted muscles. This needs to be specifically tested in the long term. However, taking into account BTX-A effects adversely affecting the mechanics of the muscles exposed as shown presently, controlling leakage of the toxin appears to be quite important for controlling the outcome of the treatment. Particularly, the spread

of BTX-A into a bi-articular muscle has effects on both proximal and distal joints and hence may even manipulate the movement in a non-targeted joint. Therefore, structural, and functional effects of BTX-A on muscles exposed also through diffusion are worth testing in the clinics.

6.5 Conclusion

The present findings show that previously reported acute BTX-A effects to persist and advance in the long term. A narrower l_{range} and elevated passive resistance of the targeted muscle are unintended mechanical effects of BTX-A, whereas the spread of BTX-A into other compartmental muscles indicates the presence of also uncontrolled mechanical effects. These findings can be clinically relevant but should be studied in patients.

7. GENERAL DISCUSSION

In this thesis, the relationship between mechanical characteristics of spastic muscles and the impaired joint motion in patients with cerebral palsy (CP) and the effectiveness of the local application of Botulinum toxin type-A (BTX-A) in the management of spasticity were investigated. The findings, therefore, provided extensive knowledge both on better understanding and management of CP. The first part of the thesis, which aims to reveal the musculoskeletal factors that may contribute to the movement pathology, a combination of invasive (i.e., intraoperative force measurements) and non-invasive (i.e., clinical measurements, 3D gait analysis, musculoskeletal modeling) methods were applied in humans. After gaining information about the muscular features relating to the pathology, then in the second part of the thesis, the effects of the BTX-A on the mechanics of exposed muscles were investigated with animal experiments (i.e., muscle force measurements and histological testing) to reveal possible implications for the management of spasticity. Both parts indicated the determinant role of epimuscular myofascial force transmission (EMFT) arising from mechanical interactions between muscles, and its clinical relevance in CP.

7.1 Spastic Muscle Mechanics of Patients with Cerebral Palsy

Because the muscle serves as a motor for movement, recognizing the changes in its structure and function due to a disease is crucial, so that muscle dysfunction can be detected, and accurate treatment can be planned later. In vivo evaluation of individual muscle's function with its effects on the joint(s), it crosses requires applying specific methodologies. The routine clinical measures of spasticity used in both diagnosis and time-course of its therapy are not very close to reflecting the muscular functioning concerning its strength and stiffness. The most widely used qualitative methods (e.g., The Gross Motor Function Classification System, the Modified Ashworth Scale, the Tardieu Scale, or manual muscle testing) are subjective and can produce imprecise and

unreliable results. Isokinetic dynamometers might have been sufficient for quantifying joint function via measuring joint torque (i.e., a required force to move a joint through a specific range of motion) but are not of clinical use because calculating the force produced by individual muscles based on joint torque is indirect and requires many assumptions, and more importantly, cannot reflect individual muscle characteristics (e.g., its stiffness). Likewise, electromyography is capable of quantifying neuromuscular electrical activity but does not provide information on direct muscle force. Accordingly, using the intraoperative approach is very advantageous for a better understanding of the muscular roots of the pathology, as it allows direct in vivo quantification of human muscle forces at their tendons.

As being the product of one of the rare groups in the world that can apply intraoperative force measurement technique and, by analyzing the muscle force-joint angle relationship in children with CP, this thesis showed that based on the significant increases in the forces of spastic knee flexors, EMFT does contribute to the joint limitation and is in line with patients' pathological gait patterns. The novel contribution of the first article published within the scope of this thesis [138] is that inter-synergistic EMFT has been shown to affect the forces exerted at the tendon of a primary knee flexor muscle, semitendinosus (ST), for the whole sagittal plane range of motion of the knee joint in patients with CP. In the ensuing studies [160, 161], spastic muscle's passive forces were directly measured for the first time and combining intraoperative experiments with gait analyses, the findings showed that inter-synergistic and inter-antagonistic EMFT cause the active state forces of muscles, spastic ST and the gracilis (GRA) to elevate, for which the higher amplitudes have been attained within the gait-relevant joint ranges and compared to which, the passive state forces remain limited even in extended knee positions. The latest modeling works assembling the intraoperatively measured muscle force data and the participants' gait analyses, demonstrated the muscle lengthâforce relationship for spastic ST and GRA, and showed significant effects of EMFT specifically in the patients' gait-relevant muscle-tendon unit length ranges as well. Within the muscles' length ranges characterizing gait, the dominant component of the exaggerated force in the shorter muscle-tendon lengths of spastic ST and GRA was shown as the active state forces, rather than passive. Further, consistent

with the clinical considerations, it was revealed that both spastic ST and GRA may be shortened muscles producing higher forces at shorter muscle lengths. However, remarkably, no strong correlation between shorter operational muscle length and higher force production was found either in passive or active conditions. This, therefore, indicated that if indeed spastic knee flexor muscles produce high forces in short muscle-belly lengths alone, elevated forces due to EMFT may be considered as a contributor to the patients' pathological gait. Otherwise, such EMFT effect may be the main determinant of the pathological condition. Thus, this thesis points out that there is a mechanical reason for co-working of muscles affecting joint movement adversely, and so, EMFT in CP has clinical implications. Based on this, one suggestion is that EMFT through intermuscular mechanical interactions is possibly different in the patients compared to that in healthy people. Yet, these issues have never been tested comparatively between healthy and CP people, and how the effect size of EMFT differs between them has not yet been clarified.

7.2 Botulinum Toxin Type-A in the Management of Spasticity

A better understanding of the effects of BTX-A on muscular mechanics has high clinical relevance as the usage of the toxin in children with CP is common for the management of spasticity. Considering the influence of spasticity, limited muscle lengthening, and restricted range of motion on the growing bones of young children, postponing orthopedic surgical interventions until the children's gait has matured is important, and thus, the combined therapy of physiotherapy and use of orthoses together with BTX-A injections is widely used in children with spastic CP. The animal part in which we sought for the therapeutic BTX-A effects on exposed muscle mechanics indicated that as clinically intended, BTX-A is successful through decreasing the muscle tone (based on the finding of active force reductions we reported within the scope of the thesis) of the injected tibialis anterior (TA) muscle long-term after injection. However, this effect is not unique for all muscle lengths studied, rather muscle length-dependent, meaning that BTX-A has complex effects and is just as hard to control. Moreover, the findings of the experiments performed within the rat anterior crural compartment

indicated that 1-month post-injection, BTX-A also yields some unintended (a narrower range of motion and higher passive force production in resting state, for the injected TA) and uncontrolled effects (altered mechanics of other compartmental muscles due to the spread of the toxin). The higher passive forces in the BTX-A group compared to that of control have been ascribed to the elevated connective tissue stiffness, based on the increased collagen content measured in the exposed muscles. Those are adverse effects of BTX-A on muscle function, and thus, have high potential clinical importance.

It is meaningful to comment on the findings, which we obtained and published [196] within the scope of this thesis, by considering two issues in the literature: First, a previous study [74] testing the acute effects of BTX-A in rats showed no significant changes in the TA muscle's length range of force exertion though, here in this thesis, BTX-A, in the long term, has been shown to lead to even a narrowing of it. This means that, unlike an expected widening, the range of motion worsens over time, or in other words, unintended BTX-A-induced changes to the injected muscle's function progress over time. Secondly, recent studies reported diminished, and unaffected EMFT due to the exposure of rat muscles to BTX-A acutely [77] and 1-month post-BTX-A injection [197], respectively, and how these effects would be in humans is unknown. Combining all, one can ultimately suggest that EMFT is more pronounced in children with CP compared to healthy children, and the short-term efficacy of BTX-A is likely based on suppression of said EMFT. Testing these deserves major attention and will inevitably lead to highly effective clinical outcomes.

7.3 Final Remarks and Future Directions

This thesis has achieved quite successful outputs by investigating the features of spastic muscles as mechanical structures and revealing that connective tissue interactions between spastic muscles have significant effects on the function of these mechanical structures, and, by showing that BTX-A is worthy of research in humans, based on the striking effects it leads on muscular mechanics showed with animal studies.

The methodological limitations should be acknowledged. The intraoperative force measurement methodology, used in this thesis, is ideal for characterizing the capacity of a muscle to produce force and to determine its contribution to restricted joint mobility though, intraoperative approaches are very rare, not only because of the impossibility to perform them in clinical routine due to limited access to the tendons and technical challenges of measuring the tendon force but also because they preclude voluntary muscle activities. Moreover, performing such intraoperative measurements in aged-matched healthy people who do not undergo surgery is not possible. Therefore, the main study limitation is the lack of a control group but testing in an aged-matched healthy group depends on the enhancement of different methodologies.

As muscle stiffness is a common clinical symptom and its management is critical during therapeutic interventions, the alterations in the mechanical (strength, stiffness) characteristics of muscles, and in the effect size of EMFT due to the disease and the BTX-A exposure need to be studied in patients. Fairly recent studies established the reliability of ultrasound shear wave elastography in children and for gastrocnemius muscle and demonstrated greater passive muscle stiffness in children with CP [198–200]. Therefore, ultrasound shear wave elastography has recently been presented as a useful tool for the study of muscle spasticity by assessing muscle stiffness through the calculation of a shear modulus. In a pilot study [201] quantifying the effects of BTX-A on passive muscle properties in children with CP, a temporary, but statistically significant, improvement in passive gastrocnemius muscle stiffness at some specific ankle joint positions between 1 and 3-months post-BTX-A was found, with no significant improvement in ankle passive range of motion or spasticity. This, therefore, suggests that BTX-A-induced changes in passive muscle stiffness may not lead to clinically meaningful improvements in the patients' mobility and indicates a condition of clinical importance. Related to the assessment of the effects of intermuscular mechanical interactions in the patients' mobility, as the muscle shear modulus is linearly related to muscle force [202] ultrasound shear wave elastography can be used to study EMFT as well. Utilizing shear wave elastography, Ates et al. [127] have recently quantified the localized changes in the shear modulus of lower limb muscles during ankle rotations performed at two different knee angles and demonstrated the existence of EMFT via

intermuscular mechanical interactions for healthy adults. However, all these studies focused on the lower leg muscles and/or investigated only passive muscle properties.

Future studies are needed to examine both passive muscle properties and active muscle properties that would represent the patient's voluntary movement and to work with different muscle groups in other parts of the limbs. For investigating whether intermuscular mechanical interactions differ in patients with CP compared to healthy individuals and in patients before and after BTX-A exposure, applying ultrasound shear wave elastography in clinical practice can potentially be a useful tool, for both understanding of CP and monitoring the muscular changes during the time-course of therapeutic interventions, all of these will undoubtedly lead to findings that will have a great clinical repercussion.

APPENDIX A. INDIVIDUAL KNEE JOINT ANGLE DATA FOR EACH LIMB TESTED

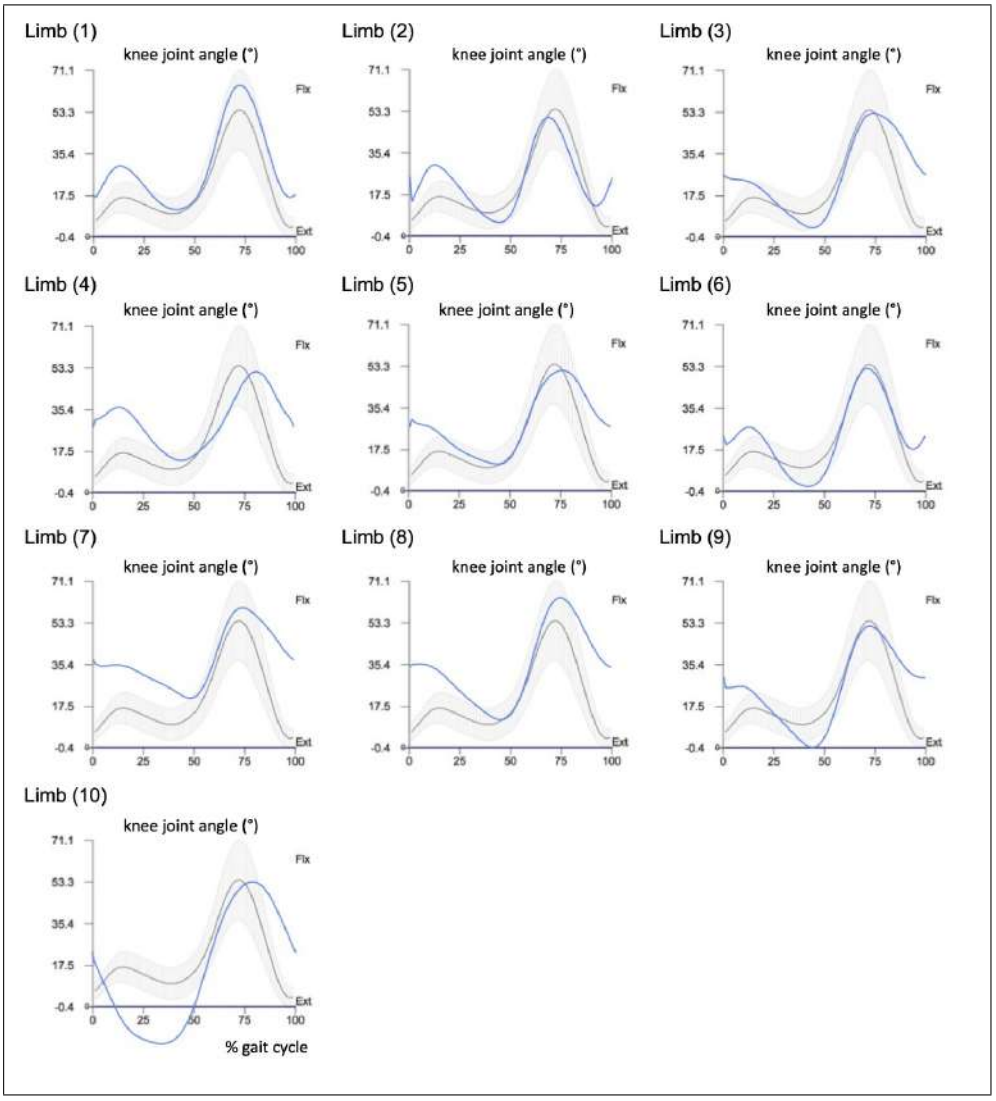

Figure A.1 Gait data showing knee joint angles in the sagittal plane per each limb tested.The blue curves show the patients' data, whereas the black curves provide the reference for typically developing children (from the database of the BTS Bioengineering system). Knee flexion (Flx) and extension (Ext) are indicated. The limbs 7-9 which show the greatest deviations from an extended knee position at the start of the gait characterize the most severe pathological movement. Note that hyperextension was observed in only one of the limbs tested (Limb 10). The patient was diagnosed with a plantar flexion-knee extension couple leading to a decision of hamstring as well as gastrocnemius release surgery.

APPENDIX B. CORRELATION ASSESSMENT BETWEEN THE SEVERITY OF THE PATHOLOGICAL GAIT AND EFFECTS OF EPIMUSCULAR MYOFASCIAL FORCE TRANSMISSION ON SPASTIC GRACILIS MUSCLE

The present data indicated that the active state forces of spastic GRA muscle elevate significantly after the added activation of other muscles. Based on that finding, here we sought a correlation between the severity of the patients' pathological gait and the increase in spastic GRA force amplitude via co-activation of other muscles. For the former, the deviation of knee angle from an extended position at the start of the gait cycle was considered as a metric that characterizes pathological movement. For the latter, the maximal percent spastic GRA force increase in condition IV compared to that in condition II, within the gait-relevant joint positions were considered as a metric that represents the peak EMFT effect. Spearman's rank correlation coefficient was calculated to test for the correlation sought after.

Figure A.1 shows knee joint angle data per each limb tested during a gait cycle. Based on the deviation of knee angle from an extended position at the start of the gait cycle, the limbs showing the most severe pathological movement are limbs 7-9. Table B.1 shows the amplitudes of those deviations as well as the corresponding maximal percent increase in spastic GRA force due to co-activation of other muscles. The Spearman's Rank correlation coefficient calculated was 0.745 (P= 0.013) indicating that there is a strong correlation between the severity of the pathological movement and the effects of added activation of synergistic and antagonistic muscles. Therefore, we conclude that the present data support the influence of EMFT in the pathological gait of patients with spastic cerebral palsy.

Table B.1
Metrics used for a correlation assessment between the patients' pathological gait and spastic GRA force increases.

Limb	Knee angle at the start of GC as deviation from knee extended position (°)	Maximal increase of spastic GRA force due to added activation of other muscles (%)
1	18.06	36.07
2	24.90	109.14
3	26.79	71.39
4	27.77	63.96
5	27.04	50.62
6	23.67	35.36
7	37.48	90.80
8	34.51	204.33
9	29.83	151.44
10	22.90	45.90

APPENDIX C. CORRELATION ASSESSMENT BETWEEN CLINICAL AND INTRAOPERATIVE MEASUREMENTS FOR SPASTIC SEMITENDINOSUS MUSCLE

C.1 Clinical and Intraoperative Measures

The mean of popliteal angle (PA) measurements according to the Modified Tardieu Scale per fast and slow-sustained stretch was considered as a representative metric of the patients' clinical condition in the knee joint.

On the other hand, data obtained based on intraoperative experimental conditions and in the tested knee angle (KA) and hip angle (HA) positions were considered in two groups:

Group A

The data collected in conditions I and II were considered to characterize spastic ST's mechanical behavior through the following metrics:

1. *Metrics based on force* (i) $\%F_{ST\_passive\ peak} \mid 120°$ (percent of peak passive state force at KA= 120°), (ii) $\%F_{ST\_peak} \mid 0°$ (percent of peak active state force at KA= 0°), (iii) $\%F_{ST\_peak} \mid 120°$ (percent of peak active state force at KA= 120°).
2. *Metrics based on the range of force exertion* (iv) Range-F_{ST} (operational KA range of F_{ST} exertion in active state i.e., joint angle range between the KA's at which, the minimum and peak F_{ST} is measured).

Note that all metrics were studied both for HA= 20° and HA= 45° (Table C.1).

Group B

The data collected in conditions III and IV were considered to characterize the influence of spastic ST's mechanical interaction with other muscles on its mechanical behavior through the following metrics:

1. *Metrics based on force* (i) $\%F_{ST\_peak} \mid 0^\circ$ (percent of peak active state force at KA= 0°), (ii) $\%F_{ST\_peak} \mid 120^\circ$ (percent of peak active state force at KA= 120°).
2. *Metrics based on the range of force exertion* (iii) Range-F_{ST} (operational KA range of F_{ST} exertion in active state i.e., joint angle range between the KA's at which, the minimum and peak F_{ST} is measured).

Note that all metrics were studied both for HA= 20° and HA= 45° (Table C.2 for condition III and Table C.3 for condition IV).

C.2 Clinical and Experimental Measures Compared

Spearman's rank correlation coefficient was calculated to test if mean PA values are correlated with the key representatives of intraoperatively measured spastic ST forces. Correlations were considered significant at $P < 0.05$.

C.3 Results

Group A

1. *Metrics based on force*: None of the metrics showed a significant correlation with the mean PA, but $\%F_{ST\_passive\ peak} \mid 120^\circ$ at HA= 20° (Spearman's rank correlation coefficient= 0.72, P= 0.02).
2. *Metrics based on the range of force exertion*: None of the metrics showed a significant correlation with the mean PA.

Table C.1
Clinical measures characterizing patients' clinical condition and intraoperative measures (Group A). PA= mean popliteal angle; $\%F_{ST\_peak}$ | 120° = percent of peak force at KA= 120°; $\%F_{ST\_peak}$ | 0° = percent of peak force at KA= 0°; $\%F_{ST\_passive\ peak}$ | 120° = percent of peak force at KA= 120°; Range-F_{ST} = operational KA range of F_{ST} exertion in active state i.e., joint angle range between the KA's at which, the minimum and peak F_{ST} is measured.

	Experimental data (HA= 45°)				Clinical data
Limb	$\%F_{ST\_peak}$ | 120°	$\%F_{ST\_peak}$ | 0°	$\%F_{ST\_passive\ peak}$ | 120°	Range-F_{ST} (°)	Mean PA (°)
1	92.3	100.0	0.0	120	62.5
2	36.2	64.8	0.0	80	67.5
3	8.0	21.7	1.3	98	60
4	20.0	100.0	15.2	120	57.5
5	30.3	100.0	0.0	120	55
6	4.2	46.0	1.3	66	65
7	8.1	59.2	92.3	66	80
8	49.0	91.5	98.2	79	80
9	32.3	53.3	93.9	44	70
10	90.6	72.7	0.0	20	72.5
	Experimental data (HA= 20°)				
Limb	$\%F_{ST\_peak}$ | 120°	$\%F_{ST\_peak}$ | 0°	$\%F_{ST\_passive\ peak}$ | 120°	Range-F_{ST} (°)	
1	40.5	100.0	0.0	120	
2	0.0	80.0	0.0	95	
3	0.0	22.4	2.3	58	
4	5.7	100.0	0.0	120	
5	32.5	100.0	7.6	120	
6	19.6	7.8	26.6	86	
7	49.2	65.0	96.8	90	
8	32.7	100.0	100.0	120	
9	19.6	100.0	98.1	120	
10	100.0	22.1	35.8	0	

Table C.2
Clinical measures characterizing patients' clinical condition and intraoperative measures (Group B, condition III). PA= mean popliteal angle; $\%F_{ST\_peak} \mid 120°$ = percent of peak force at KA= 120°; $\%F_{ST\_peak} \mid 0°$ = percent of peak force at KA= 0°; Range-F_{ST} = operational KA range of F_{ST} exertion in active state i.e., joint angle range between the KA's at which, the minimum and peak F_{ST} is measured.

	Experimental data (HA= 45°)			Clinical data
Limb	$\%F_{ST\_peak} \mid 120°$	$\%F_{ST\_peak} \mid 0°$	Range-F_{ST} (°)	Mean PA (°)
1	96.3	84.5	35	62.5
2	25.6	45.4	96	67.5
3	20.7	85.8	98	60
4	0.0	100.0	120	57.5
5	0.0	79.2	96	55
6	0.0	29.7	87	65
7	42.0	42.6	86	80
8	100.0	93.0	0	80
9	15.5	50.4	81	70
10	100.0	32.8	0	72.5
	Experimental data (HA= 20°)			
Limb	$\%F_{ST\_peak} \mid 120°$	$\%F_{ST\_peak} \mid 0°$	Range-F_{ST} (°)	
1	36.7	100.0	120	
2	0.0	71.3	95	
3	12.4	99.1	112	
4	0.1	82.3	107	
5	8.6	73.7	102	
6	18.5	97.5	108	
7	31.8	64.1	90	
8	97.7	100.0	120	
9	12.4	100.0	120	
10	70.6	58.5	97	

Table C.3
Clinical measures characterizing patients' clinical condition and intraoperative measures (Group B, condition IV). PA= mean popliteal angle; $\%F_{ST\_peak} \mid 120°$ = percent of peak force at KA= 120°; $\%F_{ST\_peak} \mid 0°$ = percent of peak force at KA= 0°; Range-F_{ST} = operational KA range of F_{ST} exertion in active state i.e., joint angle range between the KA's at which, the minimum and peak F_{ST} is measured.

	Experimental data (HA= 45°)			Clinical data
Limb	$\%F_{ST\_peak} \mid 120°$	$\%F_{ST\_peak} \mid 0°$	Range-F_{ST} (°)	Mean PA (°)
1	86.2	90.5	79	62.5
2	0.0	91.6	95	67.5
3	34.1	90.6	97	60
4	0.0	66.7	76	57.5
5	26.6	57.3	44	55
6	2.4	21.8	74	65
7	50.6	43.5	80	80
8	16.1	49.8	73	80
9	12.0	52.0	64	70
10	56.4	98.2	110	72.5
	Experimental data (HA= 20°)			
Limb	$\%F_{ST\_peak} \mid 120°$	$\%F_{ST\_peak} \mid 0°$	Range-F_{ST} (°)	
1	16.1	100.0	120	
2	0.0	77.5	91	
3	13.2	98.8	112	
4	0.5	77.6	94	
5	11.9	62.5	81	
6	17.0	97.9	107	
7	22.4	66.9	89	
8	45.5	100.0	120	
9	15.3	98.5	69	
10	100.0	78.0	0	

Group B

1. *Metrics based on force*: $\%F_{ST\_peak}$ | 120° at HA= 45° (condition III) and $\%F_{ST\_peak}$ | 120° at HA= 20° (condition IV) showed a significant correlation with the mean PA (Spearman's rank correlation coefficients= 0.71, P= 0.02)

2. *Metrics based on the range of force exertion*: Range-F_{ST} at HA= 45° (condition III) showed a significant correlation with the mean PA (Spearman's rank correlation coefficient= -0.72, P= 0.02).

C.4 Discussion

The previous studies we have conducted showed consistently no significant correlation between clinically measured metrics characterizing the patients' condition in the passive state and intraoperatively measured metrics characterizing the targeted spastic muscles' mechanics [43–45]. In contrast, the present study showed a significant correlation for Group A, which indicates a potential diagnostic value of clinically measured metrics, in the passive state. Note that the previous studies were capable of quantifying only the active state mechanics and passive state mechanics of the spastic ST muscle were quantified for the first time presently. This made the particular correlation analysis possible. In addition, the present experiment involved flexed hip positions, unlike the previously extended reference hip position. This elevated relevance of the tested joint positions for the patients' gait, but more importantly, for the present correlation assessment, for the joint positions employed during the assessment of the PA. Remarkably, the present study also showed significant correlations for Group B. Therefore, in sum, a typical clinical pre-surgical assessment may be representative of spastic ST muscle's passive state mechanics regarding the muscle's intrinsic properties (conditions I and II). However active state mechanics show relevance if the muscle's mechanical interaction with other muscles (conditions III and IV) is taken into account.

APPENDIX D. MAXIMAL AND SELECTIVE STIMULATION TO THE TARGET SPASTIC MUSCLE

In the first study in which the developed intraoperative methodology was presented [42], the success of our stimulation methodology to activate the muscles was tested in anterior cruciate ligament (ACL) reconstruction patients and reported. In short, it was shown that a randomized use of current amplitudes of 130, 140, 150, and 160 mA yields no systematic force increase as a result of increasing current amplitude, and no appreciable force variation. This indicates that the stimulated muscle is tetanized, which allows measuring the peak force of the muscle as a consistent experimental condition across different participants. In our previous studies reporting the mechanical behavior of individually activated spastic GRA [44], ST [43], and SM [45], a similar assessment led to choosing a current amplitude of 160 mA in order to ensure maximal activation of the target spastic muscle. This is also used presently.

Figure D.1 shows examples from one participant of force-time traces of the spastic ST measured in the three experimental conditions (i.e., the spastic ST was stimulated (condition II) alone, (condition III) simultaneously with its synergists GRA and biceps femoris, and (condition IV) also with its antagonist rectus femoris). This indicates that the muscle was maximally activated (i.e., tetanized) in each different test condition of the present study.

On the other hand, selective activation of the target muscle was also studied with specific tests in patients: before the actual test protocol was conducted, an additional buckle force transducer was mounted over the GRA distal tendon and in response to exclusive stimulation of either the spastic ST or the GRA using the protocol described, forces of both muscles were measured simultaneously to ensure the success of our stimulation methodology in isolating the stimulation and also maximally tetanizing the targeted muscle only (see Figure D.2 for an example to that).

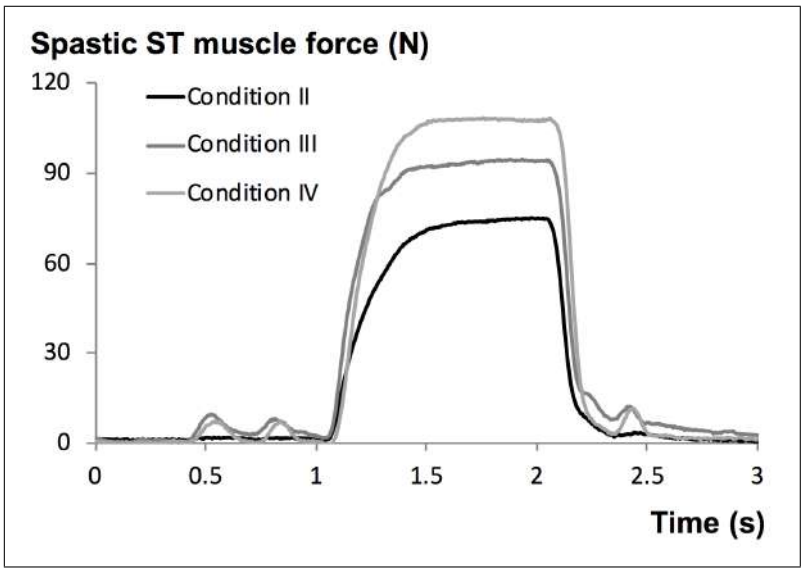

Figure D.1 Examples of typical force-time traces of spastic ST muscle in the three experimental conditions superimposed (knee angle=30°, hip angle=20°). Note that this was a consistent finding also for other knee joint angles tested in both hip joint positions.

In that example (left panel in Figure D.2), the force-time traces of spastic GRA show no change in its forces, indicating a lack of activation of this muscle in response to individual stimulation of the ST. Similarly, the force-time traces (right panel in Figure D.2) show no change in ST forces in response to selective stimulation of the GRA. Note that, this is valid also for other knee positions at hip angles of 45° and 20°. Note also that, the routine incisions performed in the surgery are not modified at all for the intraoperative experiments. Therefore, direct force measurements from the muscles that are not the targets of the surgical procedure (biceps femoris and rectus femoris muscles in the current study) are not possible. However, these are distant muscles to the ST and the tests exemplified above indicate selective activation can be achieved even for muscles in proximity. Therefore, they are not activated, unless stimulated directly and in conditions involving their added activations, the muscle stimulation protocols described above are used.

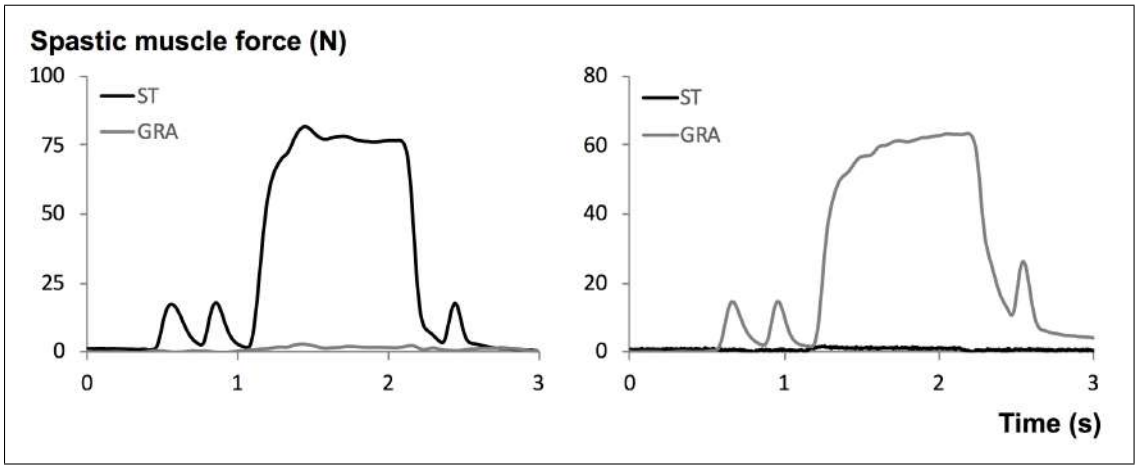

Figure D.2 Examples of typical force-time traces of spastic ST (left) and GRA (right) muscles obtained during the individual stimulation of the ST and the GRA, respectively (knee angle=30°, hip angle=45°). Note that, to determine the muscle force at each joint angle, muscle force values within the middle of the tetanus are averaged.

REFERENCES

1. Trotter, J. A., and P. P. Purslow, "Functional morphology of the endomysium in series fibered muscles," *Journal of Morphology*, Vol. 212, no. 2, pp. 109–122, 1992.

2. Oatis, C. A., *Kinesiology: The Mechanics and Pathomechanics of Human Movement, 2nd edition*, Philadelphia, Pennsylvania: Lippincott Williams & Wilkins, 2009.

3. Garies, H., M. Solomonow, R. Baratta, R. Best, *et al.*, "The isometric length-force models of nine different skeletal muscles," *Journal of Biomechanics*, Vol. 25, no. 8, pp. 903–916, 1992.

4. Huijing, P. A., "Muscular force transmission: A unified, dual or multiple system? a review and some explorative experimental results," *Archives of Physiology and Biochemistry*, Vol. 107, no. 4, pp. 292–311, 1999.

5. Purslow, P. P., and J. A. Trotter, "The morphology and mechanical properties of endomysium in series-fibred muscles: Variations with muscle length," *Journal of Muscle Research and Cell Motility*, Vol. 15, pp. 299–308, 1994.

6. Street, S. F., "Lateral transmission of tension in frog myofibers: A myofibrillar network and transverse cytoskeletal connections are possible transmitters," *Journal of Cellular Physiology*, Vol. 114, no. 3, pp. 346–364, 1983.

7. Huijing, P. A., "Epimuscular myofascial force transmission between antagonistic and synergistic muscles can explain movement limitation in spastic paresis," *Journal of Electromyography and Kinesiology*, Vol. 17, no. 6, pp. 708–724, 2007.

8. Huijing, P. A., "Muscle as a collagen fiber reinforced composite: A review of force transmission in muscle and whole limb," *Journal of Biomechanics*, Vol. 32, no. 4, pp. 329–345, 1999.

9. Huijing, P. A., "Epimuscular myofascial force transmission: A historical review and implications for new research. international society of biomechanics muybridge award lecture, taipei, 2007," *Journal of Biomechanics*, Vol. 42, no. 1, pp. 9–21, 2009.

10. Yucesoy, C. A., and P. A. Huijing, "Substantial effects of epimuscular myofascial force transmission on muscular mechanics have major implications on spastic muscle and remedial surgery," *Journal of Electromyography and Kinesiology*, Vol. 17, no. 6, pp. 664–679, 2007.

11. Maas, H., and T. G. Sandercock, "Force transmission between synergistic skeletal muscles through connective tissue linkages," *Journal of Biomedicine and Biotechnology*, Vol. 2010, p. 575672, 2010.

12. Huijing, P. A., and G. C. Baan, "Extramuscular myofascial force transmission within the rat anterior tibial compartment: Proximo-distal differences in muscle force," *Acta Physiologica Scandinavica*, Vol. 173, no. 3, pp. 297–311, 2001.

13. Maas, H., G. C. Baan, P. A. Huijing, C. A. Yucesoy, *et al.*, "The relative position of edl muscle affects the length of sarcomeres within muscle fibers: Experimental results and finite-element modeling," *Journal of Biomechanical Engineering*, Vol. 125, no. 5, pp. 745–753, 2003.

14. Maas, H., G. C. Baan, and P. A. Huijing, "Intermuscular interaction via myofascial force transmission: Effects of tibialis anterior and extensor hallucis longus length on force transmission from rat extensor digitorum longus muscle," *Journal of Biomechanics*, Vol. 34, no. 7, pp. 927–940, 2001.

15. Meijer, H. J. M., G. C. Baan, and P. A. Huijing, "Myofascial force transmission is increasingly important at lower forces: Firing frequency-related length-force characteristics of rat extensor digitorum longus," *Acta Physiologica*, Vol. 186, no. 3, pp. 185–195, 2006.

16. Yucesoy, C. A., B. H. F. J. M. Koopman, G. C. Baan, H. J. Grootenboer, *et al.*, "Extramuscular myofascial force transmission: Experiments and finite element modeling," *Archives of Physiology and Biochemistry*, Vol. 111, no. 4, pp. 377–388, 2003.

17. Yucesoy, C. A., B. H. F. J. M. Koopman, G. C. Baan, H. J. Grootenboer, *et al.*, "Effects of inter- and extramuscular myofascial force transmission on adjacent synergistic muscles: Assessment by experiments and finite-element modeling," *Journal of Biomechanics*, Vol. 36, no. 12, pp. 1797–1811, 2003.

18. Huijing, P. A., and G. C. Baan, "Myofascial force transmission: Muscle relative position and length determine agonist and synergist muscle force," *Journal of Applied Physiology*, Vol. 94, no. 3, pp. 1092–1107, 2003.

19. Maas, H., G. C. Baan, and P. A. Huijing, "Muscle force is determined also by muscle relative position: Isolated effects," *Journal of Biomechanics*, Vol. 37, no. 1, pp. 99–110, 2004.

20. Maas, H., C. A. Yucesoy, G. C. Baan, and P. A. Huijing, "Implications of muscle relative position as a co-determinant of isometric muscle force: A review and some experimental results," *Journal of Mechanics in Medicine and Biology*, Vol. 3, no. 2, pp. 145–168, 2003.

21. Yucesoy, C. A., H. Maas, B. H. F. J. M. Koopman, H. J. Grootenboer, *et al.*, "Mechanisms causing effects of muscle position on proximo-distal muscle force differences in extramuscular myofascial force transmission," *Medical Engineering and Physics*, Vol. 28, no. 3, pp. 214–226, 2006.

22. Rijkelijkhuizen, J. M., G. C. Baan, A. de Haan, C. J. de Ruiter, *et al.*, "Extramuscular myofascial force transmission for in situ rat medial gastrocnemius and plantaris muscles in progressive stages of dissection," *Journal of Experimental Biology*, Vol. 208, no. 1, pp. 129–140, 2005.

23. Bax, M., M. Goldstein, P. Rosenbaum, A. Leviton, *et al.*, "Proposed definition and classification of cerebral palsy, april 2005," *Developmental Medicine and Child Neurology*, Vol. 47, no. 8, pp. 571–576, 2005.

24. Rosenbaum, P., N. Paneth, A. Leviton, M. Goldstein, *et al.*, "A report: The definition and classification of cerebral palsy april 2006," *Developmental Medicine and Child Neurology*, Vol. 49, no. s109, pp. 8–14, 2007.

25. Graham, H. K., and P. Selber, "Musculoskeletal aspects of cerebral palsy," *Journal of Bone and Joint Surgery*, Vol. 85-B, no. 2, pp. 157–166, 2003.

26. Lance, J. W., "Symposium synopsis," in *Spasticity: Disordered Motor Control* (Feldman, R. G., R. R. Young, and W. P. Koella, eds.), pp. 485–494, Chicago: Year Book Medical Publishers, 1980.

27. Botte, M. J., V. L. Nickel, and W. H. Akeson, "Spasticity and contracture. physiologic aspects of formation," *Clinical Orthopaedics and Related Research*, Vol. 233, pp. 7–18, 1988.

28. Gracies, J. M., N. Bayle, M. Vinti, S. Alkandari, *et al.*, "Five-step clinical assessment in spastic paresis," *European Journal of Physical and Rehabilitation Medicine*, Vol. 46, no. 3, pp. 411–421, 2010.

29. O'Dwyer, N. J., and L. Ada, "Reflex hyperexcitability and muscle contracture in relation to spastic hypertonia," *Current Opinion in Neurology*, Vol. 9, no. 6, pp. 451–455, 1996.

30. Barber, L., R. Barrett, and G. Lichtwark, "Passive muscle mechanical properties of the medial gastrocnemius in young adults with spastic cerebral palsy," *Journal of Biomechanics*, Vol. 44, no. 13, pp. 2496–2500, 2011.

31. Bénard, M. R., R. T. Jaspers, P. A. Huijing, J. G. Becher, *et al.*, "Reproducibility of hand-held ankle dynamometry to measure altered ankle moment-angle characteristics in children with spastic cerebral palsy," *Clinical Biomechanics*, Vol. 25, no. 8, pp. 802–808, 2010.

32. de Bruin, M., M. J. Smeulders, M. Kreulen, P. A. Huijing, *et al.*, "Intramuscular connective tissue differences in spastic and control muscle: A mechanical and histological study," *PLoS ONE*, Vol. 9, no. 6, p. e101038, 2014.

33. Gracies, J. M., "Pathophysiology of spastic paresis. i: Paresis and soft tissue changes," *Muscle and Nerve*, Vol. 31, no. 5, pp. 535–551, 2005.

34. Smith, L. R., K. S. Lee, S. R. Ward, H. G. Chambers, *et al.*, "Hamstring contractures in children with spastic cerebral palsy result from a stiffer extracellular matrix and increased in vivo sarcomere length," *The Journal of Physiology*, Vol. 589, no. 10, pp. 2625–2639, 2011.

35. Alhusaini, A. A., J. Crosbie, R. B. Shepherd, C. M. Dean, *et al.*, "Mechanical properties of the plantarflexor musculotendinous unit during passive dorsiflexion in children with cerebral palsy compared with typically developing children," *Developmental Medicine and Child Neurology*, Vol. 52, no. 6, pp. e101–e106, 2010.

36. Elder, G. C. B., G. Stewart, K. Cook, D. Weir, *et al.*, "Contributing factors to muscle weakness in children with cerebral palsy," *Developmental Medicine and Child Neurology*, Vol. 45, no. 8, pp. 542–550, 2003.

37. Fergusson, D., B. Hutton, and A. Drodge, "The epidemiology of major joint contractures: A systematic review of the literature," *Clinical Orthopaedics and Related Research*, Vol. 456, pp. 22–29, 2007.

38. Delp, S. L., A. S. Arnold, R. A. Speers, and C. A. Moore, "Hamstrings and psoas lengths during normal and crouch gait: Implications for muscle-tendon surgery," *Journal of Orthopaedic Research*, Vol. 14, no. 1, pp. 144–151, 1996.

39. Bell, K. J., S. Ounpuu, P. A. DeLuca, and M. J. Romness, "Natural progression of gait in children with cerebral palsy," *Journal of Pediatric Orthopaedics*, Vol. 22, no. 5, pp. 677–682, 2002.

40. Crenna, P., "Spasticity and 'spastic' gait in children with cerebral palsy," *Neuroscience and Biobehavioral Reviews*, Vol. 22, no. 4, pp. 571–578, 1998.

41. Heest, A. E. V., J. H. House, and C. Cariello, "Upper extremity surgical treatment of cerebral palsy," *Journal of Hand Surgery*, Vol. 24, no. 2, pp. 323–330, 1999.

42. Yucesoy, C. A., F. Ates, U. Akgun, and M. Karahan, "Measurement of human gracilis muscle isometric forces as a function of knee angle, intraoperatively," *Journal of Biomechanics*, Vol. 43, no. 14, pp. 2665–2671, 2010.

43. Ates, F., Y. Temelli, and C. A. Yucesoy, "The mechanics of activated semitendinosus are not representative of the pathological knee joint condition of children with cerebral palsy," *Journal of Electromyography and Kinesiology*, Vol. 28, pp. 130–136, 2016.

44. Ates, F., Y. Temelli, and C. A. Yucesoy, "Human spastic gracilis muscle isometric forces measured intraoperatively as a function of knee angle show no abnormal muscular mechanics," *Clinical Biomechanics*, Vol. 28, no. 1, pp. 48–54, 2013.

45. Yucesoy, C. A., Y. Temelli, and F. Ates, "Intra-operatively measured spastic semimembranosus forces of children with cerebral palsy," *Journal of Electromyography and Kinesiology*, Vol. 36, pp. 49–55, 2017.

46. Ates, F., Y. Temelli, and C. A. Yucesoy, "Intraoperative experiments show relevance of inter-antagonistic mechanical interaction for spastic muscle's contribution to joint movement disorder," *Clinical Biomechanics*, Vol. 29, no. 8, pp. 943–949, 2014.

47. Ates, F., R. N. Ozdeslik, P. A. Huijing, and C. A. Yucesoy, "Muscle lengthening surgery causes differential acute mechanical effects in both targeted and non-targeted synergistic muscles," *Journal of Electromyography and Kinesiology*, Vol. 23, no. 5, pp. 1199–1205, 2013.

48. Maas, H., H. J. M. Meijer, and P. A. Huijing, "Intermuscular interaction between synergists in rat originates from both intermuscular and extramuscular myofascial force transmission," *Cells Tissues Organs*, Vol. 181, no. 1, pp. 38–50, 2005.

49. Yucesoy, C. A., G. C. Baan, B. H. F. J. M. Koopman, H. J. Grootenboer, *et al.*, "Prestrained epimuscular connections cause muscular myofascial force transmission to affect properties of synergistic ehl and edl muscles of the rat," *Journal of Biomechanical Engineering*, Vol. 127, no. 5, pp. 819–828, 2005.

50. Willems, M. E. T., and P. A. Huijing, "Heterogeneity of mean sarcomere length in different fibres: Effects on length range of active force production in rat muscle," *European Journal of Applied Physiology and Occupational Physiology*, Vol. 68, pp. 489–496, 1994.

51. Bakheit, A. M. O., "Management of muscle spasticity," *Critical Reviews in Physical and Rehabilitation Medicine*, Vol. 8, no. 3, pp. 235–252, 1996.

52. Damiano, D. L., K. E. Alter, and H. Chambers, "New clinical and research trends in lower extremity management for ambulatory children with cerebral palsy," *Physical Medicine and Rehabilitation Clinics of North America*, Vol. 20, no. 3, pp. 469–491, 2009.

53. Love, S. C., J. P. Valentine, E. M. Blair, C. J. Price, *et al.*, "The effect of botulinum toxin type a on the functional ability of the child with spastic hemiplegia a randomized controlled trial," *European Journal of Neurology*, Vol. 8, no. s5, pp. 50–58, 2001.

54. Criswell, S. R., B. E. Crowner, and B. A. Racette, "The use of botulinum toxin therapy for lower-extremity spasticity in children with cerebral palsy," *Neurosurgical Focus*, Vol. 21, no. 2, p. E1, 2006.

55. Graham, H. K., K. R. Aoki, I. Autti-Rämö, R. N. Boyd, *et al.*, "Recommendations for the use of botulinum toxin type a in the management of cerebral palsy," *Gait and Posture*, Vol. 11, no. 1, pp. 67–79, 2000.

56. Lukban, M. B., R. L. Rosales, and D. Dressler, "Effectiveness of botulinum toxin a for upper and lower limb spasticity in children with cerebral palsy: A summary of evidence," *Journal of Neural Transmission*, Vol. 116, pp. 319–331, 2009.

57. Ahnert-Hilger, G., and H. Bigalke, "Molecular aspects of tetanus and botulinum neurotoxin poisoning," *Progress in Neurobiology*, Vol. 46, no. 1, pp. 83–96, 1995.

58. Aoki, K. R., "Immunologic and other properties of therapeutic botulinum toxin serotypes," in *Scientific and Therapeutic Aspects of Botulinum Toxin* (Brin, M. F., J. Jankovic, and M. H. M, eds.), pp. 103–113, Philadelphia: Lippincott Williams and Wilkins, 2002.

59. Aoki, K. R., and B. Guyer, "Botulinum toxin type a and other botulinum toxin serotypes: A comparative review of biochemical and pharmacological actions," *European Journal of Neurology*, Vol. 8, no. Suppl 5, pp. 21–29, 2001.

60. Heinen, F., K. Desloovere, A. S. Schroeder, S. Berweck, *et al.*, "The updated european consensus 2009 on the use of botulinum toxin for children with cerebral palsy," *European Journal of Paediatric Neurology*, Vol. 14, no. 1, pp. 45–66, 2010.

61. Blasi, J., E. R. Chapman, E. Link, T. Binz, *et al.*, "Botulinum neurotoxin a selectively cleaves the synaptic protein snap-25," *Nature*, Vol. 365, pp. 160–163, 1993.

62. Brin, M. F., "Botulinum toxin: Chemistry, pharmacology, toxicity, and immunology," *Muscle Nerve Suppl*, Vol. 6, pp. 146–168, 1997.

63. Dolly, J. O., A. de Paiva, P. Foran, G. Lawrence, *et al.*, "Probing the process of transmitter release with botulinum and tetanus neurotoxins," *Seminars in the Neurosciences*, Vol. 6, no. 3, pp. 149–158, 1994.

64. Esquenazi, A., and N. Mayer, "Botulinum toxin for the management of muscle overactivity and spasticity after stroke," *Current Atherosclerosis Reports*, Vol. 3, pp. 295–298, 2001.

65. Kareem, A. A., "Use of botulinum toxin a in cerebral palsy," in *Cerebral Palsy - Clinical and Therapeutic Aspects* (Al-Zwaini, I. J., ed.), ch. 6, pp. 95–112, IntechOpen, 2018.

66. Simpson, L. L., "Current concepts on the mechanism of action of clostridial neurotoxins," in *Botulinum and Tetanus Neurotoxins: Neurotransmission and Biomedical Aspects* (DasGupta, B. R., ed.), pp. 5–15, Boston, MA: Springer, 1993.

67. Longino, D., T. A. Butterfield, and W. Herzog, "Frequency and length-dependent effects of botulinum toxin-induced muscle weakness," *Journal of Biomechanics*, Vol. 38, no. 3, pp. 609–613, 2005.

68. Grazko, M. A., K. B. Polo, and B. Jabbari, "Musculoskeletal aspects of cerebral palsy," *Neurology*, Vol. 45, no. 4, pp. 712–717, 1995.

69. Whelchel, D. D., T. M. Brehmer, P. M. Brooks, N. Darragh, *et al.*, "Molecular targets of botulinum toxin at the mammalian neuromuscular junction," *Movement Disorders*, Vol. 19, no. S8, pp. S7–S16, 2004.

70. Koman, L. A., J. F. Mooney, B. Smith, A. Goodman, *et al.*, "Management of cerebral palsy with botulinum-a toxin: Preliminary investigation," *Journal of Pediatric Orthopaedics*, Vol. 13, no. 4, pp. 489–495, 1993.

71. Wissel, J., F. Heinen, A. Schenkel, B. Doll, *et al.*, "Botulinum toxin a in the management of spastic gait disorders in children and young adults with cerebral palsy: A randomized, double-blind study of 'high-dose' versus 'low-dose' treatment," *Neuropediatrics*, Vol. 30, no. 3, pp. 120–124, 1999.

72. Koman, L. A., J. F. Mooney, B. P. Smith, F. Walker, *et al.*, "Botulinum toxin type a neuromuscular blockade in the treatment of lower extremity spasticity in cerebral palsy: A randomized, double-blind, placebo-controlled trial," *Journal of Pediatric Orthopaedics*, Vol. 20, no. 1, pp. 108–115, 2000.

73. Sutherland, D. H., K. R. Kaufman, M. P. Wyatt, H. G. Chambers, *et al.*, "Double-blind study of botulinum a toxin injections into the gastrocnemius muscle in patients with cerebral palsy," *Gait and Posture*, Vol. 10, no. 1, pp. 1–9, 1999.

74. Yucesoy, C. A., O. E. Arikan, and F. Ates, "Btx-a administration to the target muscle affects forces of all muscles within an intact compartment and epimuscular myofascial force transmission," Vol. 134, no. 11, p. 111002, 2012.

75. Yaraskavitch, M., T. Leonard, and W. Herzog, "Botox produces functional weakness in non-injected muscles adjacent to the target muscle," *Journal of Biomechanics*, Vol. 41, no. 4, pp. 897–902, 2008.

76. Ates, F., and C. A. Yucesoy, "Effects of botulinum toxin type a on non-injected biarticular muscle include a narrower length range of force exertion and increased passive force," *Muscle and Nerve*, Vol. 49, no. 6, pp. 866–878, 2014.

77. Yucesoy, C. A., A. N. Turkoglu, S. Umur, and F. Ates, "Intact muscle compartment exposed to botulinum toxin type a shows compromised intermuscular mechanical interaction," *Muscle and Nerve*, Vol. 51, no. 1, pp. 106–116, 2015.

78. Yucesoy, C. A., and F. Ates, "Btx-a has notable effects contradicting some treatment aims in the rat triceps surae compartment, which are not confined to the muscles injected," *Journal of Biomechanics*, Vol. 66, pp. 78–85, 2018.

79. Ates, F., and C. A. Yucesoy, "Botulinum toxin type-a affects mechanics of non-injected antagonistic rat muscles," *Journal of the Mechanical Behavior of Biomedical Materials*, Vol. 84, pp. 208–216, 2018.

80. Frasson, E., E. Dall'Ora, M. Bordignon, F. Brigo, *et al.*, "Spread of botulinum neurotoxin type a at standard doses is inherent to the successful treatment of spastic equinus foot in cerebral palsy: Short-term neurophysiological and clinical study," *Journal of Child Neurology*, Vol. 27, no. 5, pp. 587–593, 2012.

81. Turkoglu, A. N., and C. A. Yucesoy, "Simulation of effects of botulinum toxin on muscular mechanics in time course of treatment based on adverse extracellular matrix adaptations," *Journal of Biomechanics*, Vol. 49, no. 7, pp. 1192–1198, 2016.

82. Ikeda, A. J., M. F. Abel, K. P. Granata, and D. L. Damiano, "Quantification of cocontraction in spastic cerebral palsy," *Electromyography and Clinical Neurophysiology*, Vol. 38, no. 8, pp. 497–504, 1998.

83. Mirbagheri, M. M., H. Barbeau, M. Ladouceur, and R. E. Kearney, "Intrinsic and reflex stiffness in normal and spastic, spinal cord injured subjects," *Experimental Brain Research*, Vol. 141, pp. 446–459, 2001.

84. Kreulen, M., M. J. C. Smeulders, and J. J. Hage, "Restored flexor carpi ulnaris function after mere tenotomy explains the recurrence of spastic wrist deformity," *Clinical Biomechanics*, Vol. 19, no. 4, pp. 429–432, 2004.

85. Kursa, K., E. Diao, L. Lattanza, and D. Rempel, "In vivo forces generated by finger flexor muscles do not depend on the rate of fingertip loading during an isometric task," *Journal of Biomechanics*, Vol. 38, no. 11, pp. 2288–2293, 2005.

86. Smeulders, M. J. C., M. Kreulen, J. J. Hage, P. A. Huijing, *et al.*, "Overstretching of sarcomeres may not cause cerebral palsy muscle contracture," *Journal of Orthopaedic Research*, Vol. 22, no. 6, pp. 1331–1335, 2004.

87. Arnold, A. S., D. G. Thelen, M. H. Schwartz, F. C. Anderson, *et al.*, "Muscular coordination of knee motion during the terminal-swing phase of normal gait," *Journal of Biomechanics*, Vol. 40, no. 15, pp. 3314–3324, 2007.

88. He, H., K. Kiguchi, and E. Horikawa, "A study on lower-limb muscle activities during daily lower-limb motions," *International Journal of Bioelectromagnetism*, Vol. 9, no. 2, pp. 79–84, 2007.

89. Schmitz, A., A. Silder, B. Heiderscheit, J. Mahoney, *et al.*, "Differences in lower-extremity muscular activation during walking between healthy older and young adults," *Journal of Electromyography and Kinesiology*, Vol. 19, no. 6, pp. 1085–1091, 2009.

90. Yucesoy, C. A., "Epimuscular myofascial force transmission implies novel principles for muscular mechanics," *Exercise and Sport Sciences Reviews*, Vol. 38, no. 3, pp. 128–134, 2010.

91. Berthier, C., and S. Blaineau, "Supramolecular organization of the subsarcolemmal cytoskeleton of adult skeletal muscle fibers. a review," *Biology of the Cell*, Vol. 89, no. 7, pp. 413–434, 1997.

92. Purslow, P. P., "The structure and functional significance of variations in the connective tissue within muscle," *Comparative Biochemistry and Physiology Part A: Molecular and Integrative Physiology*, Vol. 133, no. 4, pp. 947–966, 2002.

93. Trotter, J. A., F. J. R. Richmond, and P. P. Purslow, "Functional morphology and motor control of series-fibered muscles," *Exercise and Sport Sciences Reviews*, Vol. 23, no. 1, pp. 167–214, 1995.

94. Kreulen, M., M. J. C. Smeulders, J. J. Hage, and P. A. Huijing, "Biomechanical effects of dissecting flexor carpi ulnaris," *The Journal of Bone and Joint Surgery*, Vol. 85-B, no. 6, pp. 856–859, 2003.

95. Katz, K., A. Rosenthal, and Z. Yosipovitch, "Normal ranges of popliteal angle in children," *Journal of Pediatric Orthopaedics*, Vol. 12, no. 2, pp. 229–231, 1992.

96. Mathur, S., J. J. Eng, and D. L. Maclntyre, "Reliability of surface emg during sustained contractions of the quadriceps," *Journal of Electromyography and Kinesiology*, Vol. 15, no. 1, pp. 102–110, 2005.

97. Gomez-Tames, J. D., J. Gonzalez, and W. Yu, "A simulation study: Effect of the inter-electrode distance, electrode size and shape in transcutaneous electrical stimulation," *Proceedings of the Annual International Conference of the IEEE Engineering in Medicine and Biology Society*, pp. 3576–3579, 2012.

98. Smeulders, M. J. C., and M. Kreulen, "Myofascial force transmission and tendon transfer for patients suffering from spastic paresis: A review and some new observations," *Journal of Electromyography and Kinesiology*, Vol. 17, no. 6, pp. 644–656, 2007.

99. Kreulen, M., and M. J. C. Smeulders, "Assessment of flexor carpi ulnaris function for tendon transfer surgery," *Journal of Biomechanics*, Vol. 41, no. 10, pp. 2130–2135, 2008.

100. Huxley, A. F., and L. D. Peachey, "The maximum length for contraction in vertebrate striated muscle," *The Journal of Physiology*, Vol. 156, no. 1, pp. 150–165, 1961.

101. Chen, X., G. N. Sanchez, M. J. Schnitzer, and S. L. Delp, "Changes in sarcomere lengths of the human vastus lateralis muscle with knee flexion measured using in vivo microendoscopy," *Journal of Biomechanics*, Vol. 49, no. 13, pp. 2989–2994, 2016.

102. Karakuzu, A., U. Pamuk, C. Ozturk, B. Acar, *et al.*, "Magnetic resonance and diffusion tensor imaging analyses indicate heterogeneous strains along human medial gastrocnemius fascicles caused by submaximal plantar-flexion activity," *Journal of Biomechanics*, Vol. 57, pp. 69–78, 2017.

103. Pamuk, U., A. Karakuzu, C. Ozturk, B. Acar, *et al.*, "Combined magnetic resonance and diffusion tensor imaging analyses provide a powerful tool for in vivo assessment of deformation along human muscle fibers," *Journal of the Mechanical Behavior of Biomedical Materials*, Vol. 63, pp. 207–219, 2016.

104. Tijs, C., J. H. van Dieën, and H. Maas, "No functionally relevant mechanical effects of epimuscular myofascial connections between rat ankle plantar flexors," *Journal of Experimental Biology*, Vol. 218, no. 18, pp. 2935–2941, 2015.

105. Huijing, P. A., A. Yaman, C. Ozturk, and C. A. Yucesoy, "Effects of knee joint angle on global and local strains within human triceps surae muscle: Mri analysis indicating in vivo myofascial force transmission between synergistic muscles," *Surgical and Radiologic Anatomy*, Vol. 33, pp. 869–879, 2011.

106. Yaman, A., C. Ozturk, P. A. Huijing, and C. A. Yucesoy, "Magnetic resonance imaging assessment of mechanical interactions between human lower leg muscles in vivo," *Journal of Biomechanical Engineering*, Vol. 135, no. 9, p. 091003, 2013.

107. Arnold, A. S., S. Salinas, D. J. Asakawa, and S. L. Delp, "Accuracy of muscle moment arms estimated from mri-based musculoskeletal models of the lower extremity," *Computer Aided Surgery*, Vol. 5, no. 2, pp. 108–119, 2000.

108. Arnold, A. S., S. R. Ward, R. L. Lieber, and S. L. Delp, "A model of the lower limb for analysis of human movement," *Annals of Biomedical Engineering*, Vol. 38, pp. 260–279, 2010.

109. Neumann, D. A., "Kinesiology of the hip: A focus on muscular actions," *Journal of Orthopaedic and Sports Physical Therapy*, Vol. 40, no. 2, pp. 82–94, 2010.

110. Lieber, R. L., and J. Fridén, "Spasticity causes a fundamental rearrangement of muscle-joint interaction," *Muscle and Nerve*, Vol. 25, no. 2, pp. 265–270, 2002.

111. Mohagheghi, A. A., T. Khan, T. H. Meadows, K. Giannikas, *et al.*, "In vivo gastrocnemius muscle fascicle length in children with and without diplegic cerebral palsy," *Developmental Medicine and Child Neurology*, Vol. 50, no. 1, pp. 44–50, 2008.

112. Tijs, C., J. H. van Dieën, and H. Maas, "Effects of epimuscular myofascial force transmission on sarcomere length of passive muscles in the rat hindlimb," *Physiological Reports*, Vol. 3, no. 11, p. e12608, 2015.

113. Olesen, A. T., B. R. Jensen, T. L. Uhlendorf, R. W. Cohen, *et al.*, "Muscle-specific changes in length-force characteristics of the calf muscles in the spastic han-wistar rat," *Journal of Applied Physiology*, Vol. 117, no. 9, pp. 989–997, 2014.

114. Haberfehlner, H., R. T. Jaspers, E. Rutz, J. G. Becher, *et al.*, "Knee moment-angle characteristics and semitendinosus muscle morphology in children with spastic paresis selected for medial hamstring lengthening," *PLoS ONE*, Vol. 11, no. 11, p. e0166401, 2016.

115. Wang, T. M., H. P. Huang, J. D. Li, S. W. Hong, *et al.*, "Leg and joint stiffness in children with spastic diplegic cerebral palsy during level walking," *PLoS ONE*, Vol. 10, no. 12, p. e0143967, 2015.

116. Yonetsu, R., A. Iwata, J. Surya, K. Unase, *et al.*, "Sit-to-stand movement changes in preschool-aged children with spastic diplegia following one neurodevelopmental treatment session - a pilot study," *Disability and Rehabilitation*, Vol. 37, no. 18, pp. 1643–1650, 2015.

117. Farmer, S. E., and M. James, "Contractures in orthopaedic and neurological conditions: A review of causes and treatment," *Disability and Rehabilitation*, Vol. 23, no. 13, pp. 549–558, 2001.

118. Shortland, A. P., C. A. Harris, M. Gough, and R. O. Robinson, "Architecture of the medial gastrocnemius in children with spastic diplegia," *Developmental Medicine and Child Neurology*, Vol. 44, no. 3, pp. 158–163, 2002.

119. Haberfehlner, H., H. Maas, J. Harlaar, I. E. Newsum, *et al.*, "Assessment of net knee moment-angle characteristics by instrumented hand-held dynamometry in children with spastic cerebral palsy and typically developing children," *Journal of NeuroEngineering and Rehabilitation*, Vol. 12, p. 67, 2015.

120. Damiano, D. L., E. Laws, D. V. Carmines, and M. F. Abel, "Relationship of spasticity to knee angular velocity and motion during gait in cerebral palsy," *Gait and Posture*, Vol. 23, no. 1, pp. 1–8, 2006.

121. Ada, L., W. Vattanasilp, N. J. O'Dwyer, and J. Crosbie, "Does spasticity contribute to walking dysfunction after stroke?," *Journal of Neurology Neurosurgery and Psychiatry*, Vol. 64, pp. 628–635, 1998.

122. Norton, B. J., H. A. Bomze, S. A. Sahrmann, and S. G. Eliasson, "Correlation between gait speed and spasticity at the knee," *Physical Therapy*, Vol. 55, no. 4, pp. 355–359, 1975.

123. Davis, R. B., S. Õunpuu, D. Tyburski, and J. R. Gage, "A gait analysis data collection and reduction technique," *Human Movement Science*, Vol. 10, no. 5, pp. 575–587, 1991.

124. Lewerenz, A., S. I. Wolf, T. Dreher, M. S. Y. Topcuoglu, *et al.*, "Mechanisms to improve foot clearance while stair ascending in patients with bilateral spastic cerebral palsy and stiff knee gait," *Gait and Posture*, Vol. 57, no. Suppl 1, pp. 60–61, 2017.

125. Yucesoy, C. A., and P. A. Huijing, "Specifically tailored use of the finite element method to study muscular mechanics within the context of fascial integrity: The linked fiber-matrix model," *International Journal for Multiscale Computational Engineering*, Vol. 10, pp. 155–170, 2012.

126. Yucesoy, C. A., and P. A. Huijing, "Assessment by finite element modeling indicates that surgical intramuscular aponeurotomy performed closer to the tendon enhances intended acute effects in extramuscularly connected muscle," *Journal of Biomechanical Engineering*, Vol. 131, no. 2, p. 021012, 2009.

127. Ates, F., R. J. Andrade, S. R. Freitas, F. Hug, *et al.*, "Passive stiffness of monoarticular lower leg muscles is influenced by knee joint angle," *European Journal of Applied Physiology*, Vol. 118, pp. 585–593, 2018.

128. Yoshitake, Y., D. Uchida, K. Hirata, D. L. Mayfield, *et al.*, "Mechanical interaction between neighboring muscles in human upper limb: Evidence for epimuscular myofascial force transmission in humans," *Journal of Biomechanics*, Vol. 74, pp. 150–155, 2018.

129. de Bruin, M., M. J. C. Smeulders, and M. Kreulen, "Flexor carpi ulnaris tenotomy alone does not eliminate its contribution to wrist torque," *Clinical Biomechanics*, Vol. 26, no. 7, pp. 725–728, 2011.

130. Yucesoy, C. A., B. H. F. J. M. Koopman, H. J. Grootenboer, and P. A. Huijing, "Finite element modeling of aponeurotomy: Altered intramuscular myofascial force transmission yields complex sarcomere length distributions determining acute effects," *Biomechanics and Modeling in Mechanobiology*, Vol. 6, pp. 227–243, 2007.

131. Fee, J. W., and F. Miller, "The leg drop pendulum test performed under general anesthesia in spastic cerebral palsy," *Developmental Medicine and Child Neurology*, Vol. 46, no. 4, pp. 273–281, 2004.

132. Sanger, T. D., M. R. Delgado, D. Gaebler-Spira, M. Hallett, *et al.*, "Classification and definition of disorders causing hypertonia in childhood," *Pediatrics*, Vol. 111, no. 1, pp. e89–e97, 2003.

133. Tardieu, C., E. H. de la Tour, M. D. Bret, and G. Tardieu, "Muscle hypoextensibility in children with cerebral palsy: I. clinical and experimental observations," *Archives of Physical Medicine and Rehabilitation*, Vol. 63, no. 3, pp. 97–102, 1982.

134. Lieber, R. L., and J. Fridén, "Muscle contracture and passive mechanics in cerebral palsy," *Journal of Applied Physiology*, Vol. 126, no. 5, pp. 1492–1501, 2018.

135. Edsfeldt, S., D. Rempel, K. Kursa, E. Diao, *et al.*, "In vivo flexor tendon forces generated during different rehabilitation exercises," *Journal of Hand Surgery: European Volume*, Vol. 40, no. 7, pp. 705–710, 2015.

136. Frost, G., J. Dowling, K. Dyson, and O. Bar-Or, "Cocontraction in three age groups of children during treadmill locomotion," *Journal of Electromyography and Kinesiology*, Vol. 7, no. 3, pp. 179–186, 1997.

137. Ates, F., Y. Temelli, and C. A. Yucesoy, "Effects of antagonistic and synergistic muscles' co-activation on mechanics of activated spastic semitendinosus in children with cerebral palsy," *Human Movement Science*, Vol. 57, pp. 103–110, 2018.

138. Kaya, C. S., Y. Temelli, F. Ates, and C. A. Yucesoy, "Effects of inter-synergistic mechanical interactions on the mechanical behaviour of activated spastic semitendinosus muscle of patients with cerebral palsy," *Journal of the Mechanical Behavior of Biomedical Materials*, Vol. 77, pp. 78–84, 2018.

139. Rodda, J. M., H. K. Graham, L. Carson, M. P. Galea, *et al.*, "Sagittal gait patterns in spastic diplegia," *Journal of Bone and Joint Surgery*, Vol. 86-B, no. 2, pp. 251–258, 2004.

140. Delp, S. L., J. P. Loan, M. G. Hoy, F. E. Zajac, *et al.*, "An interactive graphics-based model of the lower extremity to study orthopaedic surgical procedures," *IEEE Transactions on Biomedical Engineering*, Vol. 37, no. 8, pp. 757–767, 1990.

141. Benedetti, M. G., V. Agostini, M. Knaflitz, and P. Bonato, "Muscle activation patterns during level walking and stair ambulation," in *Applications of EMG in Clinical and Sports Medicine* (Steele, C., ed.), ch. 8, pp. 117–130, Croatia: InTech, 2012.

142. Bonnefoy-Mazure, A., and S. Armand, "Normal gait," in *Orthopedic Management of Children with Cerebral Palsy: A Comprehensive Approach* (Canavese, F., and J. Deslandes, eds.), ch. 16, pp. 119–213, Nova Science Publishers, Inc., 2015.

143. Wall-Scheffler, C. M., E. Chumanov, K. Steudel-Numbers, and B. Heiderscheit, "Electromyography activity across gait and incline: The impact of muscular activity on human morphology," *American Journal of Physical Anthropology*, Vol. 143, no. 4, pp. 601–611, 2010.

144. Wilke, J., R. Schleip, C. A. Yucesoy, and W. Banzer, "Not merely a protective packing organ? a review of fascia and its force transmission capacity," *Journal of Applied Physiology*, Vol. 124, no. 1, pp. 234–244, 2017.

145. Röhrle, O., and A. J. Pullan, "Three-dimensional finite element modelling of muscle forces during mastication," *Journal of Biomechanics*, Vol. 40, no. 15, pp. 3363–3372, 2007.

146. Turkoglu, A. N., P. A. Huijing, and C. A. Yucesoy, "Mechanical principles of effects of botulinum toxin on muscle length-force characteristics: An assessment by finite element modeling," *Journal of Biomechanics*, Vol. 47, no. 7, pp. 1565–1571, 2014.

147. Virgilio, K. M., K. S. Martin, S. M. Peirce, and S. S. Blemker, "Multiscale models of skeletal muscle reveal the complex effects of muscular dystrophy on tissue mechanics and damage susceptibility," *Interface Focus*, Vol. 5, no. 2, p. 20140080, 2015.

148. Bojsen-Møller, J., S. Schwartz, K. K. Kalliokoski, T. Finni, *et al.*, "Intermuscular force transmission between human plantarflexor muscles in vivo," *Journal of Applied Physiology*, Vol. 109, no. 6, pp. 1608–1618, 2010.

149. Meijer, H. J. M., J. M. Rijkelijkhuizen, and P. A. Huijing, "Effects of firing frequency on length-dependent myofascial force transmission between antagonistic and synergistic muscle groups," *European Journal of Applied Physiology*, Vol. 104, pp. 501–513, 2008.

150. van der Krogt, M. M., C. A. M. Doorenbosch, and J. Harlaar, "The effect of walking speed on hamstrings length and lengthening velocity in children with spastic cerebral palsy," *Gait and Posture*, Vol. 29, no. 4, pp. 640–644, 2009.

151. Damiano, D. L., T. L. Martellotta, D. J. Sullivan, K. P. Granata, *et al.*, "Muscle force production and functional performance in spastic cerebral palsy: Relationship of cocontraction," *Archives of Physical Medicine and Rehabilitation*, Vol. 81, no. 7, pp. 895–900, 2000.

152. Fry, N. R., M. Gough, and A. P. Shortland, "Three-dimensional realisation of muscle morphology and architecture using ultrasound," *Gait and Posture*, Vol. 20, no. 2, pp. 177–182, 2004.

153. Wren, T. A. L., A. P. Cheatwood, S. A. Rethlefsen, R. Hara, *et al.*, "Achilles tendon length and medial gastrocnemius architecture in children with cerebral palsy and equinus gait," *Journal of Pediatric Orthopaedics*, Vol. 30, no. 5, pp. 479–484, 2010.

154. Hösl, M., H. Böhm, A. Arampatzis, A. Keymer, *et al.*, "Contractile behavior of the medial gastrocnemius in children with bilateral spastic cerebral palsy during forward, uphill and backward-downhill gait," *Clinical Biomechanics*, Vol. 36, pp. 32–39, 2016.

155. Lee, S. S. M., D. Gaebler-Spira, L. Q. Zhang, W. Z. Rymer, *et al.*, "Use of shear wave ultrasound elastography to quantify muscle properties in cerebral palsy," *Clinical Biomechanics*, Vol. 31, pp. 20–28, 2016.

156. Matthiasdottir, S., M. Hahn, M. Yaraskavitch, and W. Herzog, "Muscle and fascicle excursion in children with cerebral palsy," *Clinical Biomechanics*, Vol. 29, no. 4, pp. 458–462, 2014.

157. Malaiya, R., A. E. McNee, N. R. Fry, L. C. Eve, *et al.*, "The morphology of the medial gastrocnemius in typically developing children and children with spastic hemiplegic cerebral palsy," *Journal of Electromyography and Kinesiology*, Vol. 17, no. 6, pp. 657–663, 2007.

158. Huijing, P. A., and R. T. Jaspers, "Adaptation of muscle size and myofascial force transmission: A review and some new experimental results," *Scandinavian Journal of Medicine and Science in Sports*, Vol. 15, no. 6, pp. 349–380, 2005.

159. Barber, L., R. Barrett, and G. Lichtwark, "Medial gastrocnemius muscle fascicle active torque-length and achilles tendon properties in young adults with spastic cerebral palsy," *Journal of Biomechanics*, Vol. 45, no. 15, pp. 2526–2530, 2012.

160. Kaya, C. S., F. Bilgili, N. E. Akalan, Y. Temelli, *et al.*, "Intraoperative experiments combined with gait analyses indicate that active state rather than passive dominates the spastic gracilis muscle's joint movement limiting effect in cerebral palsy," *Clinical Biomechanics*, Vol. 68, pp. 151–157, 2019.

161. Kaya, C. S., F. Bilgili, N. E. Akalan, and C. A. Yucesoy, "Intraoperative testing of passive and active state mechanics of spastic semitendinosus in conditions involving intermuscular mechanical interactions and gait relevant joint positions," *Journal of Biomechanics*, Vol. 103, p. 109755, 2020.

162. Fridén, J., and R. L. Lieber, "Spastic muscle cells are shorter and stiffer than normal cells," *Muscle and Nerve*, Vol. 27, no. 2, pp. 157–164, 2003.

163. Cankaya, A. O., U. Pamuk, and C. A. Yucesoy, "The effects of an activation-dependent increase in titin stiffness on whole muscle properties using finite element modeling," *Journal of Biomechanics*, Vol. 116, p. 110197, 2021.

164. Linke, W. A., "Titin gene and protein functions in passive and active muscle," *Annual Review of Physiology*, Vol. 80, pp. 389–411, 2018.

165. Monroy, J. A., K. L. Powers, C. M. Pace, T. Uyeno, *et al.*, "Effects of activation on the elastic properties of intact soleus muscles with a deletion in titin," *Journal of Experimental Biology*, Vol. 220, no. 5, pp. 828–836, 2017.

166. Oda, T., H. Kanehisa, K. Chino, T. Kurihara, *et al.*, "In vivo behavior of muscle fascicles and tendinous tissues of human gastrocnemius and soleus muscles during twitch contraction," *Journal of Electromyography and Kinesiology*, Vol. 17, no. 5, pp. 587–595, 2007.

167. Yanase, K., M. Yagi, S. Nakao, Y. Motomura, *et al.*, "Epimuscular myofascial force transmission from biarticular rectus femoris elongation increases shear modulus of monoarticular quadriceps muscles," *Journal of Biomechanics*, Vol. 122, p. 110421, 2021.

168. Booth, C. M., M. J. F. Cortina-Borja, and T. N. Theologis, "Collagen accumulation in muscles of children with cerebral palsy and correlation with severity of spasticity," *Developmental Medicine and Child Neurology*, Vol. 43, no. 5, pp. 314–320, 2001.

169. Adams, M. M., and A. L. Hicks, "Spasticity after spinal cord injury," *Spinal Cord*, Vol. 43, pp. 577–586, 2005.

170. Marciniak, C., L. Rader, and C. Gagnon, "The use of botulinum toxin for spasticity after spinal cord injury," *American Journal of Physical Medicine and Rehabilitation*, Vol. 87, no. 4, pp. 312–317, 2008.

171. Hyman, N., M. Barnes, B. Bhakta, A. Cozens, *et al.*, "Botulinum toxin treatment of hip adductor spasticity in multiple sclerosis: A prospective, randomised, double blind, placebo controlled, dose ranging study," *Journal of Neurology Neurosurgery and Psychiatry*, Vol. 68, no. 6, pp. 707–712, 2000.

172. Walt, A. V. D., S. Sung, T. Spelman, M. Marriott, *et al.*, "A double-blind, randomized, controlled study of botulinum toxin type a in ms-related tremor," *Neurology*, Vol. 79, no. 1, pp. 92–99, 2012.

173. Bakheit, A. M. O., A. F. Thilmann, A. B. Ward, W. Poewe, *et al.*, "A randomized, double-blind, placebo-controlled, dose-ranging study to compare the efficacy and safety of three doses of botulinum toxin type a (dysport) with placebo in upper limb spasticity after stroke," *Stroke*, Vol. 31, pp. 2402–2406, 2000.

174. Bhakta, B. B., J. A. Cozens, M. A. Chamberlain, and J. M. Bamford, "Impact of botulinum toxin type a on disability and carer burden due to arm spasticity after stroke: A randomised double blind placebo controlled trial," *Journal of Neurology Neurosurgery and Psychiatry*, Vol. 69, pp. 217–221, 2000.

175. Hammond, C., O. E. Far, and M. Seagar, "Neurotransmitter release," in *Cellular and Molecular Neurophysiology* (Canavese, F., and J. Deslandes, eds.), ch. 7, pp. 145–169, Academic Press, 2015.

176. Sheean, G. L., "Botulinum treatment of spasticity: Why is it so difficult to show a functional benefit?," *Current Opinion in Neurology*, Vol. 14, no. 6, pp. 771–776, 2001.

177. Shaari, C. M., E. George, B. L. Wu, H. F. Biller, *et al.*, "Quantifying the spread of botulinum toxin through muscle fascia," *The Laryngoscope*, Vol. 101, no. 9, pp. 960–964, 1991.

178. Grunner, J. A., J. Altman, and N. Spivack, "Effects of arrested cerebellar development on locomotion in the rat," *Experimental Brain Research*, Vol. 40, pp. 361–373, 1980.

179. Carlson, C. G., *Determination of Hydroxyproline Content as a Measure of Fibrosis in Nondystrophic and Dystrophic Skeletal Muscle*, Treat NMD, 2014. Available: http://www.treat-nmd.eu/downloads/file/sops/dmd/MDX/DMD_M.1.2.006.pdf.

180. Neter, J., M. Kutner, W. Wasserman, and C. Nachtsheim, *Applied Linear Statistical Models*, Homewood, IL: McGraw-Hill/Irwin, 4th ed., 1996.

181. Neuman, R. E., and M. A. Logan, "The determination of collagen and elastin in tissues," *Journal of Biological Chemistry*, Vol. 186, no. 2, pp. 549–556, 1950.

182. Thacker, B. E., A. Tomiya, J. B. Hulst, K. P. Suzuki, *et al.*, "Passive mechanical properties and related proteins change with botulinum neurotoxin a injection of normal skeletal muscle," *Journal of Orthopaedic Research*, Vol. 30, no. 3, pp. 497–502, 2012.

183. Ansved, T., T. Odergren, and K. Borg, "Muscle fiber atrophy in leg muscles after botulinum toxin type a treatment of cervical dystonia," *Neurology*, Vol. 48, no. 5, pp. 1440–1442, 1997.

184. Antonucci, F., C. Rossi, L. Gianfranceschi, O. Rossetto, *et al.*, "Long-distance retrograde effects of botulinum neurotoxin a," *Journal of Neuroscience*, Vol. 28, no. 14, pp. 3689–3696, 2008.

185. Elvrum, A. K. G., S. M. Brændvik, R. Sæther, T. Lamvik, *et al.*, "Effectiveness of resistance training in combination with botulinum toxin-a on hand and arm use in children with cerebral palsy: A pre-post intervention study," *BMC Pediatrics*, Vol. 12, p. 91, 2012.

186. Gracies, J. M., B. J. Singer, and J. W. Dunne, "The role of botulinum toxin injections in the management of muscle overactivity of the lower limb," *Disability and Rehabilitation*, Vol. 29, no. 23, pp. 1789–1805, 2007.

187. de Paiva, A., F. A. Meunier, J. Molgó, K. R. Aoki, *et al.*, "Functional repair of motor endplates after botulinum neurotoxin type a poisoning: Biphasic switch of synaptic activity between nerve sprouts and their parent terminals," *Proceedings of the National Academy of Sciences of the United States of America*, Vol. 96, no. 6, pp. 3200–3205, 1999.

188. Minamoto, V. B., J. B. Hulst, M. Lim, W. J. Peace, *et al.*, "Increased efficacy and decreased systemic-effects of botulinum toxin a injection after active or passive muscle manipulation," *Developmental Medicine and Child Neurology*, Vol. 49, no. 12, pp. 907–914, 2007.

189. Chin, T. Y. P., G. R. Nattrass, P. Selber, and H. K. Graham, "Accuracy of intramuscular injection of botulinum toxin a in juvenile cerebral palsy: A comparison between manual needle placement and placement guided by electrical stimulation," *Journal of Pediatric Orthopaedics*, Vol. 25, no. 3, pp. 286–291, 2005.

190. Walter, U., and D. Dressler, "Ultrasound-guided botulinum toxin injections in neurology: Technique, indications and future perspectives," *Expert Review of Neurotherapeutics*, Vol. 14, no. 8, pp. 923–936, 2014.

191. Wissel, J., A. B. Ward, P. Erztgaard, D. Bensmail, *et al.*, "European consensus table on the use of botulinum toxin type a in adult spasticity," *Journal of Rehabilitation Medicine*, Vol. 41, no. 1, pp. 13–25, 2009.

192. Picelli, A., S. Tamburin, P. Bonetti, C. Fontana, *et al.*, "Botulinum toxin type a injection into the gastrocnemius muscle for spastic equinus in adults with stroke," *American Journal of Physical Medicine and Rehabilitation*, Vol. 91, no. 11, pp. 957–964, 2012.

193. Molenaers, G., A. van Campenhout, K. Fagard, J. de Cat, *et al.*, "The use of botulinum toxin a in children with cerebral palsy, with a focus on the lower limb," *Journal of Children's Orthopaedics*, Vol. 4, no. 3, pp. 183–195, 2010.

194. Carli, L., C. Montecucco, and O. Rossetto, "Assay of diffusion of different botulinum neurotoxin type a formulations injected in the mouse leg," *Muscle and Nerve*, Vol. 40, no. 3, pp. 374–380, 2009.

195. Borodic, G. E., R. Ferrante, L. B. Pearce, and K. Smith, "Histologic assessment of doseârelated diffusion and muscle fiber response after therapeutic botulinum a toxin injections," *Movement Disorders*, Vol. 9, no. 1, pp. 31–39, 1994.

196. Kaya, C. S., E. O. Yilmaz, Z. D. Akdeniz-Dogan, and C. A. Yucesoy, "Long-term effects with potential clinical importance of botulinum toxin type-a on mechanics of muscles exposed," *Frontiers in Bioengineering and Biotechnology*, Vol. 8, p. 738, 2020.

197. Yilmaz, E. O., C. S. Kaya, Z. D. Akdeniz-Dogan, and C. A. Yucesoy, "Long-term btx-a effects on bi-articular muscle: Higher passive force, limited length range of active force production and unchanged intermuscular interactions," *Journal of Biomechanics*, Vol. 126, p. 110627, 2021.

198. Boulard, C., V. Gautheron, and T. Lapole, "Mechanical properties of ankle joint and gastrocnemius muscle in spastic children with unilateral cerebral palsy measured with shear wave elastography," *Journal of Biomechanics*, Vol. 124, p. 110502, 2021.

199. Brandenburg, J. E., S. F. Eby, P. Song, S. Kingsley-Berg, *et al.*, "Quantifying passive muscle stiffness in children with and without cerebral palsy using ultrasound shear wave elastography," *Developmental Medicine and Child Neurology*, Vol. 58, no. 12, pp. 1288–1294, 2016.

200. Lallemant-Dudek, P., C. Vergari, G. Dubois, V. Forin, *et al.*, "Ultrasound shearwave elastography to characterize muscles of healthy and cerebral palsy children," *Scientific Reports*, Vol. 11, p. 3577, 2021.

201. Brandenburg, J. E., S. F. Eby, P. Song, W. R. Bamlet, *et al.*, "Quantifying effect of onabotulinum toxin a on passive muscle stiffness in children with cerebral palsy using ultrasound shear wave elastography," *American Journal of Physical Medicine and Rehabilitation*, Vol. 97, no. 7, pp. 500–506, 2018.

202. Ates, F., F. Hug, K. Bouillard, M. Jubeau, *et al.*, "Muscle shear elastic modulus is linearly related to muscle torque over the entire range of isometric contraction intensity," *Journal of Electromyography and Kinesiology*, Vol. 25, no. 4, pp. 703–708, 2015.